

ELECTRONIC AND SPECTROELECTRONIC PROPERTIES OF ELECTROACTIVE
POLYMERS

THESIS

Presented to the Graduate Council of
Texas State University-San Marcos
in Partial Fulfillment
of the Requirements

for the Degree

Master of SCIENCE

By

Jamie R. Carberry, B.S.

San Marcos, Texas
December 2012

ELECTRONIC AND SPECTROELECTRONIC PROPERTIES OF ELECTROACTIVE
POLYMERS

Committee Members Approved:

Jennifer A. Irvin

Chang Ji

Walter Rudzinski

Approved:

J. Michael Willoughby
Dean of the Graduate College

COPYRIGHT

by

Jamie R. Carberry

2012

FAIR USE AND AUTHOR'S PERMISSION STATEMENT

Fair Use

This work is protected by the Copyright Laws of the United States (Public Law 94-553, section 107). Consistent with fair use as defined in the Copyright Laws, brief quotations from this material are allowed with proper acknowledgement. Use of this material for financial gain without the author's express written permission is not allowed.

Duplication Permission

As the copyright holder of this work I, Jamie R. Carberry, authorize duplication of this work, in whole or in part, for educational or scholarly purposes only.

ACKNOWLEDGMENTS

I would like to give a large thank you to Dr. Jennifer Irvin as well as Dr. Jody Neef for never hesitating to provide guidance, assistance, and support whenever it was needed. I'm also going to thank Dr. Chang Ji and Dr. Walter Rudzinski, committee members, who were willing to provide valuable insight and Dr. Beall for his help with modeling studies.

Special thanks should be given to those lab mates who were in the lab alongside me to give me support in the lab as well as outside the lab. Not one day will pass by that the phrase "you clam" doesn't bring to mind the amazing group. In particular, Blake Bowden, who put up with me as his lab partner for two years, Katie Winkel, who would give valued advice and never allow me to go off the beaten path, Makda Araya, who was the one I could depend on going to lunch with to get out of the lab, and James Warren, who helped to problem solve and to ensure that Chipotle Friday was always met.

Finally, words alone cannot express the thanks needed for my family who would never let me down. My mom, my sisters, and my brother were there for every good time and bad. You guys are, and will always be, the world to me. No matter how close or how far I may go, down the road I know they will be there.

This manuscript was submitted on July 19th, 2012.

TABLE OF CONTENTS

	Page
ACKNOWLEDGMENTS	v
LIST OF TABLES	viii
LIST OF EQUATIONS	ix
LIST OF SCHEMES	x
LIST OF FIGURES	xi
ABSTRACT	xv
 CHAPTER	
I. INTRODUCTION TO ELECTROACTIVE POLYMERS	1
History of Electroactive Polymers	1
Band Gap	2
Redox-Active Polymers	5
Oxidative Polymerization	6
Chronoamperometry	13
Applications	15
Electrochemical Capacitors	15
Light-Emitting Diodes	15
Polymer Solar Cells	17
Motivation for Research	18
II. ISOPYRAZOLES	20
Background	20
Experimental	22
Materials	22
Instrumentation	23

Results and Discussion	24
Monomer and Polymer Electrochemistry	24
BEIPZ-TMS Electropolymerization Attempts	24
BEIPz Electropolymerization and Resultant Polymer	
Electrochemistry	25
Spectroelectrochemistry	42
Conclusions	43
III. PYRIMIDINES	45
Background	45
Experimental	47
Materials	47
Instrumentation	48
Results and Discussion	49
Monomer and Polymer Electrochemistry	49
Electrolyte: EMIBTI	49
Electrolyte: BMPBTI	57
Spectroelectrochemistry	63
Molecular Modeling and X-Ray Diffraction	68
Conclusions	72
IV. FERROCENE-CONTAINING POLYMERS	74
Background	74
Experimental	76
Materials	76
Instrumentation	77
Results and Discussion	77
Electrodeposition	77
Conclusion	81
V. CONCLUDING REMARKS	82
Conclusion	82
Future Work	83
REFERENCES	85

LIST OF TABLES

Table	Page
1. Tabulated data for each pyrimidine and isopyrazole monomer and its respective polymer in 0.1 M BMPBTI/CH ₃ CN. Values for the band gap determination are discussed in the spectroelectrochemistry section below	62
2. Oxidation and reduction potentials for electrodeposited ferrocene-containing copolymers, 1A-C and 2A-C, in 0.1 M NaCl/H ₂ O with corresponding diffusion coefficients, D. WE: Pt (0.2 cm diameter); RE: Ag wire; CE: Pt wire.....	81

LIST OF EQUATIONS

Equation	Page
1. Conversion of wavelength to electron volts.....	3
2. Randles-Sevcik equation.....	11
3. Theory for Surface-Immobilized redox centers	12
4. Cottrell equation.....	14

LIST OF SCHEMES

Scheme	Page
1. Synthesis of BTIPz	21
2. Synthesis of BEIPz-TMS	21
3. Deprotection of BEIPz-TMS to form BEIPz	22
4. Synthesis of 2,5-bis(thien-2-yl)pyrimidine (BTPm)	46
5. Copolymerization of 3-Phenyl[5]ferrocenophane-1,5-dimethylene with Various N-substituted Maleimides	76
6. Copolymerization of Vinylferrocene with Various N-substituted Maleimides	76

LIST OF FIGURES

Figure	Page
1. Common conducting polymers	2
2. Band gap grows smaller with increasing conjugation	3
3. UV-Vis spectrum for conjugated monomer, its neutral polymer, and its p-doped polymer. Inset: expanded to show shift in band gap (see Chapter 3)	4
4. Representation of n-and p-doping processes when electrons are removed (p-doping) or added (n-doping) to the neutral polymer.....	5
5. Redox-active polymers	6
6. Oxidative polymerization of thiophene	7
7. Electrochemical cell.....	9
8. Electrolytes	10
9. Cottrell Plot for 0.01 M ferrocene-containing copolymer 2A. Parameters: induction period: 0 V for 15 seconds, forward step period: 0.5 V for 120 seconds, and relaxation period: 0.5 V for 120 seconds.	14
10. Depiction of light emitting diode (OLED).....	16
11. Monomers of interest	18
12. Various copolymers of interest derived from (1) ferrocenophene and (2) vinylferrocene with various N-substituted maleimides	19
13. Depiction of synthesized monomers BTIPz, BEIPz, and BEIPz-TMS	20

14. Electropolymerization of 0.01M BEIPz in 0.1M BMPBTI/CH ₃ CN at 100 mV/s for 5 cycles from -2.3 to +1.2 V. WE: Pt (0.2 cm diameter); RE: Ag wire; CE: Pt wire	27
15. Electropolymerization of 0.01M EDOT and 3-methoxythiophene (ThOMe) in 0.1M BMPBTI /CH ₃ CN at 100 mV/s on gold working electrodes; the first cycle is shown for each electrode. RE: silver wire; CE: Pt wire.....	28
16. Electropolymerization of 0.01M bithiophene in 0.1M BMPBTI/CH ₃ CN at 100 mV/s for 5 cycles from -2.55 to +1.0 V. WE: Au (0.2 cm diameter); RE: Ag wire; CE: Pt wire	29
17. Electropolymerization of 0.01M BEIPz in 0.1M BMPBTI/CH ₃ CN at 100 mV/s for 1 cycles from -2.35 to +1.2 V. WE: Au (0.2 cm diameter); RE: Ag wire; CE: Pt wire	30
18. Electropolymerization of 0.01M BEIPz in 0.1M TMABF ₄ /CH ₃ CN at 100 mV/s for 5 cycles from -1.5 to +1.0 V. WE: Au (0.2 cm diameter); RE: Ag wire; CE: Pt wire	31
19. Cyclic voltammogram of PBEIPz in 0.1M TMABF ₄ /PC at 100 mV/s for 50 cycles from -2.35 to +0.9 V. WE: Au (0.2 cm diameter); RE: Ag wire; CE: Pt wire.	33
20. Electropolymerization of 0.01M BEIPz in 0.1M BMPBTI/CH ₃ CN at 100 mV/s for 5 cycles from -1.6 to +1.0 V. WE: Au (0.2 cm diameter); RE: Ag wire; CE: Pt wire	34
21. Cyclic voltammetry of PBEIPz grown in 0.1M BMPBTI/CH ₃ CN and cycled in 0.1M BMPBTI/CH ₃ CN at 100, 200, and 400 mV/s from -2.3 to +0.4 V. WE: Au (0.2 cm diameter); RE: Ag wire; CE: Pt wire	35
22. Electropolymerization of 0.01M BEIPz in 0.1M TMABF ₄ /CH ₃ CN at 30 mV/s for 60 cycles from -1.6 to +1.05 V. WE: Pt (0.2 cm diameter); RE: Ag wire; CE: Pt wire	36
23. Cyclic voltammogram of PBEIPz in 0.1M TMABF ₄ /PC and TMABF ₄ /CH ₃ CN at 100 mV/s. WE: Pt (0.2 cm diameter); RE: Ag wire; CE: Pt wire.....	37
24. Electropolymerization of 0.01M BEIPz in 0.1M TBAP/CH ₃ CN at 100 mV/s for 5 cycles from -1.45 to +1.15 V. WE: Au (0.2 cm diameter); RE: Ag wire; CE: Pt wire	38
25. Cyclic voltammogram of PBEIPz in 0.1M TBAP/CH ₃ CN at 100, 200, and 400 mV/s from -1.3 to +0.25 V. WE: Au (0.2 cm diameter); RE: Ag wire; CE: Pt wire	39

26. Cyclic voltammogram of PBEIPz in 0.01 M BMPBTI/CH ₃ CN, TMABF ₄ /CH ₃ CN, TBAP/PC, and TBAP/CH ₃ CN at 100 mV/s. WE: Au (0.2 cm diameter); RE: Ag wire; CE: Pt wire.....	40
27. Cyclic voltammogram of PBEIPz in 0.1M BMPBTI/CH ₃ CN at 100, 200, and 400 mV/s from -1.45 to +0.5 V. WE: Au (0.2 cm diameter); RE: Ag wire; CE: Pt wire	41
28. Monomer energy gap, E _g , depicted for BEIPz.....	43
29. Structure of 2,5-bis(thien-2-yl)pyrimidine (BTPy).....	46
30. Structural representation of (a) BTPm and (b) BEPm	47
31. Repeated potential scanning electropolymerization of BTPm (0.005 M in 0.1 M EMIBTI/CH ₃ CN) vs. Fc/Fc ⁺ at 100 mV/s from -1.6 to +0.2 V	50
32. PBTPm cyclic voltammetry in 0.1 M EMIBTI/CH ₃ CN.....	51
33. Repeated potential scanning oxidative electropolymerization of BEPm (0.01 M in 0.1 M EMIBTI/CH ₃ CN) Vs. Fc/Fc ⁺ at 100 mV/s from -1.35 to +0.5 V	52
34. PBEPm cyclic voltammetry in 0.1 M EMIBTI/CH ₃ CN.....	54
35. Repeated potential scanning electropolymerization of BEPm (0.01 M in 0.1 M EMIBTI/CH ₃ CN) Vs. Fc/Fc ⁺ at 100 mV/s from -1.8 to +0.5 V	55
36. PBEPm cyclic voltammetry in 0.1 M EMIBTI/CH ₃ CN.....	56
37. Repeated potential scanning electropolymerization of BTPm (0.005 M in 0.1 M BMPBTI/CH ₃ CN) Vs. Fc/Fc ⁺ at 100 mV/s	57
38. PBTPm cyclic voltammetry in 0.1 M BMPBTI/CH ₃ CN. Inset: The linear relationship between peak current and scan rate reveals that the polymer film is adhered to the electrode and is electroactive	58
39. Repeated potential scanning electropolymerization of BEPm (0.01 M in 0.1 M BMPBTI/CH ₃ CN) Vs. Fc/Fc ⁺ at 100 mV/s	59
40. PBEPm cyclic voltammetry in 0.1 M BMPBTI/CH ₃ CN.....	60
41. Cyclic voltammetry of PBEPm (dashes line, prepared from 0.005 M BEPm) vs. PBTPm (solid line, prepared from 0.005 M BTPm) in 0.1 M BMPBTI/CH ₃ CN at 450 mV/s.....	61

42. Monomer energy gap, E_g , depicted for BTPm and BEPm using 1.25×10^{-3} M monomer concentrations. Inset: magnified portion of energy gap determination	63
43. Spectroelectrochemistry of PBEPm in 0.1 M BMPBTI/ CH_3CN electrochemically deposited on an ITO working electrode from -0.9 V (A) to 1.2 V (N).....	65
44. Spectroelectrochemistry of PBTPm in 0.1 M BMPBTI/ CH_3CN electrochemically deposited on an ITO working electrode from -1.05 V (A) to 1.65 V (N).....	66
45. BTPm conformers.....	67
46. Determination of torsion angles through plane intersection	68
47. Molecular models of BTPm and BEPm showing torsion angles occurring on the opposite side of the pyrimidine nitrogens	69
48. Molecular model of BTPm with distance of 3.4\AA between each monomer	70
49. Molecular model of BTPm with distance of 3.9\AA between each monomer	71
50. A typical ferrocene-containing vinyl monomer	75
51. Cyclic Voltammogram of copolymer 1A-C at 100 mV/s. WE: Pt (0.2 cm diameter); RE: Ag wire; CE: Pt wire	78
52. Cyclic voltammogram of copolymer 2A-C at 100 mV/s. WE: Pt (0.2 cm diameter); RE: Ag wire; CE: Pt wire	79

ABSTRACT

ELECTRONIC AND SPECTROELECTRONIC PROPERTIES OF ELECTROACTIVE POLYMERS

by

Jamie R. Carberry, B.S.

Texas State University-San Marcos

December 2012

SUPERVISING PROFESSOR: JENNIFER A. IRVIN

Using stable n-doping and ferrocene derived polymers, electronic and spectroelectronic properties can be observed. Through choosing electron donators and electron acceptors, properties can be adjusted to produce polymers that can show lower, desirable, band gaps. Utilizing 3,4-ethylenedioxythiophenes as donor groups alongside the nitrogen-containing acceptor groups, oxidation potentials can be decreased as well. Using high molecular weight ferrocene-containing copolymers, chronoamperometry shows electrochemical reversibility making these copolymers very stable.

CHAPTER I

INTRODUCTION

History of Electroactive Polymers

In 1958, Natta and colleagues first prepared polyacetylene (PA, Figure 1) as a highly complex, insoluble black powder, making it difficult to characterize.¹ Because of its complex nature, the polymer was not of high interest until 1977.² Shirakawa and colleagues made polyacetylene into thin free-standing films that could be doped, making them conductive, leading to the creation of inherently conducting polymers.²

Polyacetylene was shown to have high conductivity, but its poor stability in air kept it from practical use. However, polyacetylene's unusual electronic properties led to research into other conducting polymers (Figure 1), such as polyaniline (PANI), poly(p-phenylene) (PPP), and poly(p-phenylenevinylene) (PPV).³ Alongside these polymers being investigated are polyheterocycles (Figure 1) including polypyrrole (PPy), polythiophene (PT), and poly(3,4-ethylenedioxythiophene) (PEDOT).^{4,5,3} The common factor in all of these polymers that leads to their conductive nature is conjugation: alternating double and single bonds that aid in resonance delocalization in the doped state. In many cases, stability of these polymers is much better than that of polyacetylene, and the polymer properties can be adjusted by incorporation of a variety of functional groups.

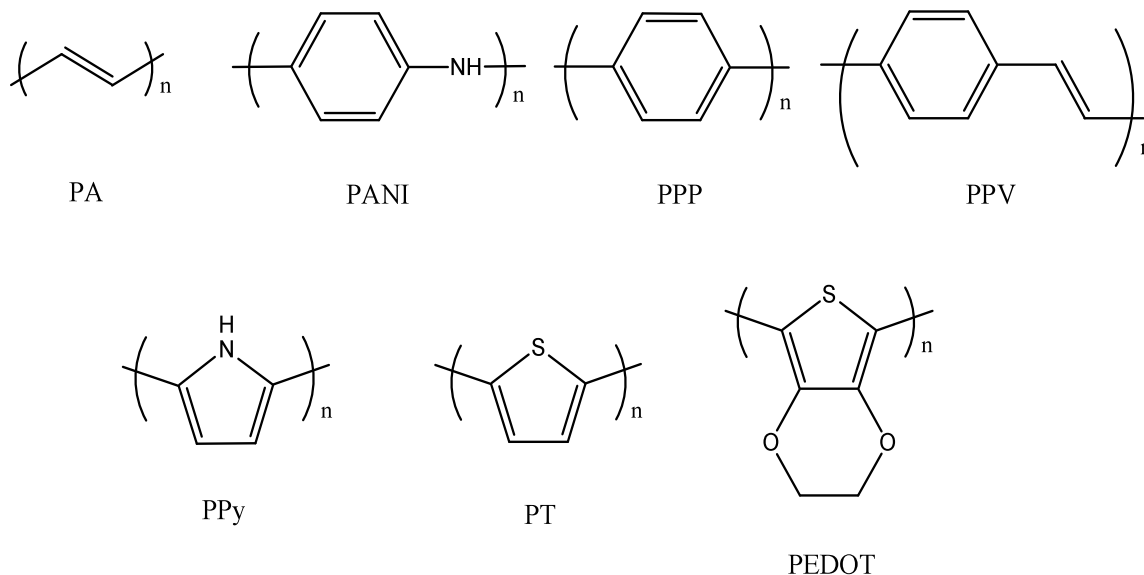


Figure 1. Common conducting polymers: polyacetylene (PA), polyaniline (PANI), poly(p-phenylene) (PPP), poly(phenylenevinylene) (PPV), polypyrrole (PPy), polythiophene (PT), and poly(3,4-ethylenedioxythiophene) (PEDOT).

Band Gap

All metals, semiconductors, and insulators possess their own individual characteristic energy structures (Figure 2) giving a range of electrical characteristics. One important characteristic is the energy gap (E_g) between the bonding (valence) and the antibonding (conductance) orbitals. For a material to become conductive, the electrons must obtain the required energy to move from the highest occupied molecular orbital (HOMO) to the lowest unoccupied molecular orbital (LUMO). The necessary energy required for electron promotion can be gained through absorption of either heat (phonons) or light (photons).⁶ Promotion of electrons is often difficult due to the large difference in energy between the HOMO and LUMO, but that energy difference can be

decreased by incorporation of aromatic or non-aromatic pi bonds into the molecule.⁷ In conjugated polymers, many molecular orbitals of similar energy overlap and become bands, and the energy gap is then known as a band gap (Figure 2).^{8,9} With a smaller band gap, electrons can easily be excited from the valence band to the conductance band. To reduce the band gap, planar molecules are desired due to their increased conjugation providing a greater pi orbital alignment.^{10,11}

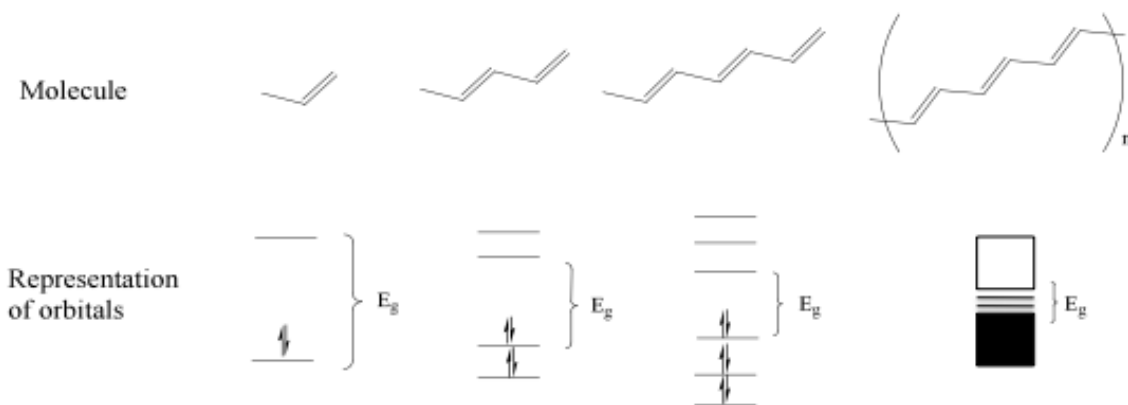


Figure 2. Band gap grows smaller with increasing conjugation.

Band gap is usually determined spectroscopically with the aid of an ultraviolet-visible (UV-Vis) spectrophotometer. In a UV-Vis spectrum, the onset of the π to π^* transition is easily visible for most conjugated molecules and electroactive polymers (EAPs). The energy at which this onset occurs is defined as the band gap. To determine the band gap, wavelength can be converted to energy through the following inverse relationship,

$$Energy(eV) = \frac{1240}{\lambda(nm)} \quad (\text{Equation 1})$$

where eV is the amount of energy gained from the charge of one electron's movement over one volt, and λ is the wavelength in nm.^{12,13} Increasing conjugation lowers the band gap, shifting the absorption to lower eV or higher wavelengths (Figure 3). As conjugation length increases from monomer to neutral polymer, the band gap is shifted to lower energies.

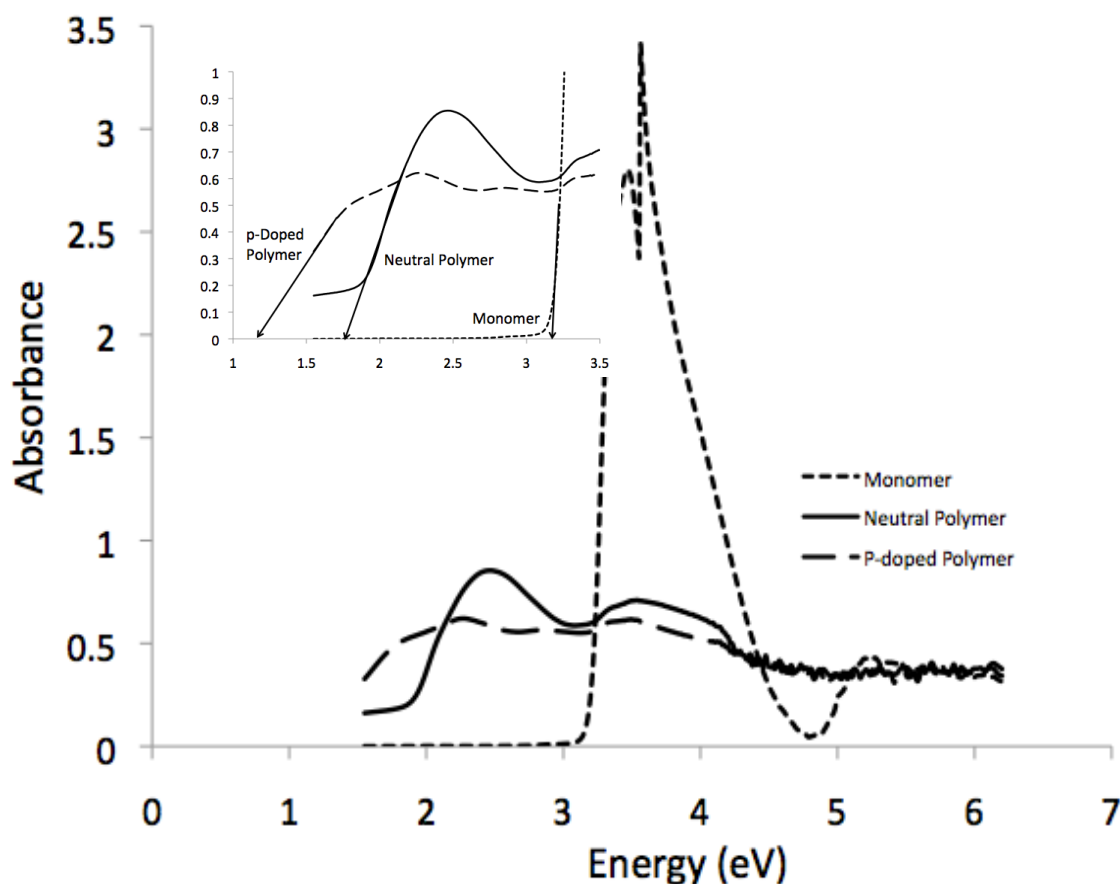


Figure 3. UV-Vis spectrum for conjugated monomer, its neutral polymer, and its p-doped polymer. Inset: expanded to show shift in band gap (see Chapter 3).

Minimizing the band gap for electroactive polymers (EAPs) through hybridization of the orbitals can create two new bands (Figure 2) between the original conducting and

valence bands. Thus, as a neutral polymer is doped, its E_g decreases further, as can be seen in Figure 3. This process is known as doping.¹⁴ Positive doping, or p-doping, is understood as a process that involves reversible oxidation of the neutral polymer backbone and the accompanying changes in the electronic structure.¹⁵ Conversely, n-doping involves reduction of neutral polymers (Figure 4). Stability in the n-doped state is typically poor due to instability of the carbanions formed during n-doping.¹⁶

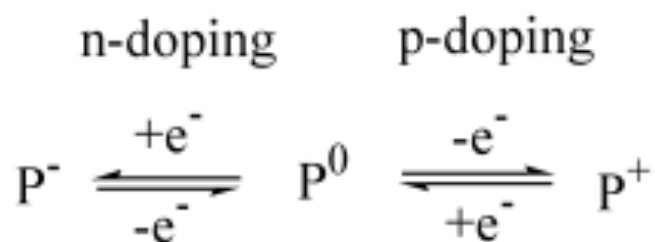


Figure 4. Representation of n-and p-doping processes when electrons are removed (p-doping) or added (n-doping) to the neutral polymer.

Redox-Active Polymers

In addition to conjugated polymers, another class of electroactive polymers are the redox active polymers. While these polymers are not wholly conjugated and are at best poorly conductive, they contain groups capable of undergoing oxidation and reduction reactions, such as ferrocene groups seen in Figure 5.

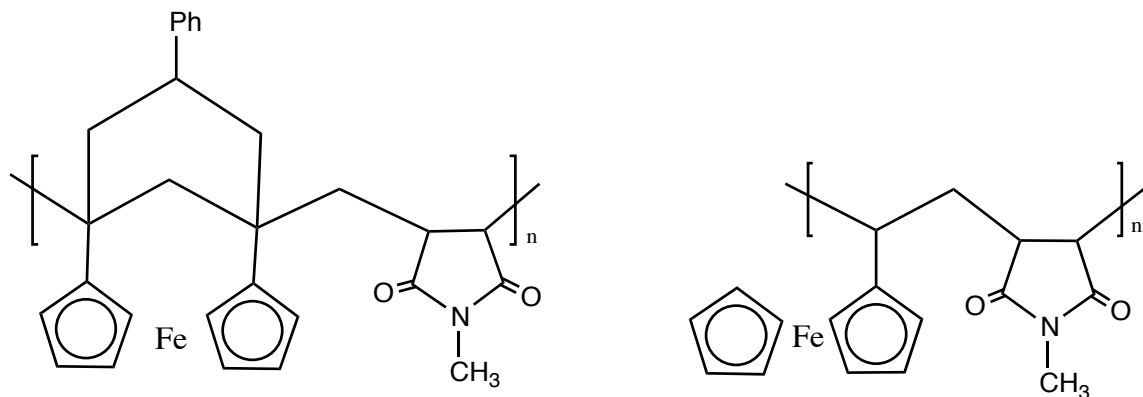


Figure 5. Redox-active polymers.

The redox-active groups can be contained within the main chain or pendant to the main chain.¹⁷ The ability of these polymers to undergo redox reactions in the presence of chemical or electrochemical oxidizing/reducing reagents has led to the study of redox-active polymers as sensors for a variety of chemical and biological analytes.^{18,19}

Oxidative Polymerization

To produce conducting polymers, oxidative polymerization can be performed in the presence of an electrolyte, either electrochemically or chemically (Figure 6).^{20,21} When the oxidizing agent removes an electron from the monomer, polymerization begins. A radical cation is produced and can then proceed to react with another radical cation molecule or an unreacted monomer molecule to form a dicationic dimer or a radical cationic dimer, respectively. During radical-radical coupling, the unpaired

electrons form a bond, leaving the dicationic dimer. Upon reacting the radical cation with the monomer molecule, a radical cationic dimer is produced, which can lose a second electron to form a dicationic dimer. Once the dicationic dimer has been produced through either method, it will proceed to lose two protons to form a neutral dimer. This process will continue to repeat, forming the wanted polymer.

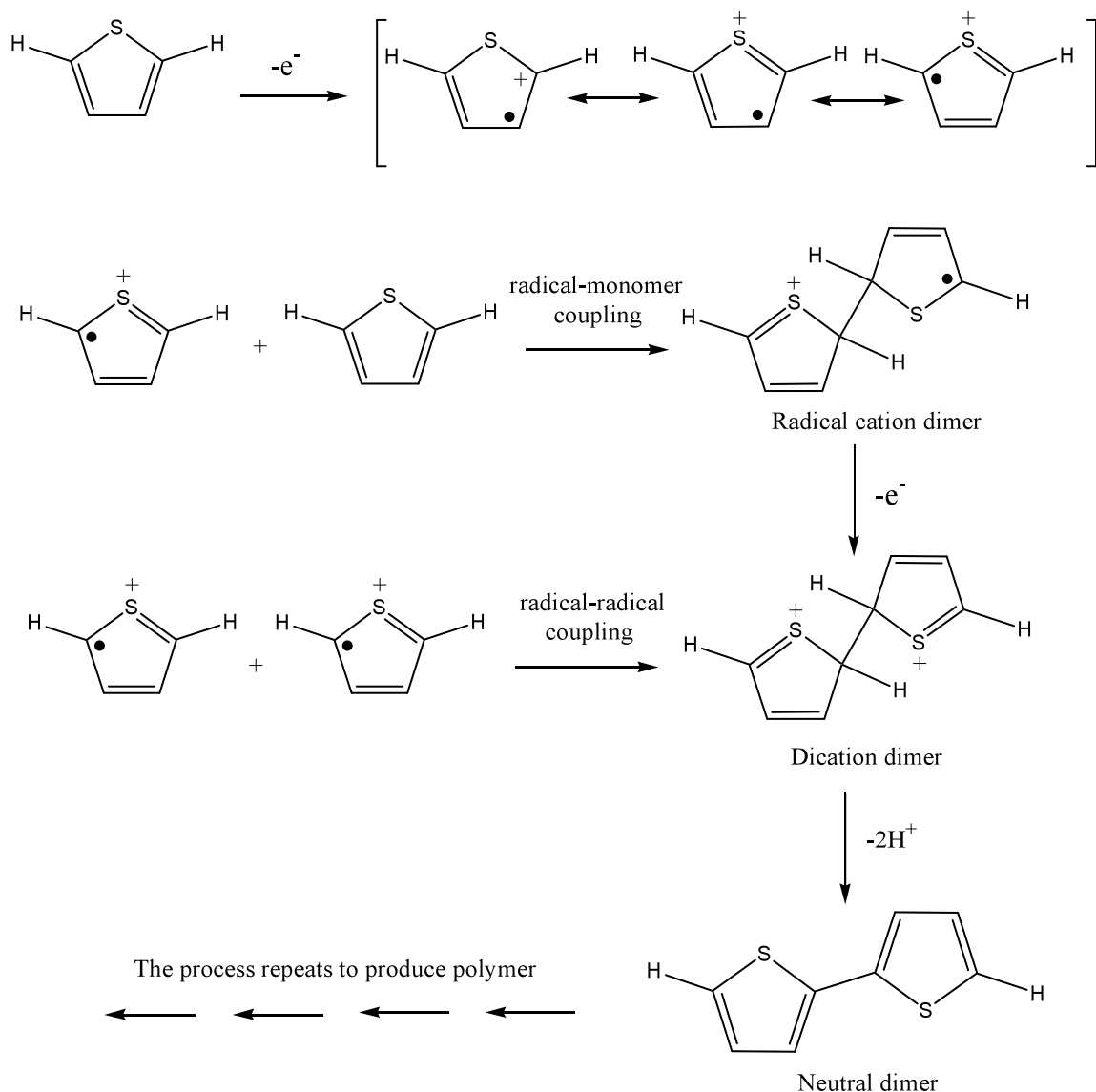


Figure 6. Oxidative polymerization of thiophene.

Using electrochemical polymerization, the potentials can be conveniently controlled preventing any potential side reactions. When chemical oxidants are used, that control is lost, and the monomer and polymers can undergo detrimental, irreversible oxidation processes (over-oxidation), producing materials with inferior electronic properties.²² For understanding the reduction and oxidation processes, cyclic voltammetry becomes instrumental. With the electroactive monomers and respective polymers, the electrochemistry is intricate; for ease of understanding, it is easiest to start with a discussion of electrochemistry of freely diffusing molecules and their associated reversible redox processes before moving on to a discussion of the electrochemistry of insoluble polymers.

Cyclic voltammetry (CV) is a process in which a potential is applied to the working electrode from a potentiostat, creating a measurable current response. A conventional three-electrode cell, containing working, reference, and counter electrodes, is depicted in Figure 7. Redox processes of the analyte occur at the working electrode, which is typically a conductive, unreactive species such as platinum, gold, or glassy carbon. The counter electrode is a suitably large piece of metal (such as platinum) that can be used as an electron source or electron sink. The reference electrode may be something with relatively well-controlled electrochemistry, such as the Ag/Ag^+ electrode, or it may be something less consistent, such as a silver wire, in which case it is referred to as a pseudo-reference electrode. Pseudo-reference electrodes are convenient for comparing electrochemistry in a variety of electrolytes, and they are relatively small and easy to use. However, use of a pseudo-reference electrode requires subsequent electrochemical experiments using a well-understood redox reaction such as the

ferrocene/ferrocinium (Fc/Fc^+) couple.²³

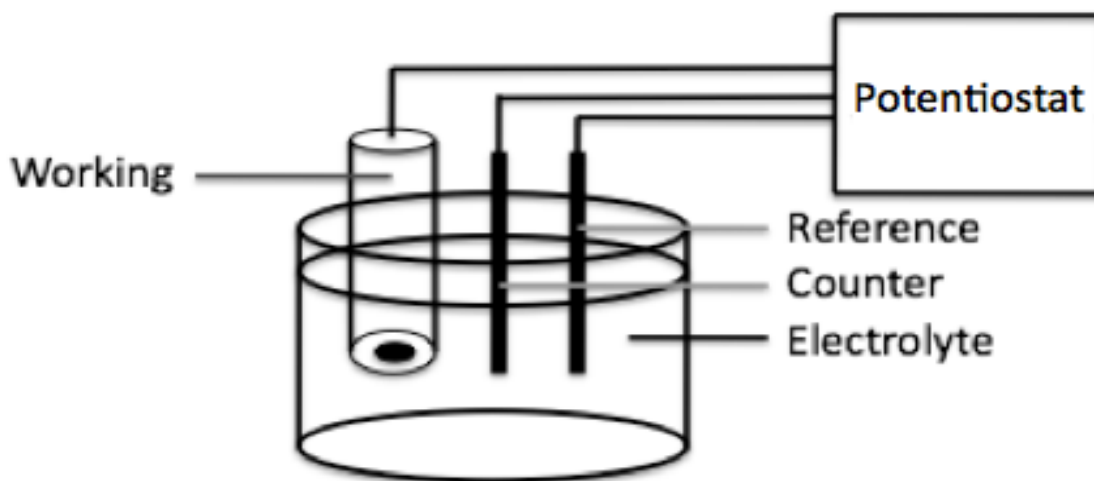


Figure 7. Electrochemical cell.

To transfer current and to balance generated charges during the electrochemical process, a supporting electrolyte is introduced. Ionic liquids such as 1-ethyl-3-methylimidazolium bis(trifluoromethylsulfonyl)imide (EMIBTI), and 1-butyl-1-methylpyrrolidinium bis(trifluoromethylsulfonyl)imide (BMPBTI) show great electrochemical and thermal stability and are not as volatile as organic electrolyte solutions providing a good alternative to the traditional electrolytes (Figure 8).²⁴ Additional electrolytes used are also depicted in Figure 8.

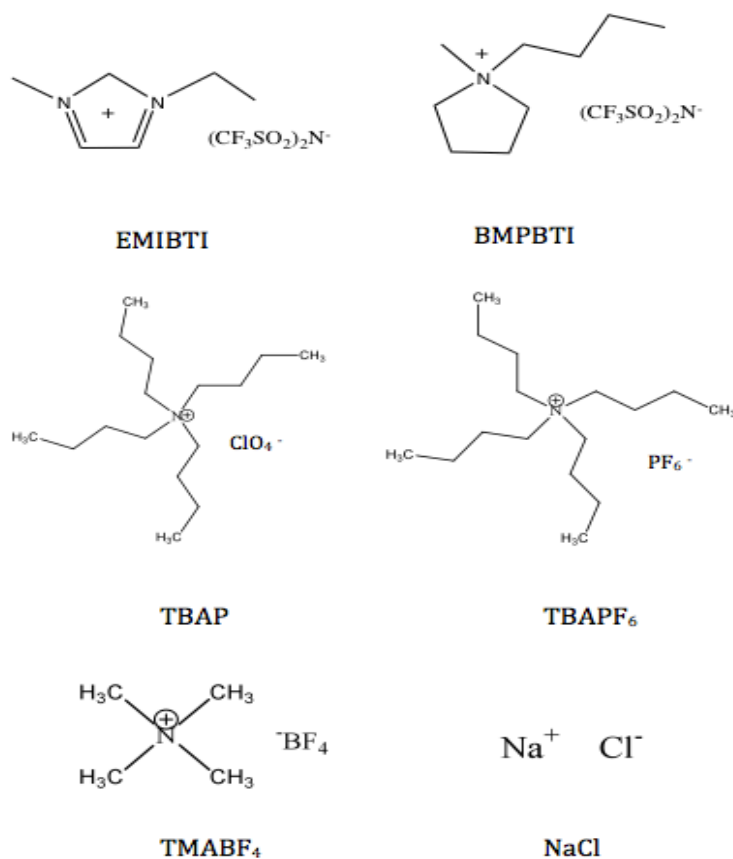


Figure 8. Electrolytes: 1-ethyl-3-methylimidazolium bis(trifluoromethylsulfonyl)imide (EMIBTI), 1-butyl-1-methylpyrrolidinium bis(trifluoromethylsulfonyl)imide (BMPBTI), Tetrabutylammonium perchlorate (TBAP), Tetrabutylammonium hexafluorophosphate (TBAPF₆), Tetrabutylammonium tetrafluoroborate (TMABF₄), and Sodium chloride (NaCl).

With increasing potential of the working electrode (anodic scanning), freely diffusing species that are electroactive are oxidized, in turn producing a current response which decreases as the reduced species' concentration decreases near the working electrode.²⁶ When the highest potential is reached, the direction of the scan is reversed (cathodic scanning), causing the oxidized species to become reduced. When this reduced species is near the working electrode the current response will increase, and when the

reduced species diffuses away from the electrode the current response will decrease. The current at the peak potential can be identified using the Randles-Sevcik equation given by:

$$i_p = (2.69 \times 10^5) n^{3/2} A D^{1/2} C^b v^{1/2} \quad (\text{Equation 2})$$

where i_p is the peak current, n is the number of transferred electrons, A is the electrodes surface area (cm^2), D is the diffusion constant ($\text{cm}^2 \text{s}^{-1}$), C^b is the bulk concentration (mol cm^{-3}) and v is the scan rate (V s^{-1}).^{25,26} Therefore, peak current is directly proportional to the square root of scan rate in a diffusion controlled system.

For electroactive polymer electrochemistry there are slight differences. An irreversible process is observed during the polymerization of electroactive monomers when the monomer diffuses to the electrode surface with an applied potential. Once diffused to the electrode surface, the monomer is irreversibly oxidized creating an electroactive polymer film. In most cases, the polymer is insoluble in the electrolyte solution and is adhered to the electrode.

To continue studying the electroactive polymer deposited on the working electrode, all of the monomer must be removed to prevent further oxidative polymerization, isolating the polymer redox process(es). Due to the immobilization of the polymer on the electrode surface, the semi-reversible redox process is not observed; therefore the process is not diffusion controlled. Instead of the Randles-Sevcik equation applying, the theory for surface immobilized redox centers applies for the peak current and is shown by:

$$i_p = \frac{n^2 F^2 \Gamma v}{4RT} \quad (\text{Equation 3})$$

where i_p is the peak current, n is the number of transferred electrons, F is Faradays constant (96,485.3365 C/mol), and Γ is the amount of reactant initially present at the electrode surface.²⁶ For the surface immobilized species, the peak current is shown to be linearly dependent on scan rate. A comparison of Equations 2 and 3 reveals that an evaluation of the effect of scan rate on current response can reveal whether an electrochemical process is diffusion controlled or whether the polymer is well-adhered to the surface of the working electrode.

The electron density of the monomer plays a large role in how well it can be oxidatively polymerized. When there is an increase in electron density, there is a decrease in oxidation potential due to stabilization of the cations, formed during oxidation, from the electron donating groups.²⁷ Electron accepting groups contain atoms that are more electronegative than carbon, so acceptors can better stabilize the negative charges created during the n-doping process. Electron rich (donor) groups, such as thiophene rings, are readily oxidized, but cannot stabilize a negative charge well making them unsatisfactory for n-doping. Groups containing more electronegative atoms than carbon (acceptors) can stabilize negative charges well, making them good for n-doping, however, they are hard to oxidize. It has been found that monomers with a donor-acceptor-donor (D-A-D) structure can be oxidized relatively easily but are still able to stabilize negative charge.²⁸ Thus, implementing the D-A-D approach will be beneficial in the preparation of electrochemically polymerized n-doping polymers.

Using a working electrode, a polymer coating can be obtained by applying a voltage to a monomer solution via electropolymerization. A catalyst is not necessary for the production of the rapidly grown conducting polymer. With the ability to control film thickness and polymer placement, electropolymerization can be beneficial for practical applications.²⁸ Limitations for electropolymerization are largely due to the costly instrumentation as well as the time necessary to perform the polymerization restricting the commercial utility of the process.²⁸ Electrochemical polymerization will not occur for electron deficient monomers with high oxidation potentials.

Chronoamperometry

Chronoamperometry is an electrochemical technique in which the potential of the working electrode is stepped for a given period of time and the current response, caused by a faradic process at the electrode surface, is plotted versus time.²⁹ A high charging current is produced during chronoamperometry which exponentially decays over time. This decay, described below by the Cottrell equation, is caused by the faradaic current created by electron transfer.³⁰ To begin the experiment, an induction period is set with given parameters, for a brief amount of time to allow the cell to equilibrate. Once the induction period has finished, the forward step period begins where the working electrodes potential is stepped to a predetermined potential for a set amount of time to allow the polymer to deposit onto the electrode. After the polymer has been deposited, a relaxation period occurs, holding the potential of the working electrode at the initial

potential for a short period of time. At this point, current is plotted as a function of time producing a chronoamperogram and allowing further analysis of the polymer in monomer-free electrolyte.

Diffusion coefficients for each CME's were determined utilizing the Cottrell equation given by,

$$Q = 2zFAC\left(\frac{Dt}{\pi}\right)^{\frac{1}{2}} \quad (\text{Equation 4})$$

where Q is the consumed charge obtained from a Cottrell Plot in Coulombs (Figure 9) for each individual polymer, z is the charge transfer from the polymer by chloride ion incorporated during oxidation ($z = 1$), F is Faraday's constant ($96,485 \text{ C mol}^{-1}$), A is electrode surface area (cm^2), C is concentration (mol cm^{-3}), D is linear diffusion coefficient ($\text{cm}^2 \text{ s}^{-1}$), and t is time (s).^{30,31}

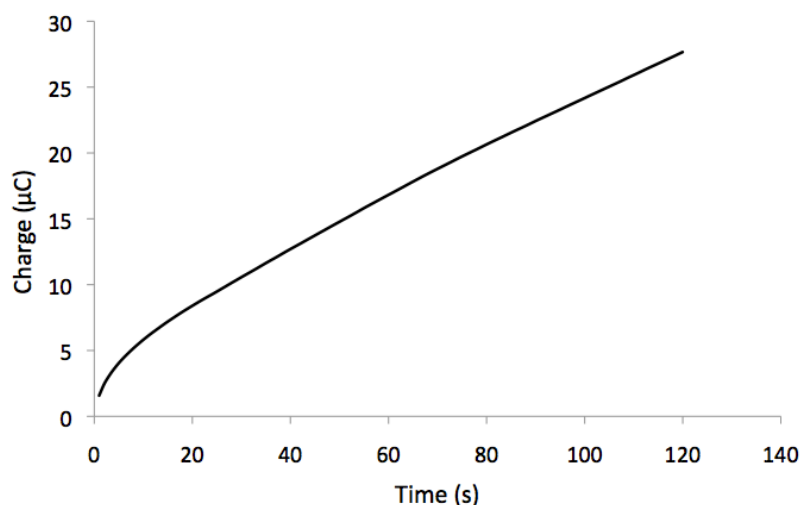


Figure 9. Cottrell Plot for 0.01 M ferrocene-containing copolymer 2A. Parameters: induction period: 0 V for 15 seconds, forward step period: 0.5 V for 120 seconds, and relaxation period: 0.5 V for 120 seconds.

Applications

Electrochemical Capacitors (EC's)

The electrochemical capacitor (EC) is a charge storage device in which electrical energy is stored via oxidation and reduction of redox-active materials such as polymers, carbonaceous materials (such as graphite, fullerenes, or amorphous carbon), or metal oxides.³² Two electrodes are constructed from redox-active materials on opposing sides of an organic or aqueous electrolyte solution.³²

To charge the capacitor, a voltage bias is applied, oxidizing or reducing the redox-active materials. To compensate for the charges formed during the redox process, ions from the electrolyte shift in the direction of the electrodes, the cathode becomes negatively charged while the anode becomes positively charged. Utilizing EAPs as the electrodes creates the ability for charge to be stored throughout the entire material, creating greater storage capacity, rather than at the electrolyte/electrode interface.³³

Light-Emitting Diodes (LED's)

Light-emitting diodes (LED's) are illumination devices created through rapid decay of excited molecular states.³⁴ The difference in energy between the excited and ground state depicts which color is observed. LED's have been used in many electronic devices such as televisions, radios, cell phones, calculators, digital cameras and watches.^{35,12} The most common form of LED is the organic light-emitting diode (OLED), which utilizes a multi-layer design sandwiching the organic semiconductor material, between the cathode and a transparent anode (Figure 10). The organic molecules show electrical conductivity due to the delocalization of pi electrons, which is

a result of conjugation throughout all/part of the molecule.³⁶ To perform, a voltage is applied over the OLED giving the anode and cathode a positive and negative charge respectively. With an applied voltage to the electrodes, holes (positive charges) are injected into the electron-blocking layer (EBL) while electrons are injected into the hole-blocking layer (HBL). When the holes and electrons intersect, excitons are created which emit photons, light, as they begin to decay to the ground state in the emitting layer (Figure 10).³⁷ The EBL and emitting layers can be combined with a p-doped EAP that emits, or the HBL and emitting layer can be combined with an n-doped emissive EAP.

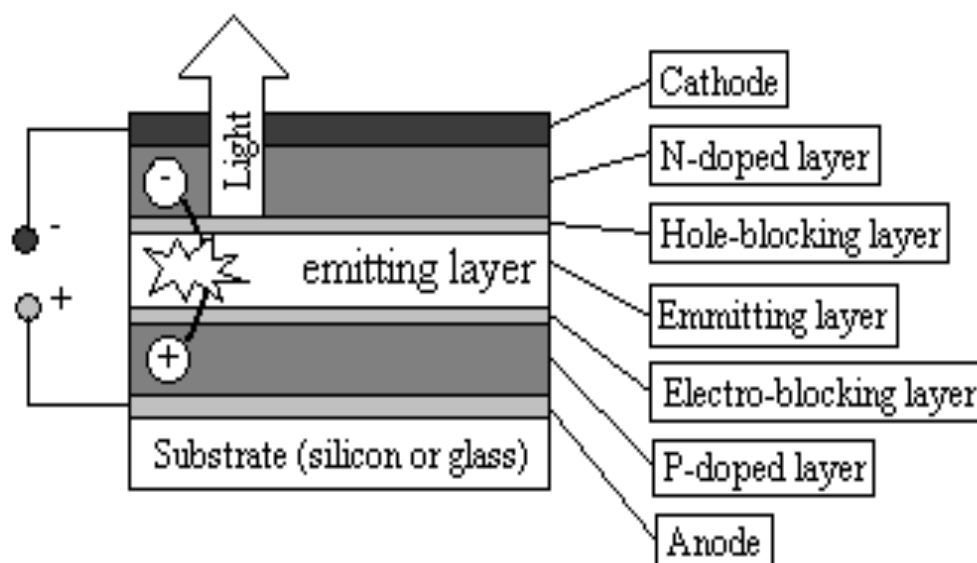


Figure 10. Depiction of light emitting diode (OLED).³⁷

A commonly seen anode is indium tin oxide (ITO), which is transparent and drives injection of holes into the HOMO level of the organic layer. Additionally, metals

are utilized as cathode materials to promote injection of electrons into the LUMO of the organic layer. Eliminating layers, by substitution of a single polymer film, could simplify the process.

Polymer Solar Cells (PSC's)

Polymer solar cells (PSC's), a type of photovoltaic device, produce energy from light, following a reverse process of LED's. Excitons, or photoexcited electron hole-pairs, are created through an absorptive layer being struck by photons of visible light. At the donor-acceptor interface, the excitons are divided into holes and electrons. The holes are transferred across the donor material to be collected at the cathode while the electrons are transferred across the acceptor material to the anode. Radiative recombination is prevented by a short transfer time of excitons.⁷

Recent research on PSC's is largely focused on the search for more efficient materials.^{7,38} Electron acceptors such as fullerene derivatives are currently in use for most bulk heterojunction PSC's, but efficiencies are poor, driving the search for better materials.^{39,40} EAPs are commonly used as the hole transport and absorptive layers in many PSC's. Stable n-doping EAPs could replace fullerenes as acceptors in PSC's. Ideally, to enhance the photocurrent, the polymeric material should obtain a broad, high absorbance.⁴¹ Through increasing charge transport capabilities, charge separation can be accomplished by tuning the band gap of the polymer.¹³ For donor polymers a high band gap is preferred whereas with an acceptor polymer a low bandgap is preferred.⁴² With rapid charge transport, a thicker absorptive layer can be formed, increasing the photocurrent as well.⁴³

Motivation for Research

The demand for stable n-doping polymers for use in EC's, LED's, and PSC's has necessitated research into novel n-doping polymers with improved electrochemical stability. It appears that the donor-acceptor-donor approach is the most promising path to stable n-doping polymers. Our research group has focused its efforts in this area to the synthesis of high nitrogen heterocyclic acceptor units flanked by thiophene- and EDOT-based donor units. Other members of the Irvin Research Group have synthesized a variety of D-A-D monomers (Figure 11) to explore the effectiveness of various acceptor groups. The research described herein is focused on characterizing the electrochemical and spectroelectrochemical properties of these monomers and the polymers prepared from them.

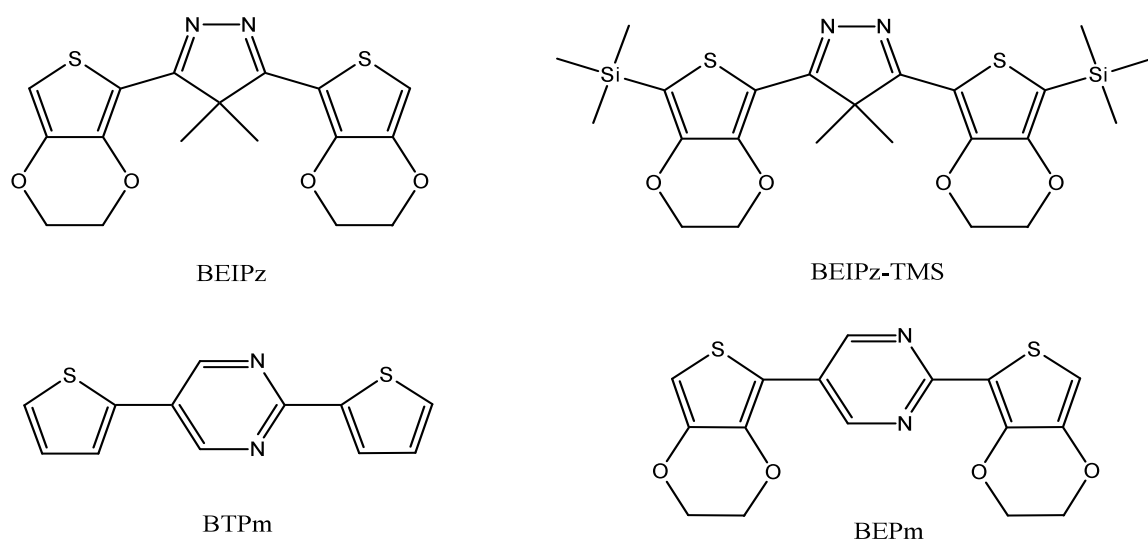


Figure 11. Monomers of interest.

Cyclic voltammetry was used to electrochemically polymerize the monomers shown in Figure 11. A variety of electrolytes, counter electrodes, and potential windows were explored for polymerization. After polymerization, polymer electrochemistry was studied to determine the effect of the different donor and acceptor groups on electronic properties. Both p-doping and n-doping processes were studied for all the polymers. Spectroelectrochemistry was also employed to determine the optical band gaps of the polymers.

A series of high molecular weight ferrocene-containing redox-active polymers was electrochemically characterized using cyclic voltammetry and chronoamperometry for both soluble and surface-immobilized polymers. These polymers were derived from various N-substituted maleimides with ferrocenophane or vinylferrocene (Figure 12). The resulting copolymers were studied in aqueous media, as prepared by Dr. Charles Neef, providing insight into the development of solution cast amorphous films. In aqueous sodium chloride solutions, oxidative electrochemical deposition produced films with satisfactory redox activity making these copolymers good targets for use as chemically modified electrodes that can eventually be utilized as sensors.

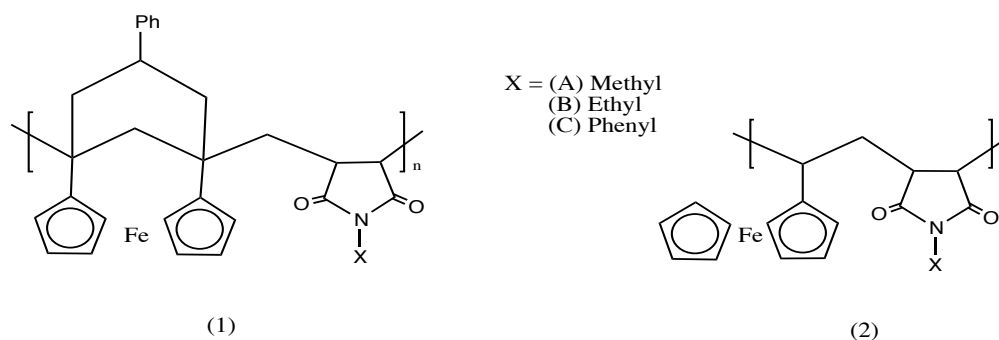


Figure 12. Various copolymers of interest derived from (1) ferrocenophane and (2) vinylferrocene with various N-substituted maleimides.

CHAPTER II

ISOPYRAZOLES

Background

Bisarylisopyrazoles show promise as donor-acceptor-donor materials because of their ability to increase stability of n-doping polymers. The previously reported 3,5-bis(thien-2-yl)isopyrazole (BTIPz, Figure 13) showed reasonably stable n- and p-doping processes although its high oxidation potential limited possible use.¹⁶ The introduction of ethylenedioxy substituents to thiophene-based monomers has been shown to reduce monomer and polymer oxidation potentials.⁴⁴ To that end, the ethylenedioxy-substituted analogue to BTIPz was prepared by another member of the Irvin Research Group.⁴⁶ The new monomer, 3,5-bis(3,4-ethylenedioxythien-2-yl)isopyrazole (BEIPz, Figure 13) was found to decompose during purification. Modification of the precursor with trimethylsilyl protecting groups produced a more stable molecule (BEIPz-TMS, Figure 13).

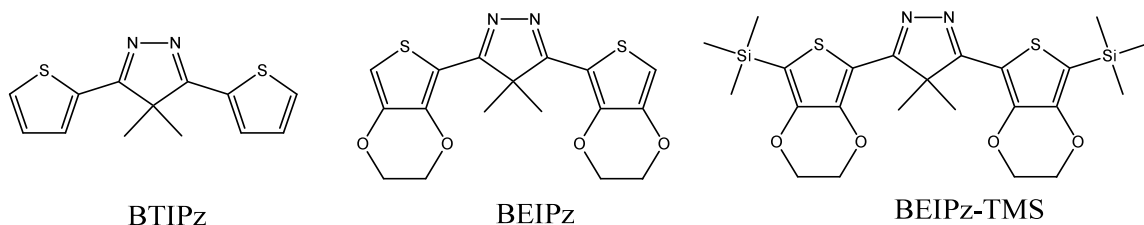
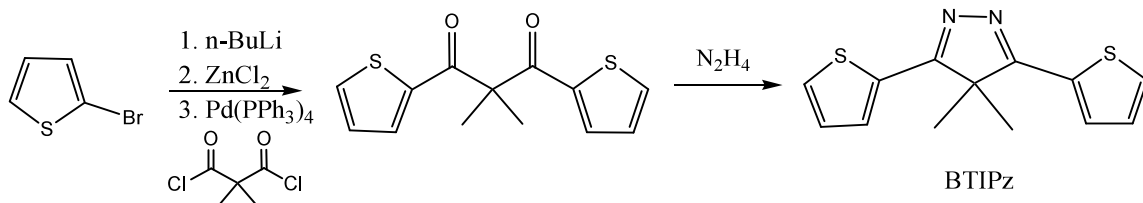


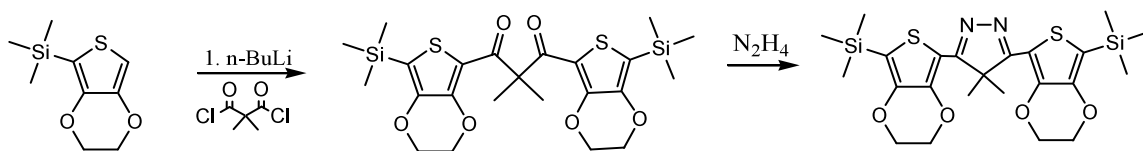
Figure 13. Depiction of synthesized monomers BTIPz, BEIPz, and BEIPz-TMS.

The isopyrazole, (BEIPz, Figure 13), another D-A-D monomer synthesized by another graduate student, Katie Winkel, used a reaction similar to the one used to prepare BTIPz (Figure 13).¹⁶ For BTIPz, 2-bromothiophene was used to couple with dimethylmalonyl chloride, with the bromine used to ensure coupling only occurred at the 2-position of the thiophene (Scheme 1).



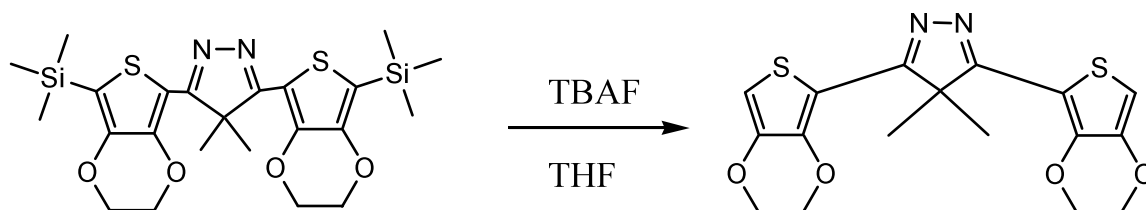
Scheme 1. Synthesis of BTIPz.

Coupling of 3,4-ethylenedioxy-2-trimethylsilylthiophene with dimethylmalonyl chloride was accomplished via nucleophilic acyl substitution of the acyl chloride with the lithiated species (Scheme 2). Functionalization of EDOT with the trimethylsilyl (TMS) group proved necessary; without the TMS group, side reactions and decomposition proved problematic, likely due to the low oxidation potential of EDOT-containing monomers.⁴⁵ This procedure simplified purification while also improving stability of the resultant monomer precursor (BEIPz-TMS, Figure 13, Scheme 2).



Scheme 2. Synthesis of BEIPz-TMS.

It was possible to remove the TMS groups using TBAF to produce BEIPz (Figure 13, Scheme 3).⁴⁵ Due to this lowering of oxidation potential by the attachment of EDOT, a lower band gap was anticipated in comparison to that of BTIPz.⁴⁶



Scheme 3. Deprotection of BEIPz-TMS to form BEIPz.

Prior studies on TMS-protected monomers have been performed showing good stability in air with polymerization occurring at low oxidation potentials.⁴⁵ This chapter will cover work focused on determining the electrochemical properties of BEIPz-TMS and BEIPz.

Experimental

Materials

Acetonitrile (CH_3CN , anhydrous 99.8%) and propylene carbonate (PC, anhydrous 99.7%) were purchased from Sigma Aldrich and placed in an argon atmosphere dry box. Tetrabutylammonium fluoride (TBAF, 1.0 M in tetrahydrofuran (THF)), 3-methoxythiophene, and 2,2'-bithiophene were purchased from Acros and stored between 2°C and 8°C prior to use. Tetramethylammonium tetrafluoroborate (TMABF_4) was

purchased from Sigma Aldrich, recrystallized twice from methanol/water, and dried in a vacuum oven for twenty-four hours prior to use. Ionic liquid electrolyte 1-butyl-1-methylpyrrolidinium bis(trifluoromethylsulfonyl)imide (BMPBTI) was synthesized in the laboratory via aqueous ion exchange and purified by using column chromatography (silica gel) followed by heating with stirring under vacuum to remove residual water.^{45,47} Tetrabutylammonium perchlorate (TBAP) was purchased from Fluka and was recrystallized from acetone and dried under vacuum prior to use.⁴⁸ BEIPz, and BEIPz-TMS were synthesized in the laboratory by Katie Winkel.^{46,34}

Instrumentation

All electrochemical experiments were performed in an argon atmosphere dry box using a Pine WaveNow potentiostat. Electropolymerizations were conducted on solutions containing 0.01 M monomer and 0.1 M electrolyte in either CH₃CN or PC. The working (WE), auxiliary (CE), and pseudo-reference (RE) electrodes were a platinum or gold button electrode (0.2 cm diameter, Bioanalytical Systems Inc.), a platinum wire, and a silver wire, respectively. The potential of the silver wire electrode was calibrated using the ferrocene/ferrocinium (Fc/Fc⁺) couple.⁴⁹ Cycling of the polymer films was accomplished using monomer-free 0.1 M electrolytes (BMPBTI, TMABF₄, and TBAP) in either CH₃CN or PC.

UV-Vis spectroelectrochemistry was carried out using a Cary 100 UV-Visible Spectrophotometer with 10 mm quartz cuvettes (Fischer Scientific). BEIPz was dissolved in CH₃CN and placed in spectrophotometer for 80 seconds from 190 to 900 nm

and diluted until a peak was observed below an absorption of 5 au. Polymer growth onto an (ITO) coated glass slide (Delta Technologies, 5-15 Ω) was attempted from -1 V to 1.6 V with a silver wire counter electrode and platinum wire reference electrode over 120 scans at 100 mV/s. Excess time was allotted to observe if low concentration was a factor; however, the polymer did not adhere to the ITO-coated glass slide, creating the inability to continue with polymer spectroelectrochemistry.

Results and Discussion

Monomer and Polymer Electrochemistry

BEIPZ-TMS Electropolymerization Attempts

As was discussed previously, trimethylsilyl-protected EDOT can be electropolymerized without first removing the TMS groups.⁴⁵ Electropolymerizing BEIPz-TMS without removing TMS groups is desirable due to the questionable stability of BEIPz and the decrease in number of reactions needed to prepare an electropolymerizable monomer. Electropolymerization of BEIPz-TMS was attempted using 0.01 M BEIPz-TMS in a 0.1 M TEABF₄/PC at 100 mV/s. Repeated attempts at electropolymerizing BEIPz-TMS were unsuccessful; the polymer would not deposit on either gold or platinum working electrodes. Electropolymerization of EDOT-TMS was proposed to involve coordination to the electrode surface⁴⁵; it is possible that the added steric bulk prevents coordination so that polymerization can not occur.

TMS groups are readily removed from BEIPz-TMS by exposure to tetrabutylammonium fluoride (TBAF). While this was previously accomplished prior to electrochemical studies on BEIPz, it was hoped that it would be possible to accomplish *in situ* TMS removal by addition of TBAF during electropolymerization. To explore this possibility, TBAF (0.1 mL of a 1.0 M solution in THF) was added to a 0.01 M BEIPz-TMS /0.1 M TMABF₄/CH₃CN solution, immediately prior to electropolymerization. Electropolymerization was attempted immediately after addition of TBAF and again 30 minutes and 24 hours after addition. All attempts were unsuccessful. Changing the solvent to PC was also unsuccessful. The deprotection mechanism is thought to involve two steps.⁴⁵ In the first step, fluoride anion acts as a nucleophile and adds to the vacant silicon d orbital, causing the silicon-carbon bond to break and resulting in carbanion formation. In the second step, water is added, and the carbanion acts as a base and removes a proton from a water molecule, forming a carbon-hydrogen bond. In the case of BEIPz-TMS, this process must occur on both sides of the molecule to generate two C-H bonds, resulting in BEIPz formation (Scheme 3). It is likely that the deprotection failed due to an unavailability of water (or any acidic protons) to complete the deprotection process. Water is deliberately excluded from n-doping polymer electrochemistry experiments, because the n-doped polymers readily react with water.

BEIPz Electropolymerization and Resultant Polymer Electrochemistry

Electropolymerizations of BEIPz were performed by cycling the applied potential between -2.3 and +1.2 V vs. Fc/Fc⁺ (all potentials are vs. Fc/Fc⁺ unless otherwise

specified) in a BMPBTI/CH₃CN electrolyte solution using a platinum working electrode (Figure 14). Previous studies with the analogous thiophene monomer (BTIPz) have shown that cycling into the n-doping region of the growing polymer results in polymers with improved current response and capacities during polymer n-doping.¹⁶ The initial cyclic voltammetric (CV) scan of BEIPz showed a peak ($E_{p,m}$) at ca. +0.88 V followed by reduction to the neutral polymer ($E_{c,p}$) at ca. -0.67 V, which is typical for the polymerization of thiophene monomers. However, two additional reduction peaks were observed in the first CV scan. A reduction at -1.78 V (E_{irr}) was irreversible and was not observed in subsequent scans. An additional reduction peak (E_{n-d}) observed at -2.15 V was reversible and was consistent with n-doping of the growing polymer film. Additionally, monomer onset was observed at ca. +0.66 V. However, a loss in current from monomer oxidation was observed with each additional scan, indicating a lack of electroactivity within the growing polymer film. The lack of electroactivity may be due to the depletion of the monomer in solution. Each time monomer is consumed during oxidation to form polymer, or during the irreversible reduction process, less is available to polymerize during subsequent scans. This is normally avoided by making sure there is excess monomer available to polymerize, but in this case the irreversible reduction made that impossible.

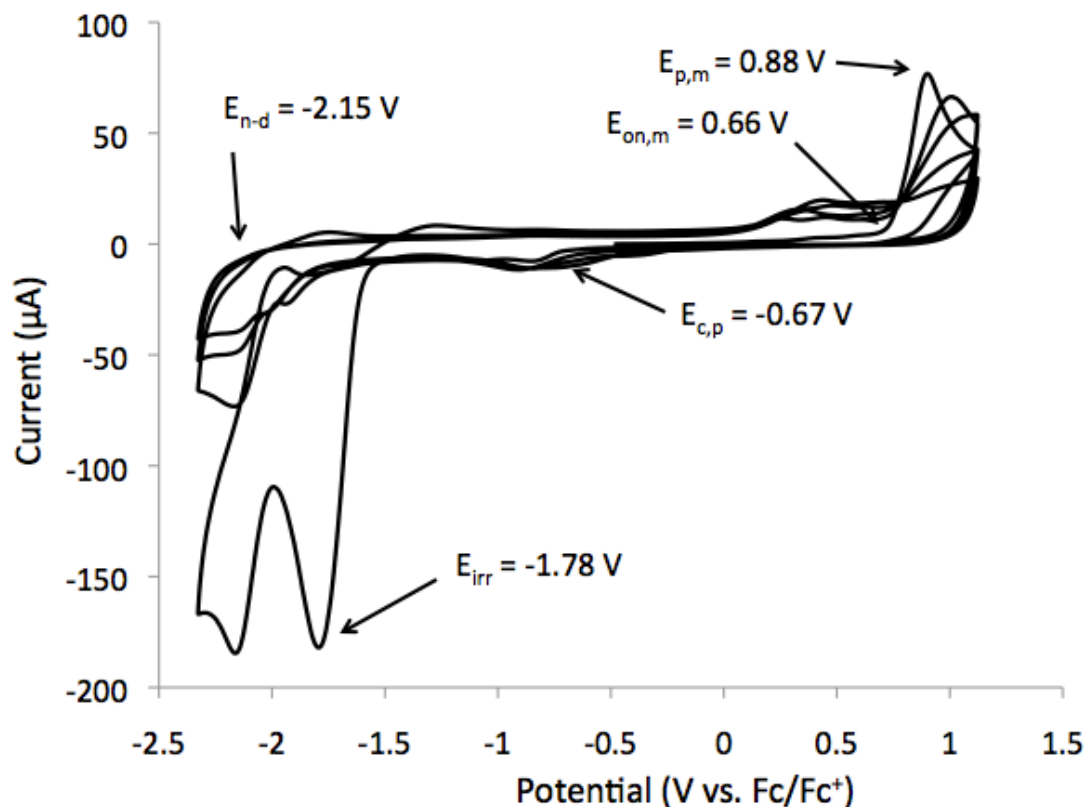


Figure 14. Electropolymerization of 0,01M BEIPz in 0.1M BMPBTI/CH₃CN at 100 mV/s for 5 cycles from -2.3 to +1.2 V. WE: Pt (0.2 cm diameter); RE: Ag wire; CE: Pt wire.

The first irreversible reduction was unanticipated. Because this process was not observed with BTIPz, it seems likely that the process was related to the incorporation of the ethylenedioxy substituent. In order to better understand this process, a similar experiment was conducted with EDOT and with 3-methoxythiophene (ThOMe). Both of these monomers also exhibited irreversible reduction processes when scanning to n-doping potentials during polymerization (Figure 15). The irreversible reduction peaks were observed at -1.95 V for both EDOT and ThOMe. In past studies, it has been found that alkali metals will reductively cleave alkyl aryl ethers.⁵⁰ It has also been found that palladium can facilitate catalytic reduction while deprotecting allyl aryl ethers.⁵¹ It seems likely that the irreversible reduction processes observed in BEIPz, EDOT, and ThOMe

are due to electrochemically induced cleavage of the alkyl aryl ethers. Cleavage of at least one C-O bond of the ether linkage could cause poisoning of the electrode and interfere with the polymerization.

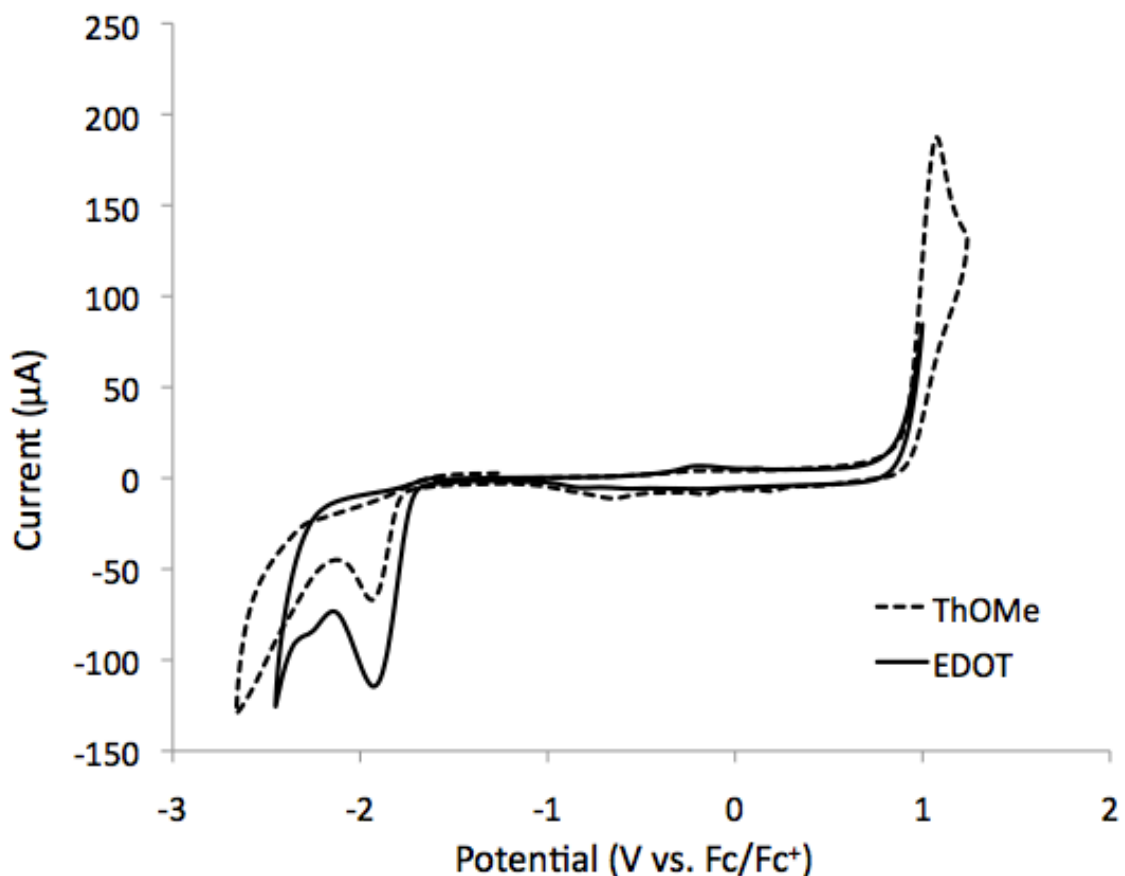


Figure 15. Electropolymerization of 0.01M EDOT and 3-methoxythiophene (ThOMe) in 0.1M BMPBTI /CH₃CN at 100 mV/s on gold working electrodes; the first cycle is shown for each electrode. RE: silver wire; CE: Pt wire.

To further confirm that this effect was limited to monomers containing ether substituents, a similar experiment was conducted with 2,2'-bithiophene. Upon cycling bithiophene to n-doping potentials, an irreversible reduction is observed (Figure 16). The initial cyclic voltammetry (CV) scan of bithiophene showed onset of monomer oxidation ($E_{on,m}$) at ca. 0.74 V and a peak ($E_{p,m}$) at ca. 0.84 V. A reduction at -1.86 V (E_{irr}) was

irreversible and was not observed in subsequent scans. This reductive process appears to be somewhat smaller than those observed for ether-containing monomers, and it does not interfere with subsequent electropolymerization (as evidenced by the increasing magnitude of the $E_{p,m}$ peak in subsequent scans rather than the decrease observed with BEIPz). It is possible that an ion trapping process is occurring with poly(bithiophene); this effect is often observed in n-doping polymers⁵² and is shown to have no effect on reproducibility of the polymer redox properties.

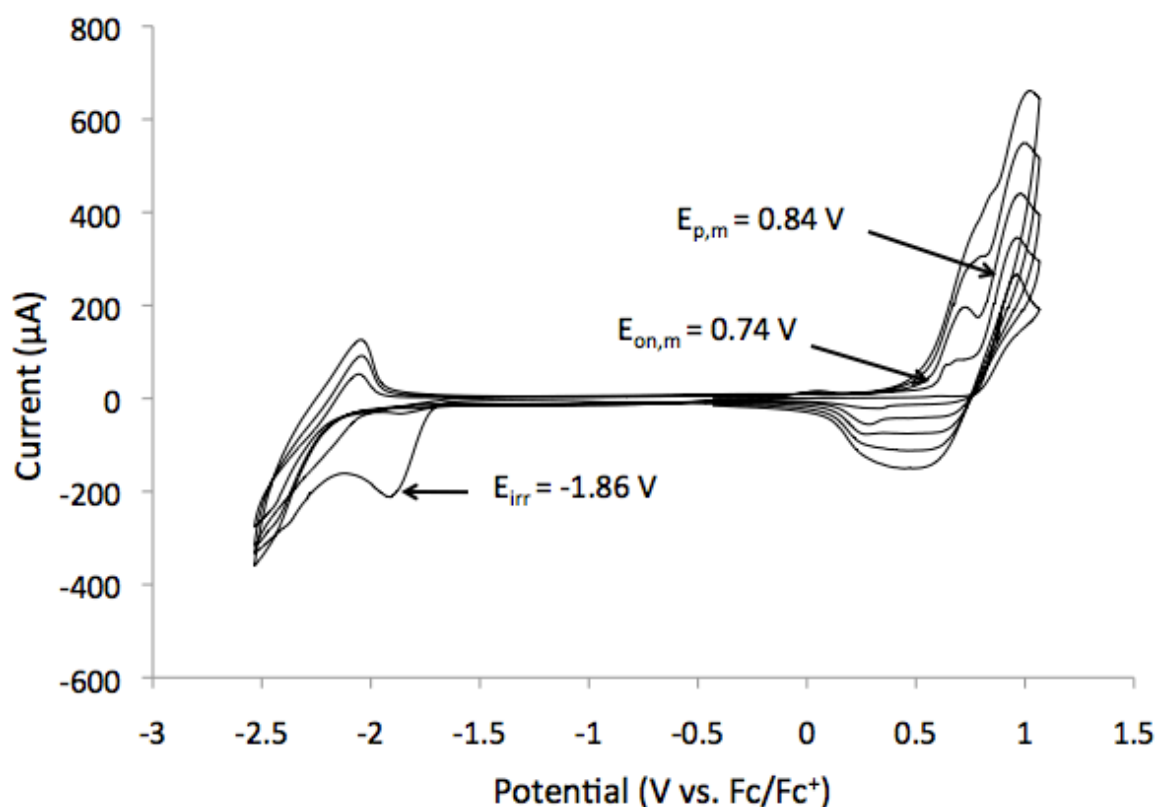


Figure 16. Electropolymerization of 0.01M bithiophene in 0.1M BMPBTI/CH₃CN at 100 mV/s for 5 cycles from -2.55 to +1.0 V. WE: Au (0.2 cm diameter); RE: Ag wire; CE: Pt wire.

Using a gold electrode irreversible reduction was not only observed during EDOT and ThOMe polymerization, but also during polymerization of BEIPz (Figure 17) when scanning from -2.35 to +1.2 V. The monomer oxidation peak can be seen at ca. +0.95 V and the monomer onset is seen at ca. +0.75 V. Two peaks have been observed in the first CV just as were seen when the platinum electrode was used. The irreversible reduction peaks at ca. -1.64 V and, as with BEIPz polymerization on a platinum electrode, is not seen in subsequent scans. A second, reversible, reduction peak was observed at ca. -1.96 V.

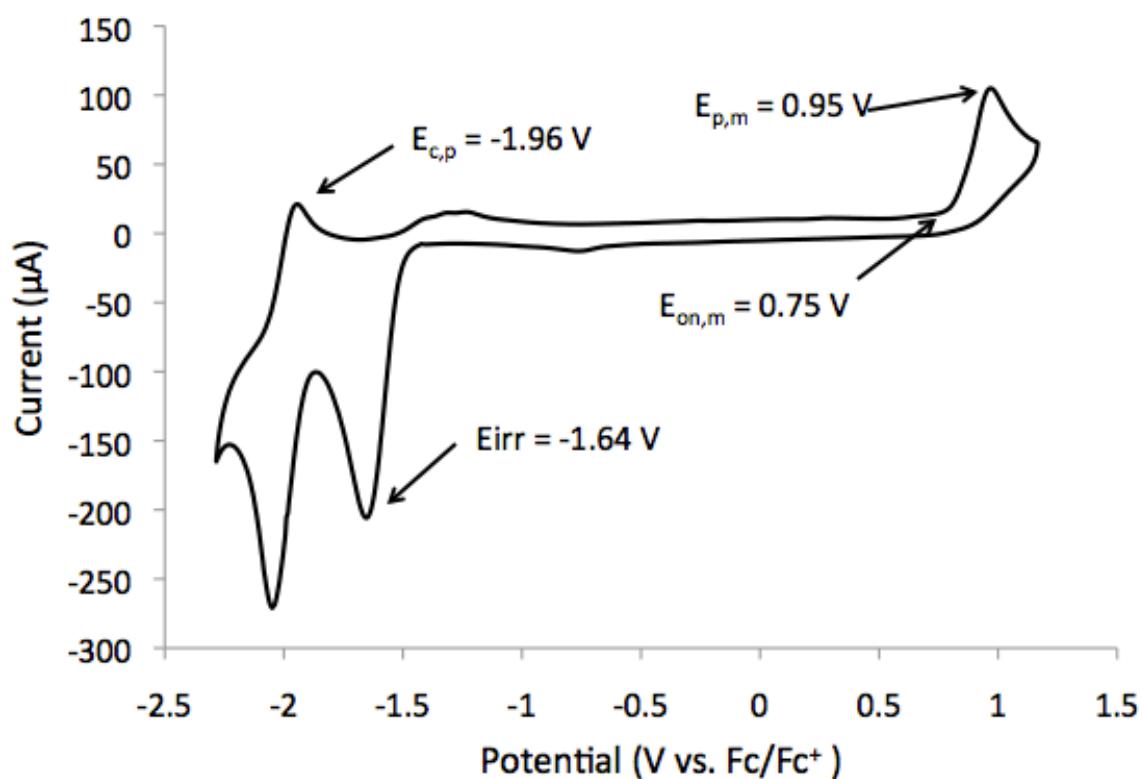


Figure 17. Electropolymerization of 0.01M BEIPz in 0.1M BMPBTI/CH₃CN at 100 mV/s for 1 cycles from -2.35 to +1.2 V. WE: Au (0.2 cm diameter); RE: Ag wire; CE: Pt wire.

In order to prevent the irreversible reduction, BEIPz was electropolymerized through repetitive cycling from -1.5 to +1.0 V (Figure 18). Monomer onset ($E_{on,m}$) is seen at 0.35 V and the monomer peak ($E_{p,m}$) is centered at 0.78 V. The electrolyte was also changed to TMABF₄ in CH₃CN, as reported by Witker and colleagues, to see if electrochemical response could be improved.¹⁶ With each scan, the current response decreases, indicating a poorly-behaved electropolymerization in comparison to the reported well-behaved electroactive BTIPz.¹⁶

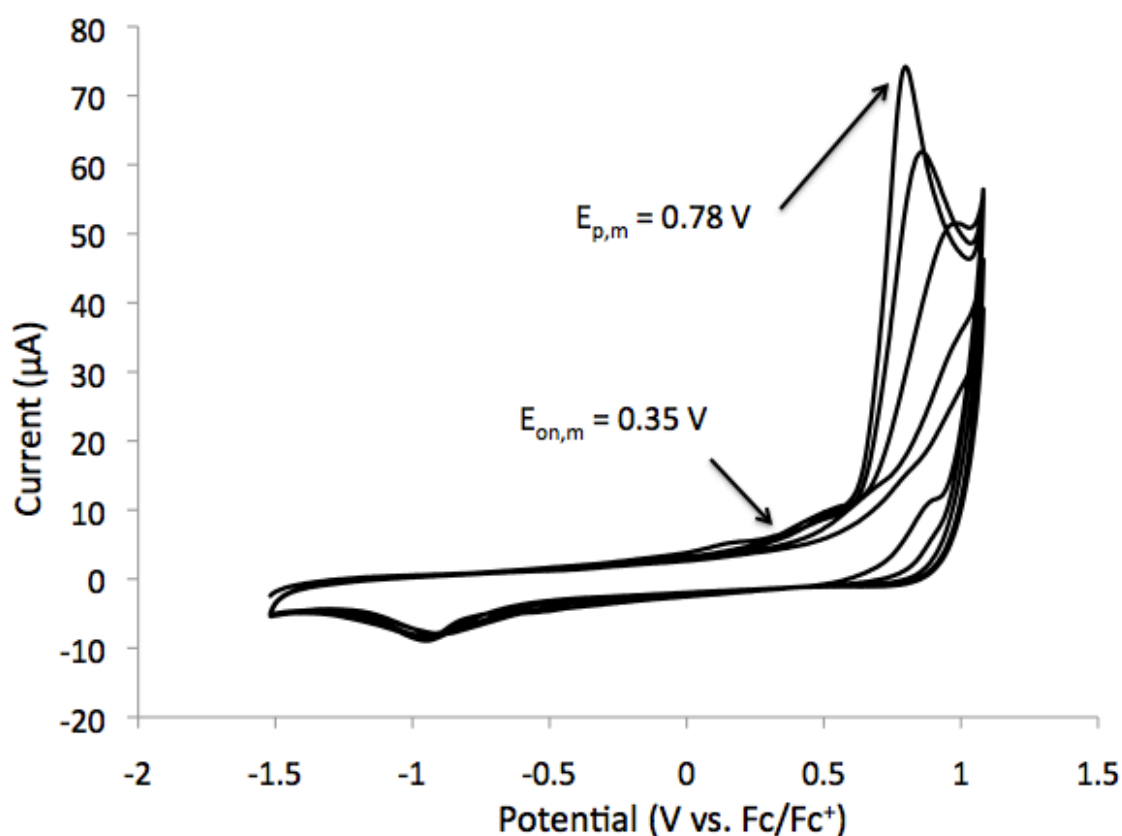


Figure 18. Electropolymerization of 0,01M BEIPz in 0.1M TMABF₄/CH₃CN at 100 mV/s for 5 cycles from -1.5 to +1.0 V. WE: Au (0.2 cm diameter); RE: Ag wire; CE: Pt wire.

The stability of the resultant polymer (PBEIPz) was tested by cycling the polymer film from -2.35 to +0.9 V fifty times in 0.1 M TMAF₄/PC as reported by Witker and colleagues, to get a greater current response and allow the polymer to become more solvent swollen in PC, providing better access to ions for the n-doping process.¹⁶ As can be seen in Figure 19, PBEIPz shows good stability, with little or no change in current response. The first scan shows lack of oxidative onset in comparison to the following scans possibly due to stabilization of the system. The n-doping process is not seen, probably due to purposely not scanning to n-doping potentials during polymerization. The reduction seen at -1.4 V to -2.4 V seems to be coupled to the initial potential oxidation scan. The first scan shows a shoulder corresponding to polymer oxidation however, this process is not seen in successive scans depicting the polymer has permanently oxidized and remains in the oxidized state. With each successive scan the reduction peak is lost as well due to the polymer becoming oxidized. With this, ion trapping can be speculated as the cause.⁵²

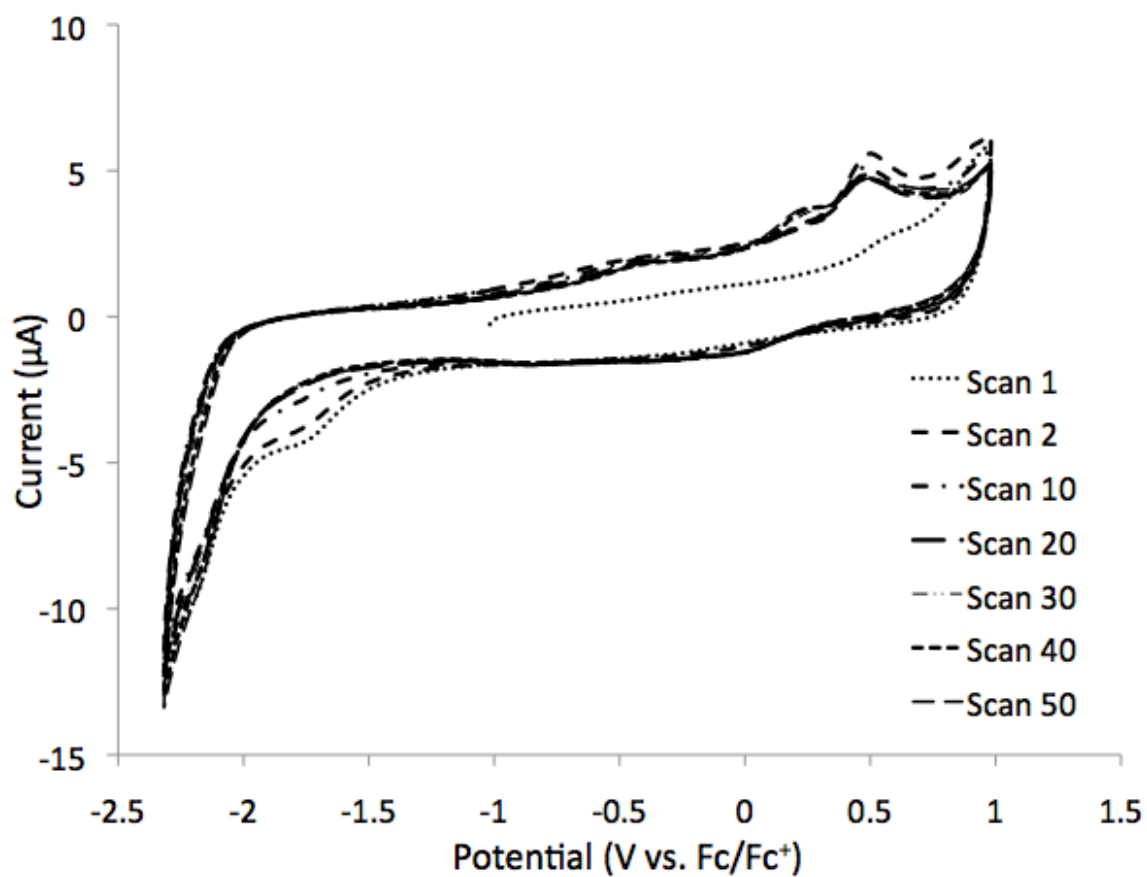


Figure 19. Cyclic voltammogram of PBEIPz in 0.1M TMABF₄/PC at 100 mV/s for 50 cycles from -2.35 to +0.9 V. WE: Au (0.2 cm diameter); RE: Ag wire; CE: Pt wire.

To compare electrolytes, 0.1 M BMPBTI/CH₃CN was used as the supporting electrolyte during another oxidative polymerization (Figure 20). The reduction process is more prominent, with a greater current response, giving an onset ($E_{on,m}$) at about 0.2 V and reduction centered at -0.9 V in comparison to that of the TMAFB₄/CH₃CN electrolyte with a reduction centered at -0.45 V (Figure 17).

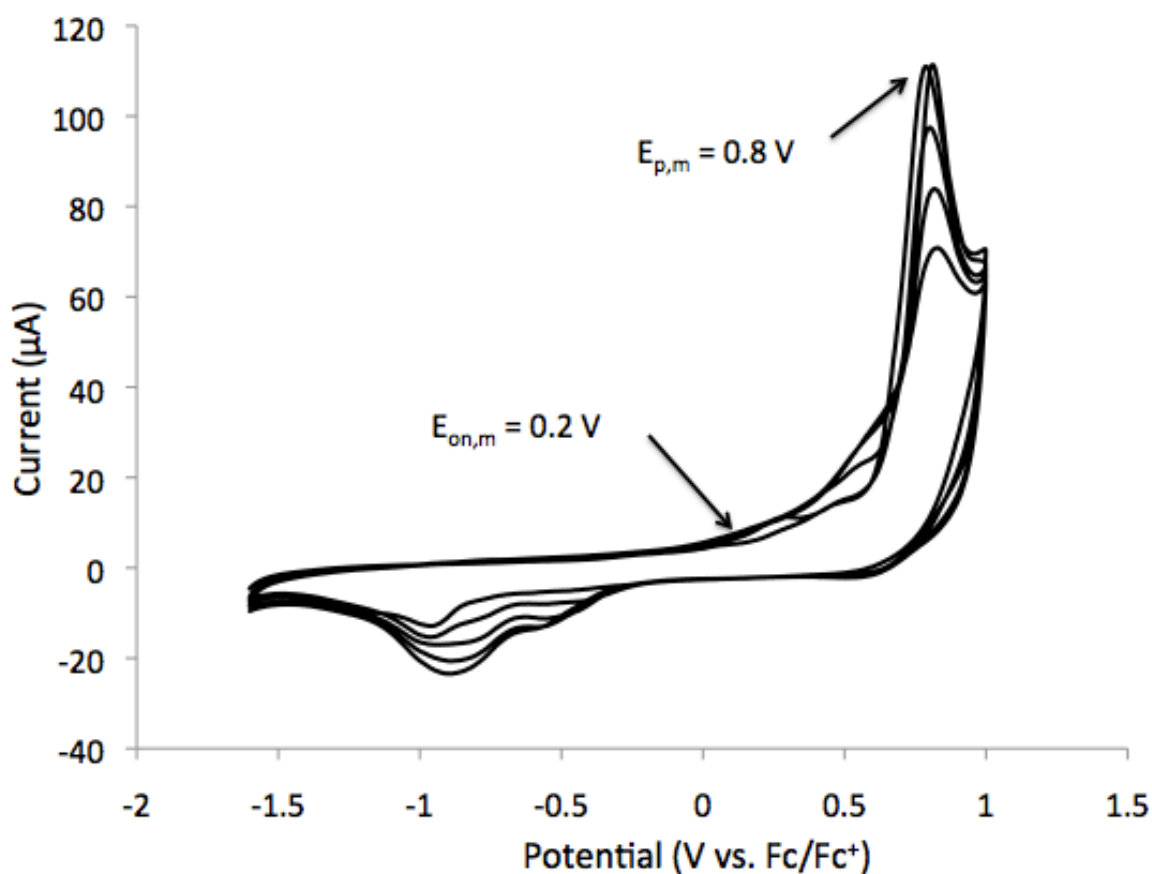


Figure 20. Electropolymerization of 0,01M BEIPz in 0.1M BMPBTI/CH₃CN at 100 mV/s for 5 cycles from -1.6 to +1.0 V. WE: Au (0.2 cm diameter); RE: Ag wire; CE: Pt wire.

To better view the polymer oxidation and reduction processes, the polymer's electrochemistry was studied in monomer-free 0.1 M BMPBTI/CH₃CN electrolyte at

100, 200 and 400 mV/s (Figure 21). It is evident that the polymer film prepared in BMPBTI/CH₃CN provides a better current response and redox process than does the film prepared in TMABF₄/PC (Figure 19). The linear dependence of current response on scan rate (Figure 21 inset) indicates that the polymer film is electroactive and adhered to the electrode.

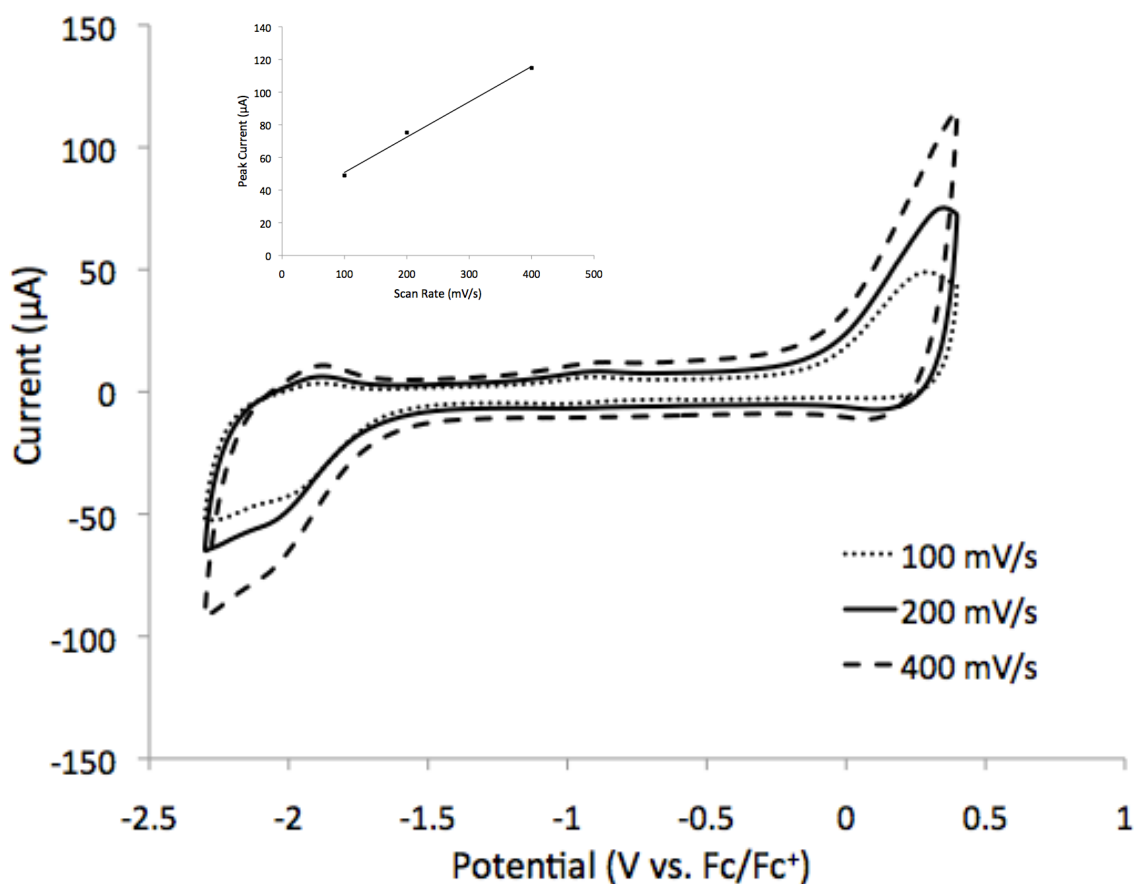


Figure 21. Cyclic voltammetry of PBEIPz grown in 0.1M BMPBTI/CH₃CN and cycled in 0.1M BMPBTI/CH₃CN at 100, 200, and 400 mV/s from -2.3 to +0.4 V. WE: Au (0.2 cm diameter); RE: Ag wire; CE: Pt wire. Inset: The linear relationship between peak current and scan rate reveals that the polymer film is adhered to the electrode and is electroactive.

Successive oxidation polymerization cycles, of 0.01 M BEIPz dissolved in 0.1 M TMABF₄/CH₃CN using a platinum working electrode, were performed from -1.6 to +1.05 V at 30 mV/s for 60 scans to provide a thicker polymer film (Figure 22). Since polymerizing to n-doping potentials shows an irreversible reduction, the smaller window was chosen. At approximately +0.84 V polymer oxidation seems to depreciate very quickly possibly due to trapped ions, as found in studies for other isopyrazole species.¹⁶ Onset of monomer oxidation ($E_{\text{on,m}}$) appears at +0.25 V.

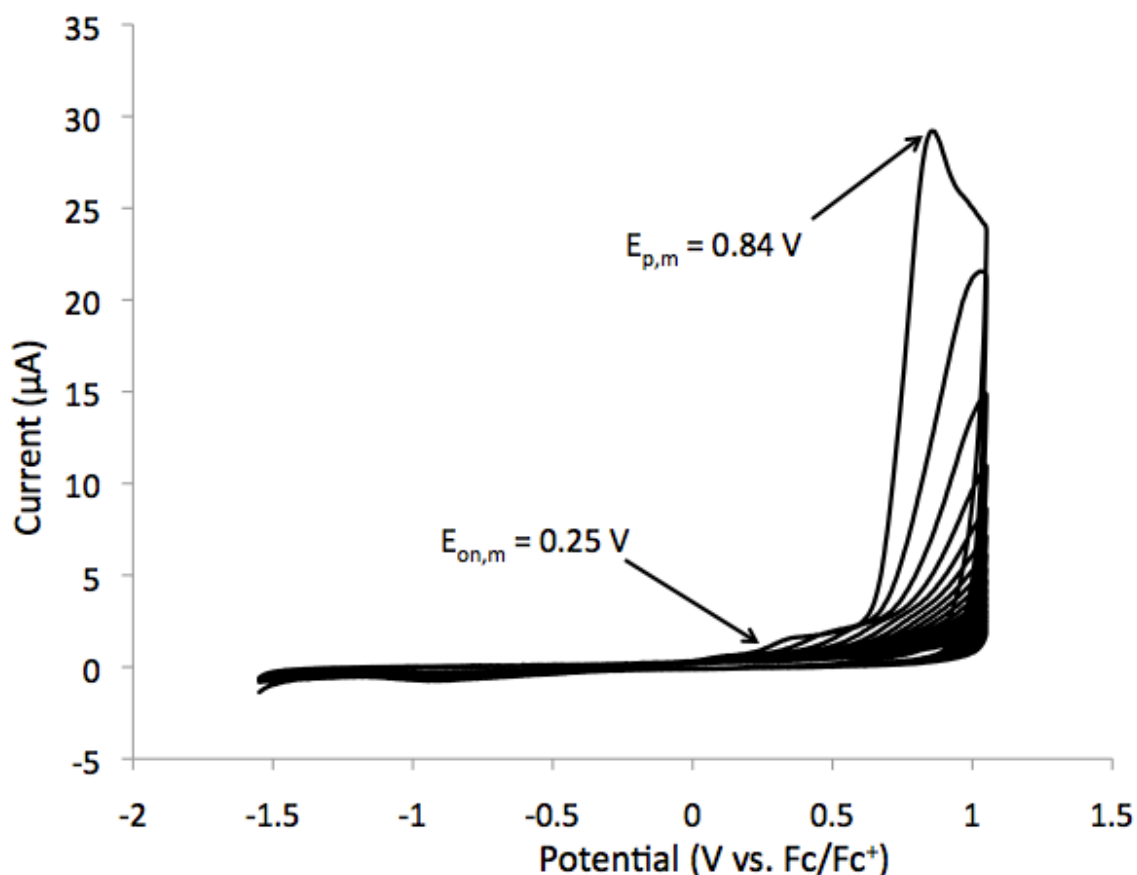


Figure 22. Electropolymerization of 0.01M BEIPz in 0.1M TMABF₄/CH₃CN at 30 mV/s for 60 cycles from -1.6 to +1.05 V. WE: Pt (0.2 cm diameter); RE: Ag wire; CE: Pt wire.

After electropolymerization, the resultant polymer (PBEIPz) film was rinsed with electrolyte and placed into 0.1 M TMABF₄/CH₃CN and 0.1 M TMABF₄/PC monomer free electrolyte solutions. Upon cycling in propylene carbonate, the n-doping process was observed to be more defined than that of cycling in acetonitrile (Figure 23). This could be due to the polymer becoming more solvent swollen in PC, providing better access to ions for n-doping.

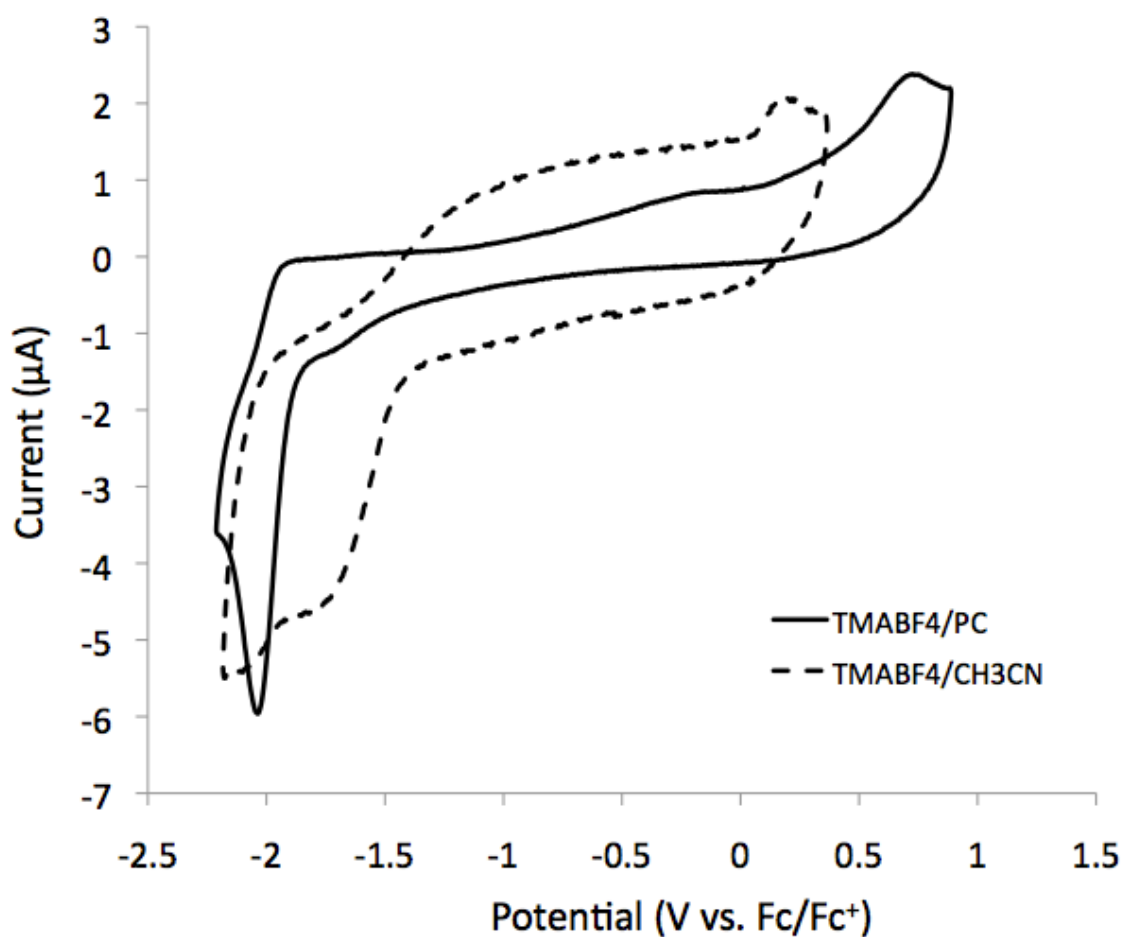


Figure 23. Cyclic voltammogram of PBEIPz in 0.1M TMABF₄/PC and TMABF₄/CH₃CN at 100 mV/s. WE: Pt (0.2 cm diameter); RE: Ag wire; CE: Pt wire.

Electropolymerization of BEIPz was also accomplished using a 0.01 M BEIPz monomer dissolved in a 0.1 M TBAP/CH₃CN solution at 100 mV/s. In CH₃CN, onset of monomer oxidation ($E_{on,m}$) can be seen at ca. +0.35 V, with a peak at approximately ca. +1.0 V (Figure 24). With the TBAP/CH₃CN electrolyte, polymer reduction and oxidation processes are more apparent ranging from -1.45 to -0.25 V and +0.35 to +0.95 V respectively.

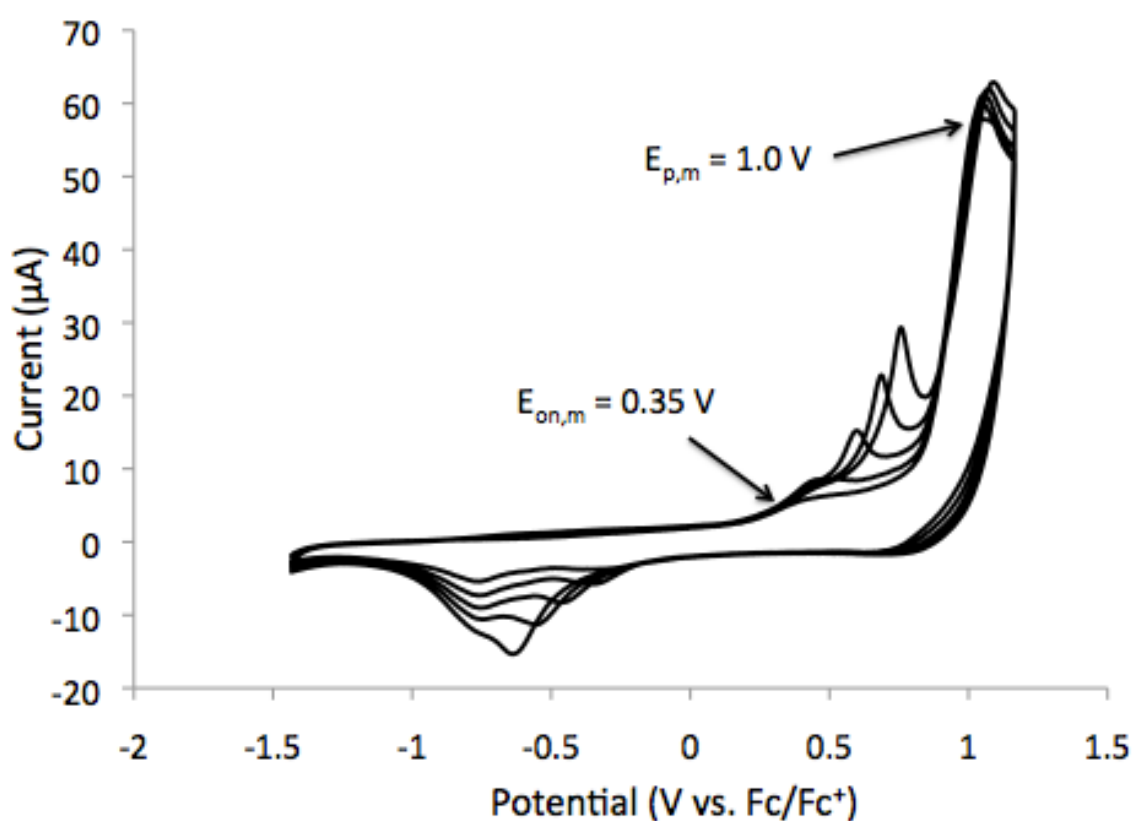


Figure 24. Electropolymerization of 0.01M BEIPz in 0.1M TBAP/CH₃CN at 100 mV/s for 5 cycles from -1.45 to +1.15 V. WE: Au (0.2 cm diameter); RE: Ag wire; CE: Pt wire.

To view the polymer oxidation and reduction processes better, the polymer's electrochemistry was studied in monomer-free 0.1M TBAP/CH₃CN electrolyte at 100,

200 and 400 mV/s (Figure 25). The linear dependence of current response on scan rate (Figure 25 inset) indicates that the polymer film is electroactive and adhered to the electrode.

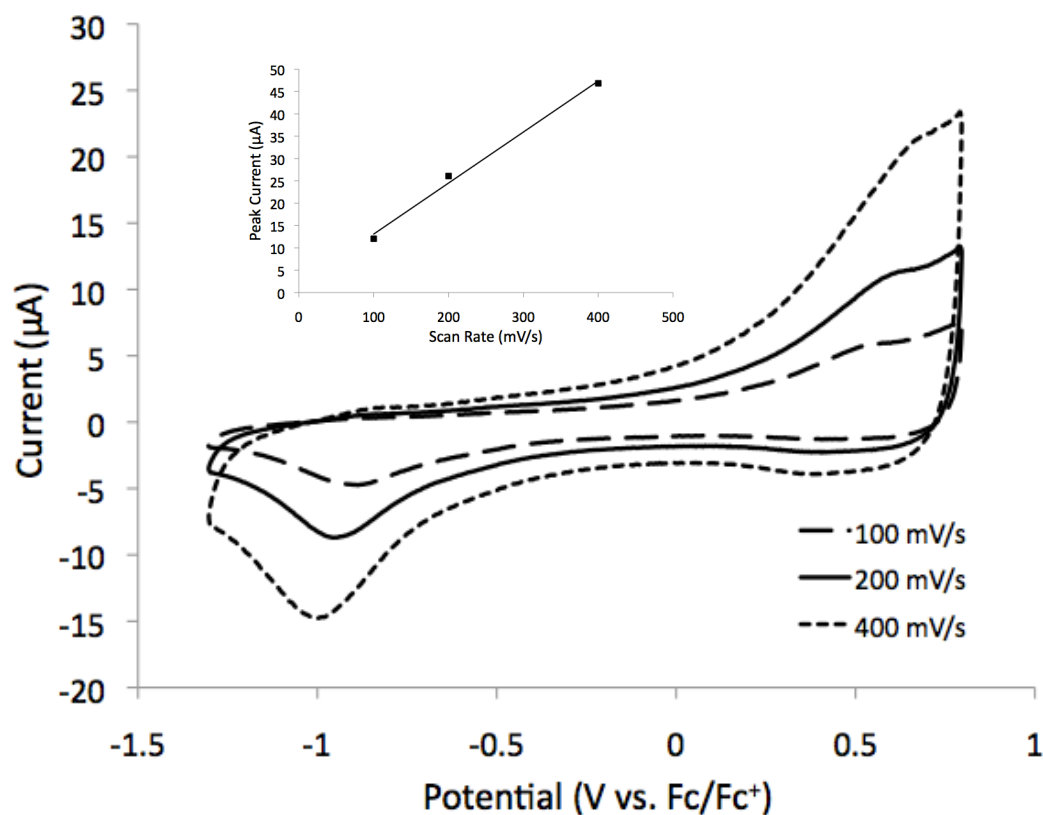


Figure 25. Cyclic voltammogram of PBEIPz in 0.1M TBAP/CH₃CN at 100, 200, and 400 mV/s from -1.3 to +0.25 V. WE: Au (0.2 cm diameter); RE: Ag wire; CE: Pt wire. The linear relationship between peak current and scan rate reveals that the polymer film is adhered to the electrode and is electroactive

To determine which electrolyte system worked better, all four electrolytes/solvent systems, BMPBTI/CH₃CN, TMABF₄/CH₃CN, TBAP/PC, and TBAP/CH₃CN were compared with PBEIPz after electropolymerization of 0.01M BEIPz in 0.1MTBAP/CH₃CN (Figure 26). Using TMABF₄ and TBAP/CH₃CN the window observed seems to be shifted too high for wanted use. The best electrolyte system found was BMPBTI/CH₃CN due to the lower oxidation potential alongside the good current response.

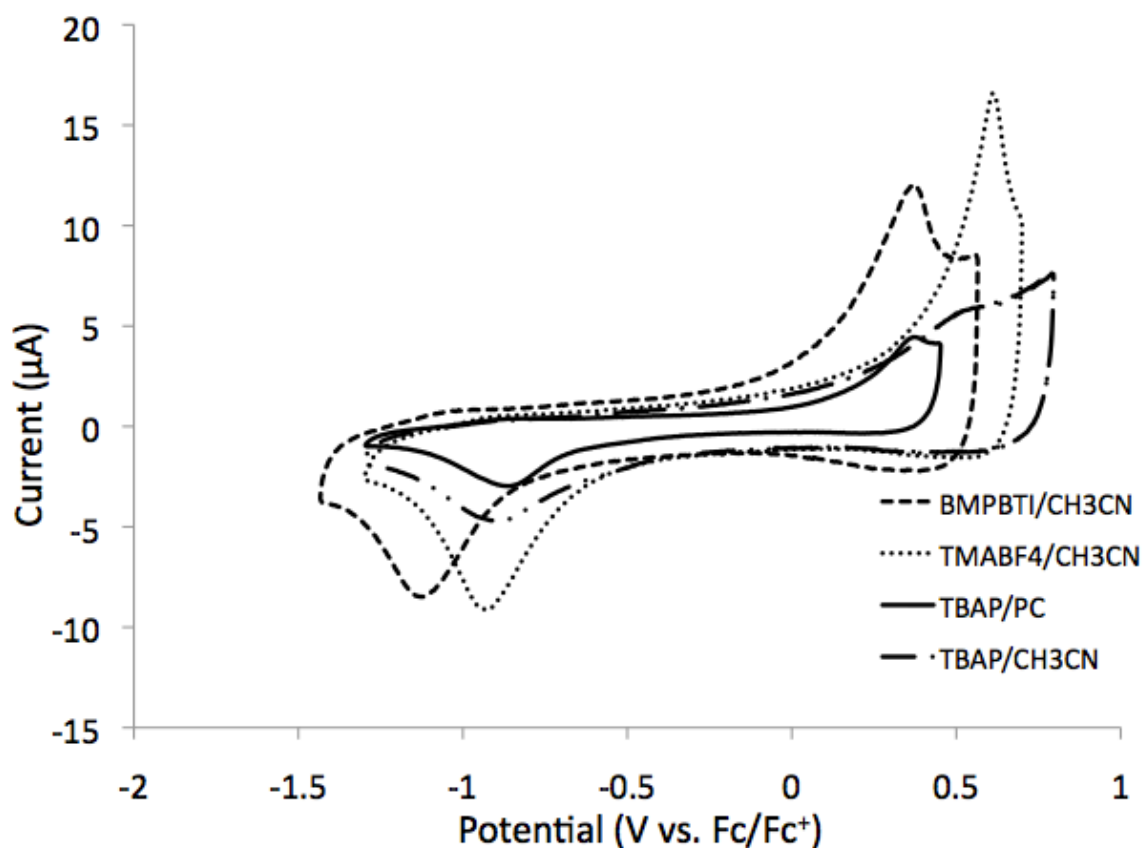


Figure 26. Cyclic voltammogram of PBEIPz in 0.01 M BMPBTI/CH₃CN, TMABF₄/CH₃CN, TBAP/PC, and TBAP/CH₃CN at 100 mV/s. WE: Au (0.2 cm diameter); RE: Ag wire; CE: Pt wire.

Once the electrolyte best suited for cyclic voltammetry was found, the polymer film was placed in monomer free 0.1 M BMPBTI/CH₃CN electrolyte and cycled at 100, 200, and 400 mV/s (Figure 27). It can be seen that the linear dependence of current response on scan rate indicates that the polymer film is electroactive and adhered to the electrode (Figure 27 inset). Both reduction and oxidation processes can be seen with increased current response when cycled in a different electrolyte solution than grown in originally. This phenomenon was also seen by Witker et al.¹⁶

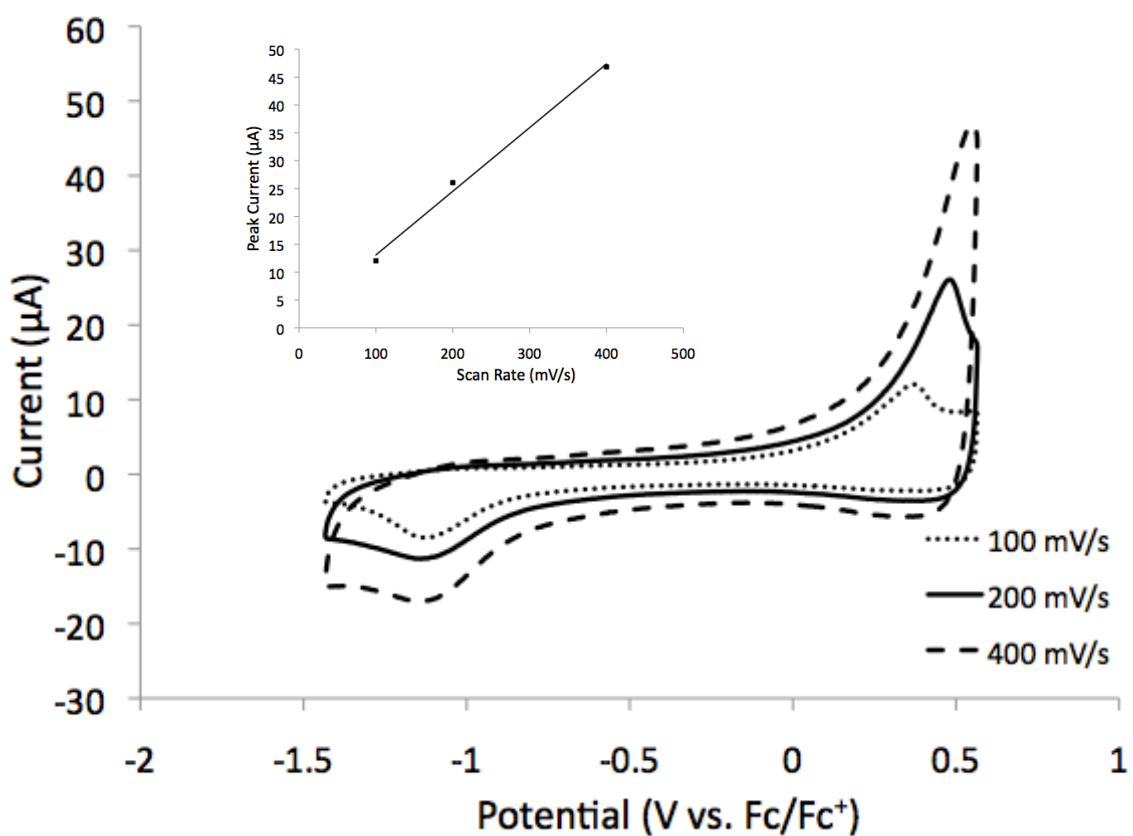


Figure 27. Cyclic voltammogram of PBEIPz in 0.1M BMPBTI/CH₃CN at 100, 200, and 400 mV/s from -1.45 to +0.5 V. WE: Au (0.2 cm diameter); RE: Ag wire; CE: Pt wire. Inset: The linear relationship between peak current and scan rate reveals that the polymer film is adhered to the electrode and is electroactive.

Spectroelectrochemistry

Through careful selection of donor and acceptor groups of a D-A-D compound, the π -system's HOMO and LUMO energy levels can be controlled; in this way, polymers can be designed to provide specific p- and n-doping properties.⁵³ When an optical response is observed upon introduction to electrolyte species, the polymer shows potential for use in sensor materials. These highly electroactive and structurally controlled electrochromic properties have been shown with other EDOT containing D-A-D molecules.³³

Attempts were made to determine the spectroelectrochemical behavior of PBEIPz. Unfortunately, PBEIPz would not adhere to an ITO-coated glass electrode. It is possible to estimate band gap from the polymer's electrochemically-determined oxidation and reduction potentials from $E_{g(\text{echem})} = E_{\text{ox,on}} - E_{\text{red,on}}$, where $E_{\text{ox,on}}$ is the onset of the polymer oxidation and $E_{\text{red,on}}$ is the onset of the polymer reduction.⁴² Using this method and the following values: $E_{\text{ox,on}} = -0.1$ V, $E_{\text{red,on}} = -1.6$ V determined from the cyclic voltammogram shown in Figure 21, the estimated (electrochemical) E_g value for the polymer is 1.5 V, which is (as expected) considerably lower than the observed (optical) E_g of BEIPz (2.5 eV, Figure 28).

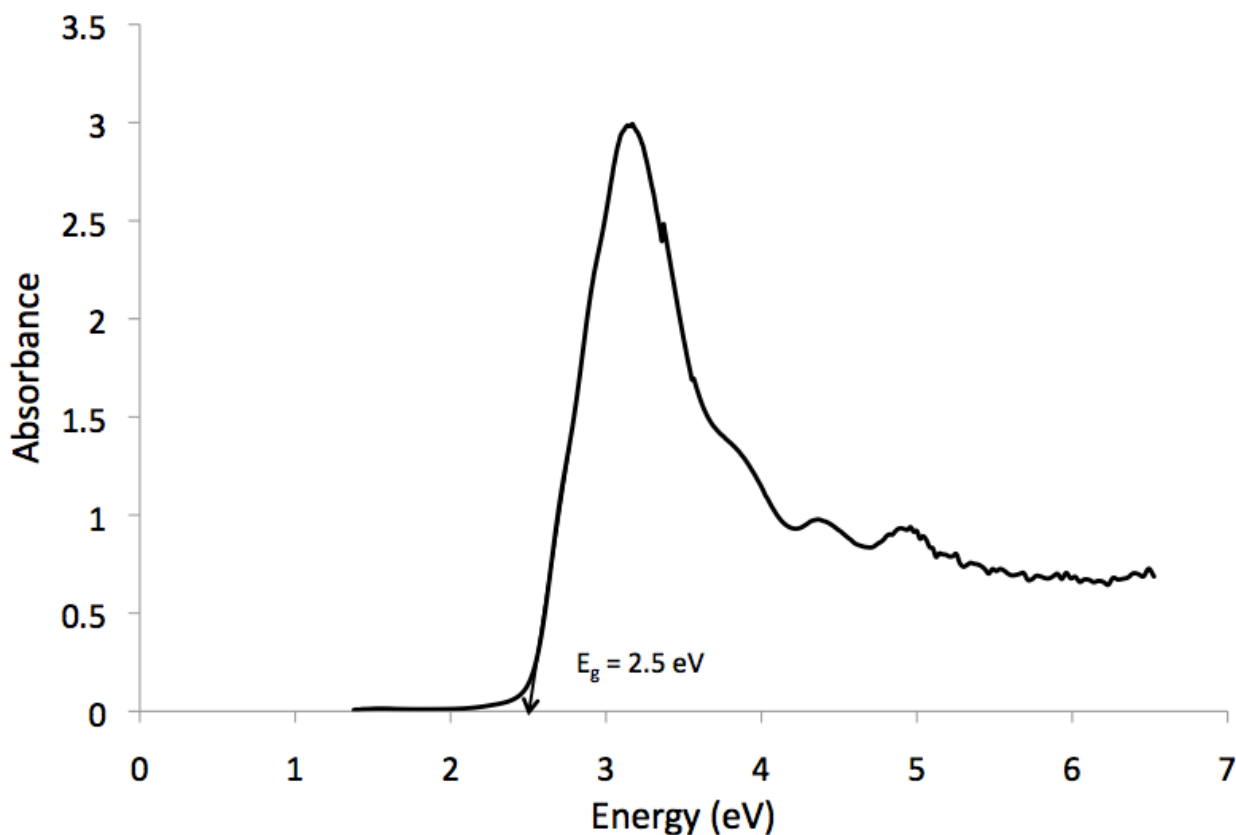


Figure 28. Monomer energy gap, E_g , depicted for BEIPz.

Conclusions

Irreversible reduction made it impossible to avoid electrochemically induced cleavage of the alkyl aryl ethers observed in BEIPz, EDOT, and ThOMe using a gold and platinum working electrode. Electropolymerization of BEIPz in $\text{TMABF}_4/\text{CH}_3\text{CN}$ showed monomer peak reduction due to the polymer becoming oxidized. Oxidative polymerization in BMPBTI provides a better current response and redox process for PBEIPz than the film prepared in TMABF_4/PC when grown on gold electrode. Providing a thicker film in TMABF_4 while changing the solvent from PC to CH_3CN showed that PC provides a more defined voltammogram. The polymer presumably becomes more

solvent swollen in PC, providing better access to ions for n-doping. When switching to TBAP on a gold working electrode, PBEIPz redox processes were found to be more apparent. However, after electropolymerization all four electrolytes/solvent systems, BMPBTI/CH₃CN, TMABF₄/CH₃CN, TBAP/PC, and TBAP/CH₃CN were compared to one-another. The best electrolyte system found was BMPBTI/CH₃CN due to the lower oxidation potential accompanied by good current response. Linear dependence of current response on scan rate also indicated that the polymer film were electroactive and adhered to the electrode. Deprotection of BEIPz TMS failed due to an unavailability of water (or any acidic protons) to complete the deprotection process.

Attempts were made to determine the spectroelectrochemical behavior of PBEIPz. Unfortunately, PBEIPz would not adhere to an ITO-coated glass electrode. The estimated (electrochemical) E_g value for PBEIPz was 1.5 V, which was (as expected) considerably lower than the observed (optical) E_g of BEIPz, 2.5 eV.

CHAPTER III

PYRIMIDINES

Background

With most n-doping polymers, degradation occurs within the first few redox cycles. This instability is thought to be caused by the formation of highly reactive carbanions during reduction, causing rapid, irreversible oxidation by water or air.⁵⁴ Many applications such as energy storage devices, electrochromics, sensors, photovoltaics, and biomedical devices would benefit from stable n-doping polymers.⁵⁵ To obtain stable, conductive, n-doping polymers, charge trapping must be prevented by increasing electron affinity along the polymer chain.⁵⁶ Nitrogen is better able to stabilize negative charges formed during reduction. By incorporating high nitrogen heterocycles that contain electron withdrawing imine-type nitrogens, electron affinity can be increased.⁵⁷ The electron affinities and ionization potentials of these high nitrogen heterocycles determine the success of the polymers' electrochemistry, creating a better n-doping polymer, by stabilizing the negative charge more effectively.

2,5-Bis(thien-2-yl)pyridine (BTPy) (Figure 29) was synthesized and its electronic properties were reported previously.⁵⁸ Previous findings showed an unstable n-doping process not useful for practical use therefore something more stable was needed.

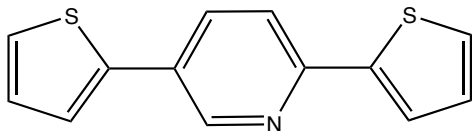
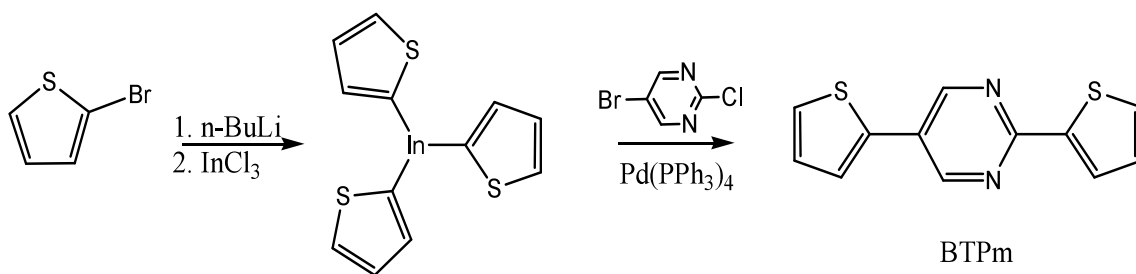


Figure 29. Structure of 2,5-bis(thien-2-yl)pyrimidine (BTPy).

With only one nitrogen in pyridine in comparison to the two found in pyrimidine, BTPm (pyrimidine species) should be better able to stabilize negative charge than BTP (pyridine species). Acceptor ability is related to electron affinity;⁵⁹ the estimated electron affinity of pyrimidine (-0.46 eV) is slightly higher than that of pyridine (-0.61).⁵⁷ Thus, 2,5-bis(thien-2-yl)-pyrimidine (BTPm) is expected to be more stable in the n-doped state than BTPy. BTPy was synthesized previously but its electronic properties were not reported (Scheme 4).^{53,60}



Scheme 4. Synthesis of 2,5-bis(thien-2-yl)pyrimidine (BTPm).

The focus of this chapter is donor-acceptor-donor (D-A-D) molecules utilizing pyrimidine acceptor groups between two thiophene donor groups. Electron rich thiophene donor groups sandwiching the nitrogen-rich heterocycles are expected to facilitate oxidative polymerization while pyrimidine acceptor groups should stabilize the n-doped polymer. Replacing the thiophene donor groups with 3,4-ethylenedioxythiophene (EDOT) donor groups has been shown to lower monomer and

polymer oxidation potentials. Both BTPm and its EDOT analog 2,5-bis(3,4-ethylenedioxythien-2-yl)pyrimidine (BEPm) were synthesized previously in the Irvin Research Group via the Sarandese coupling method shown in Scheme 4 so that their electrochemical properties could be determined (Figure 30).^{60,46}

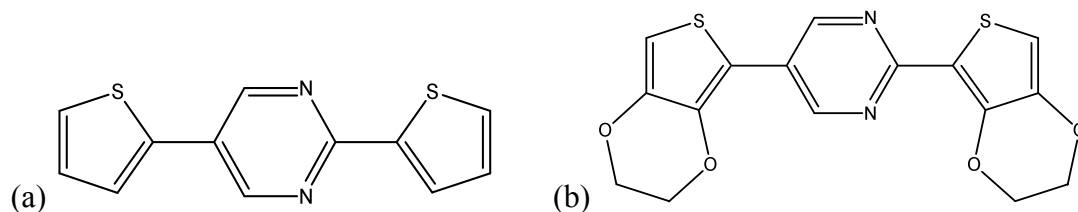


Figure 30. Structural representation of (a) BTPm and (b) BEPm.

Experimental

Materials

Acetonitrile (CH_3CN , anhydrous 99.8%) and propylene carbonate (PC, anhydrous 99.7%) were purchased from Sigma Aldrich and placed in an argon atmosphere dry box for use. Ferrocene was purchased from Acros, placed in an argon atmosphere glovebox, and used as received. Each electrolyte, 1-ethyl-3-methylimidazolium bis(trifluoromethylsulfonyl)imide (EMIBTI) and 1-butyl-1-methylpyrrolidinium bis(trifluoromethylsulfonyl)imide (BMPBTI), was synthesized in the laboratory via aqueous ion exchange and purified using column chromatography (silica gel) followed by heating with stirring under vacuum to remove residual water.^{47,34}

Structural identity was confirmed from ^1H NMR using either a Varian INOVA 400 MHz NMR or a Bruker Avance III 400 MHz NMR. BTPm and BEPm were synthesized using Sarandeses coupling methodology by Katie Winkel.^{46,34}

Instrumentation

Cyclic voltammetry experiments were conducted using a Pine WaveNow potentiostat in an argon atmosphere on solutions containing 0.005 or 0.01 M monomer, as specified below, and 0.1 M electrolyte (either EMIBTI or BMPBTI as specified below) in CH_3CN . The working (WE), auxiliary (CE), and pseudo-reference (RE) electrodes were a platinum or gold button (0.2 cm diameter, Bioanalytical Systems Inc.), a platinum wire, and a silver wire respectively. All cyclic voltammograms are referenced to the ferrocene/ferrocenium couple in each given electrolyte.

UV-Vis spectroelectrochemistry was carried out using a Cary 100 UV-Visible Spectrophotometer with 10 mm quartz cuvettes (Fisher Scientific). In this case the working, auxiliary, and pseudo-reference electrodes were an indium tin oxide (ITO) coated glass slide (Delta Technologies, 5-15 Ω), a platinum wire, and a silver wire respectively. Electropolymerization was accomplished outside of the spectrophotometer, depositing polymer onto the ITO glass slide by cycling from -0.9 to 1.2 V and -1.05 to 1.6 V for BEPm and BTPm respectively. Each polymer was grown over 5 cycles at a scan rate of 100 mV/s. Once polymer was deposited, monomer-free electrolyte solution was placed in the cuvette, and the platinum counter electrode was replaced with a clean ITO-coated glass slide to be put into the spectrophotometer. The polymer films were

kept at approximately constant potentials beginning at the most reduced state for 80 seconds (using a voltammetry experiment in which the voltage was changed, for instance, from -1.00 V to -0.9 V at a scan rate of 0.01 mV/s, as the wavelength was scanned from 190 to 900 nm until each spectrum was obtained. Potentials were increased by 0.2 V each time until the fully oxidized state was reached. UV-visible spectra of the monomers were acquired by dissolving the monomers in CH₃CN and recording the spectra of the solutions from 190 to 900 nm. Monomer concentrations were chosen to provide solution absorption less than 5 absorbance units (au).

Molecular modeling calculations were accomplished using the Cerius 2 software package from Accelrys. The X-ray crystal structure of BTPm (recrystallized from acetonitrile) was determined by fellow graduate student Makda Araya using a Rigaku single crystal micro diffractometer integrated with ACCESS Mini 1.0 Mercury 2, solved using Crystal Structures 4.0 and refined using Diamond.⁶¹

Results and Discussion

Monomer and Polymer Electrochemistry

Electrolyte: EMIBTI

As was discussed in Chapter 2, scanning to n-doping potentials during electropolymerization has been shown to improve the polymer n-doping electrochemical response.¹⁶ To determine whether or not this approach would improve BTPm

electrochemistry, electropolymerization of BTPm was accomplished using a 0.005 M BTPm monomer dissolved in a 0.01 M EMIBTI/CH₃CN solution. The low monomer concentration was necessary due to poor solubility of BTPm in CH₃CN. Propylene carbonate was also examined as a potential solvent for electropolymerization but it proved to be even less effective than CH₃CN at dissolving BTPm. In CH₃CN, onset of monomer oxidation ($E_{\text{on,m}}$) can be seen (Figure 31) at 0.83 V, with a peak ($E_{\text{p,m}}$) at approximately +1.16 V. Five full cycles were employed to ensure significant polymer deposition on the electrode.

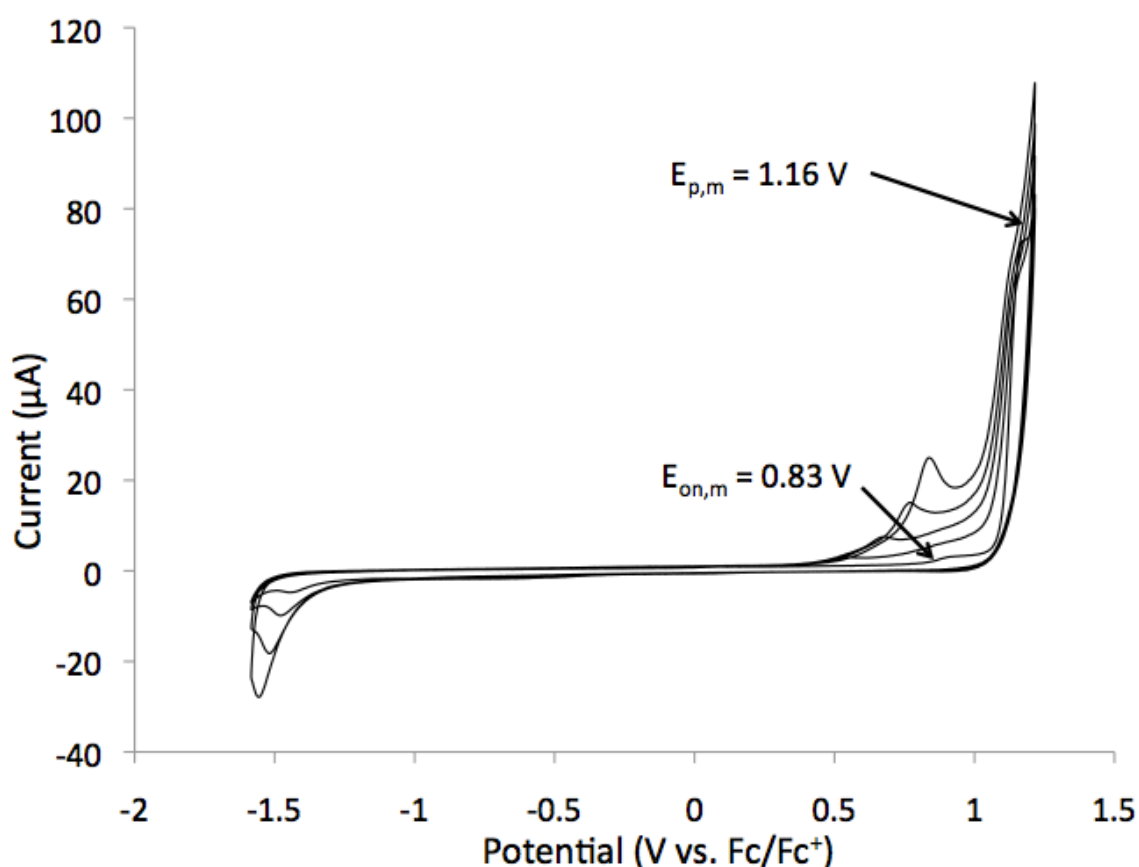


Figure 31. Repeated potential scanning electropolymerization of BTPm (0.005 M in 0.1 M EMIBTI/CH₃CN) vs. Fc/Fc⁺ at 100 mV/s from -1.6 to +0.2 V.

After electropolymerization, the resultant polymer (PBTPm) film was rinsed with electrolyte solution and placed into monomer free electrolyte solution (0.1 M EMIBTI/CH₃CN). The polymer electrochemistry was investigated as a function of scan rate. Cyclic voltammetry was conducted at rates of 100, 200, 300, 350, and 500 mV/s. It can be seen (Figure 32) the $E_{a,p}$ is observed at +1.3 V whereas the $E_{p,m}$ is at a lower potential of +1.16 V (Figure 31). The linear dependence of current response on scan rate (Figure 32 inset) indicates that the polymer film is electroactive and adhered to the electrode according to the theory of surface immobilized redox centers.²⁶

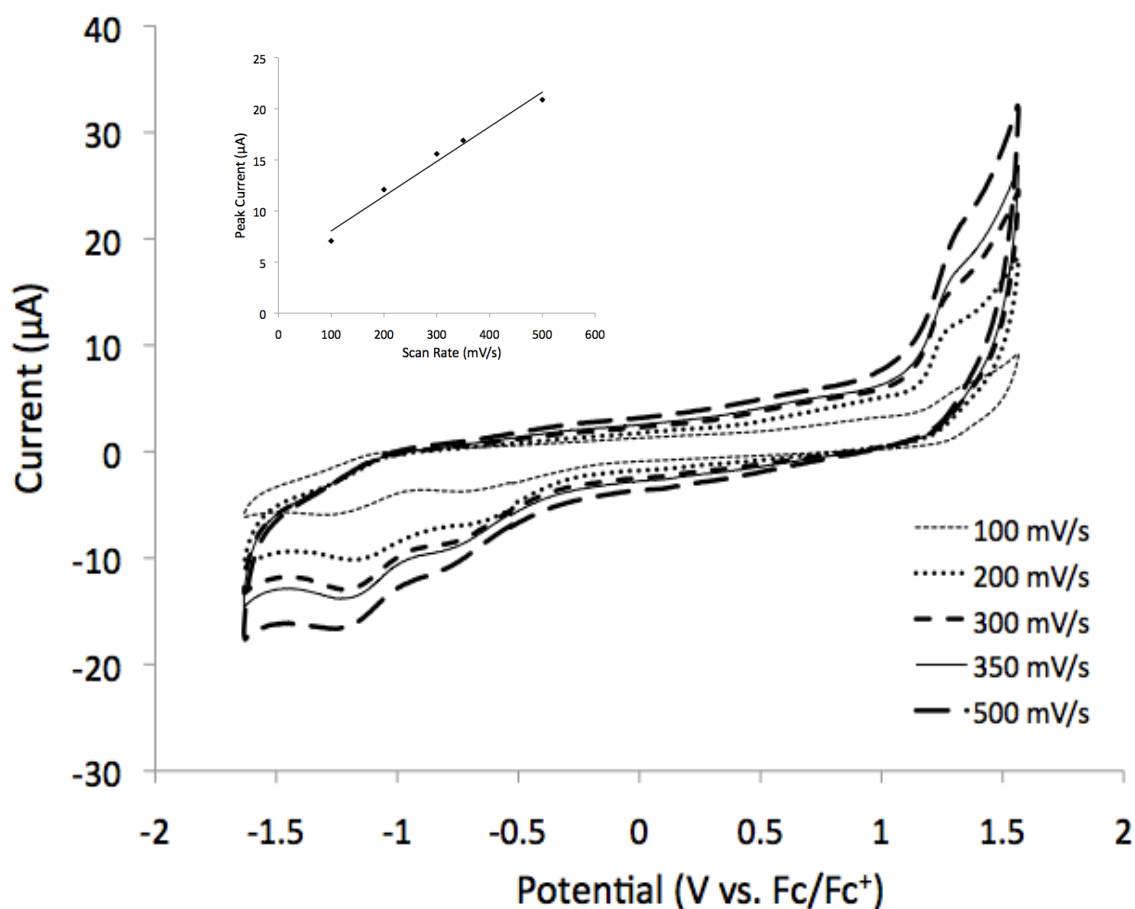


Figure 32. PBTPm cyclic voltammetry in 0.1 M EMIBTI/CH₃CN. Inset: The linear relationship between peak current and scan rate reveals that the polymer film is adhered to the electrode and is electroactive.

To obtain a lower oxidation potential for both the monomer and polymer, BEPm was synthesized to increase the donor groups' electron density.⁴⁶ Oxidative electropolymerization of BEPm was accomplished using a 0.01 M BEPm monomer dissolved in a 0.01 M EMIBTI/CH₃CN solution. BEPm appeared to be more soluble in CH₃CN than BTPm was. In CH₃CN, onset of monomer oxidation ($E_{\text{on,m}}$) can be seen (Figure 33) at +0.45 V, with a peak ($E_{\text{p,m}}$) at approximately +0.45 V. Five full cycles were employed to ensure significant polymer deposition on the electrode. Significantly, addition of electron-donating ethylenedioxy substituents resulted in BEPm monomer oxidation potentials ca. 0.53 V lower than in BTPm.

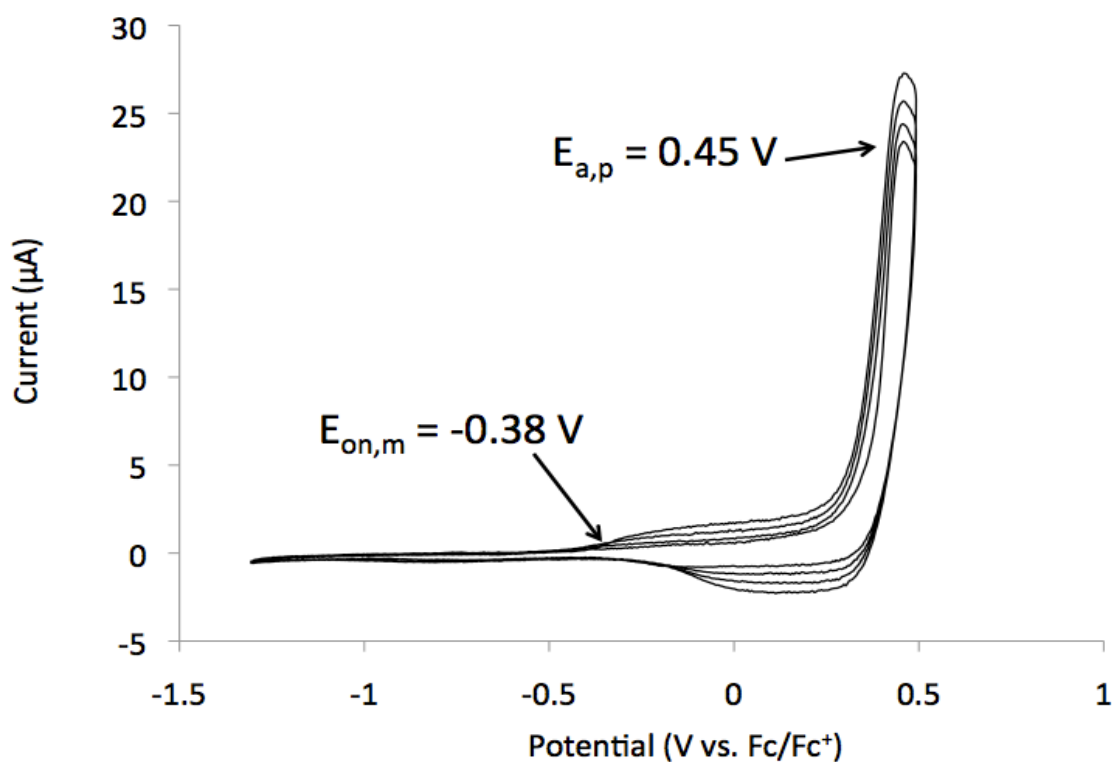


Figure 33. Repeated potential scanning oxidative electropolymerization of BEPm (0.01 M in 0.1 M EMIBTI/CH₃CN) Vs. Fc/Fc⁺ at 100 mV/s from -1.35 to +0.5 V.

After oxidative electropolymerization, the resultant polymer (PBEPm) film was rinsed with electrolyte and placed in monomer free electrolyte solution (0.1 M EMIBTI/CH₃CN). The polymer electrochemistry was investigated as a function of scan rate. Cyclic voltammetry was conducted at rates of 100, 200, 300, 350, and 500 mV/s (Figure 34). The linear dependence of current response on scan rate (Figure 34 inset) indicates that the polymer film is electroactive and adhered to the electrode. The voltammograms reveal a significant p-doping current response, but the n-doping portion is relatively insignificant, particularly in comparison to the voltammograms of PBTPm (Figure 32); it is possible that the electron donating ethylenedioxy substituents lowered the reduction potential enough that only the edge of the reduction process is accessible within the electrochemical stability window of the electrolyte solution.

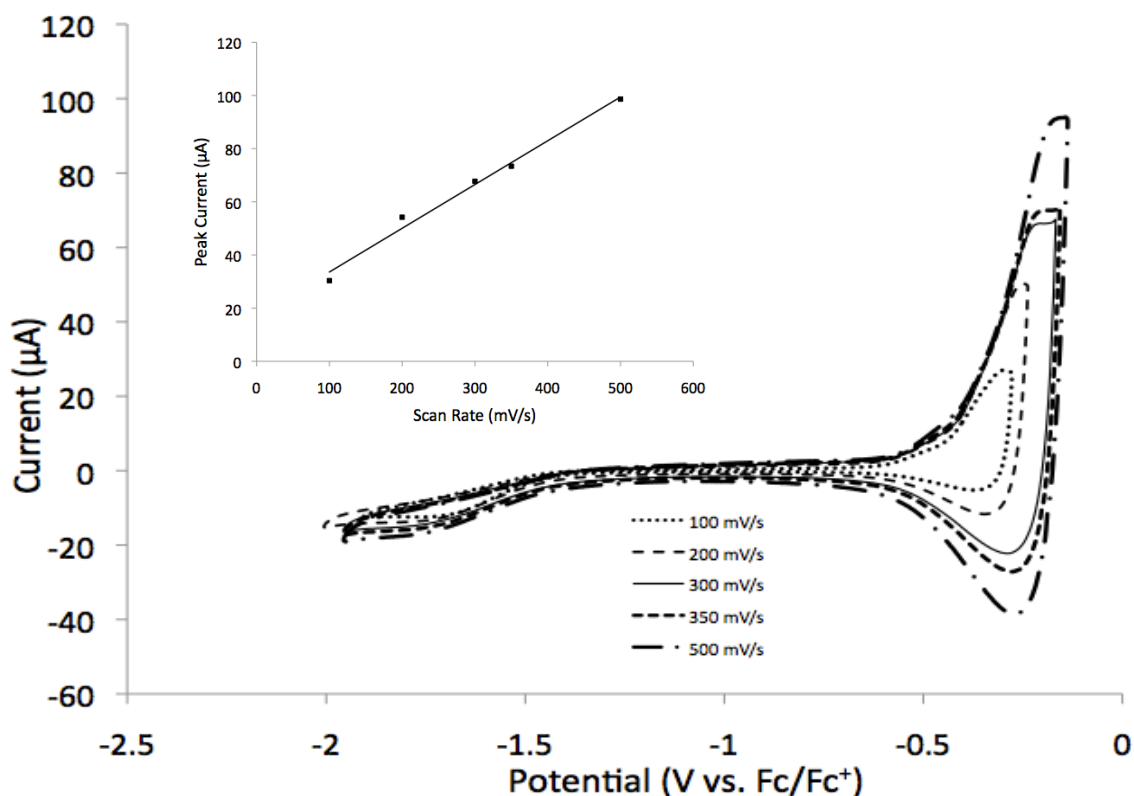


Figure 34. PBEPm cyclic voltammetry in 0.1 M EMIBTI/CH₃CN. Inset: The linear relationship between peak current and scan rate reveals that the polymer film is adhered to the electrode and is electroactive.

As observed with BTPm, scanning to n-doping potentials during electropolymerization has not improved the polymer n-doping electrochemical response. To determine whether or not this approach would improve BEPm electrochemistry, further electropolymerization of BEPm was accomplished using a 0.01 M BEPm monomer dissolved in a 0.01 M EMIBTI/CH₃CN solution. In CH₃CN, onset of monomer oxidation ($E_{\text{on,m}}$) can be seen at +0.25 V, with a peak ($E_{\text{p,m}}$) at approximately +0.45 V (Figure 35). Five full cycles were employed to ensure significant polymer deposition on the electrode. The lack of an irreversible process may be due to the pyrimidine ring

containing a better acceptor, more electron withdrawing, than the isopyrazole, creating more stabilized ether linkages.

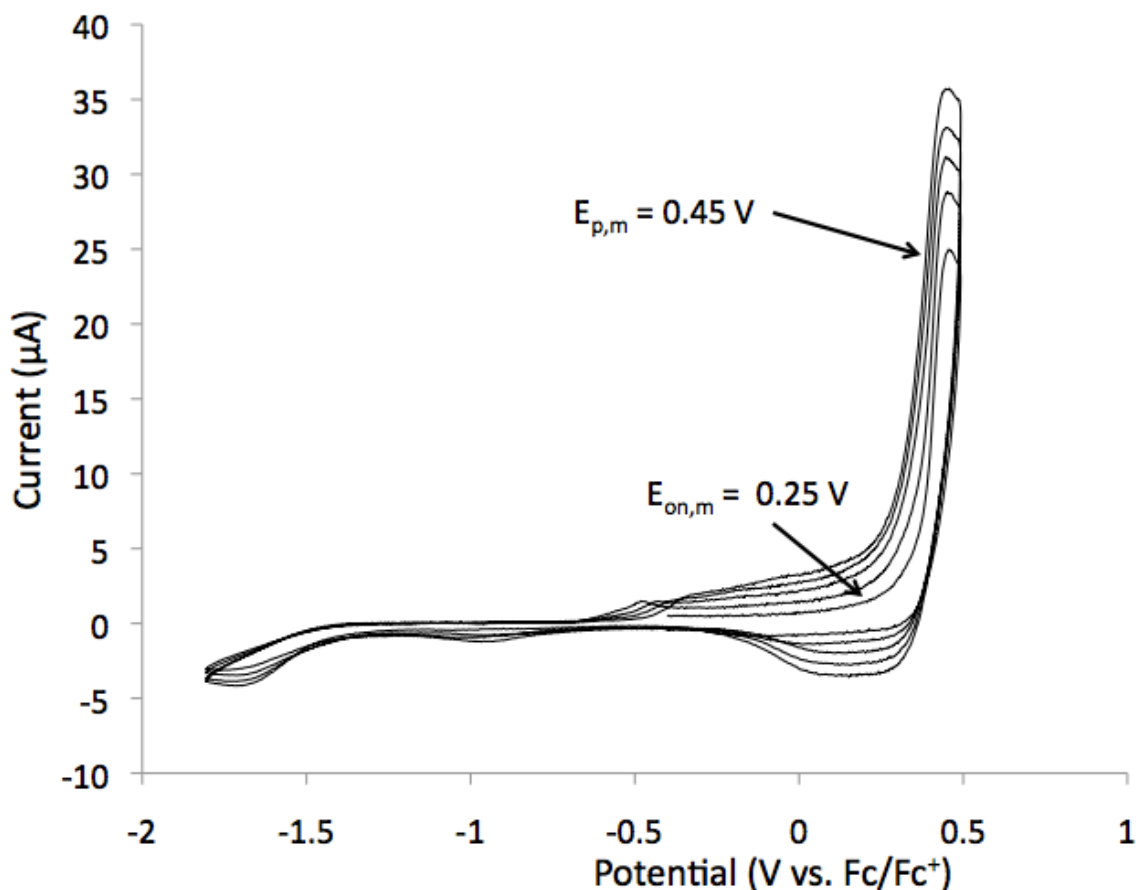


Figure 35. Repeated potential scanning electropolymerization of BEPm (0.01 M in 0.1 M EMIBTI/CH₃CN) Vs. Fc/Fc⁺ at 100 mV/s from -1.8 to +0.5 V.

After electropolymerization, the resultant polymer (PBEPm) film was rinsed with electrolyte and placed into monomer free electrolyte solution (0.1 M EMIBTI/CH₃CN). The polymer electrochemistry was investigated as a function of scan rate. Cyclic voltammetry was conducted at rates of 100, 200, 300, and 350 mV/s. The linear dependence of current response on scan rate (Figure 36 inset) indicates that the polymer film is electroactive and adhered to the electrode. The n-doping process is not seen when

using EMIBTI as the supporting electrolyte possibly due to the small electrolyte window. The polymer p-doping electrochemistry has significantly increased in current (Figure 36) after polymerizing to n-doping potentials.

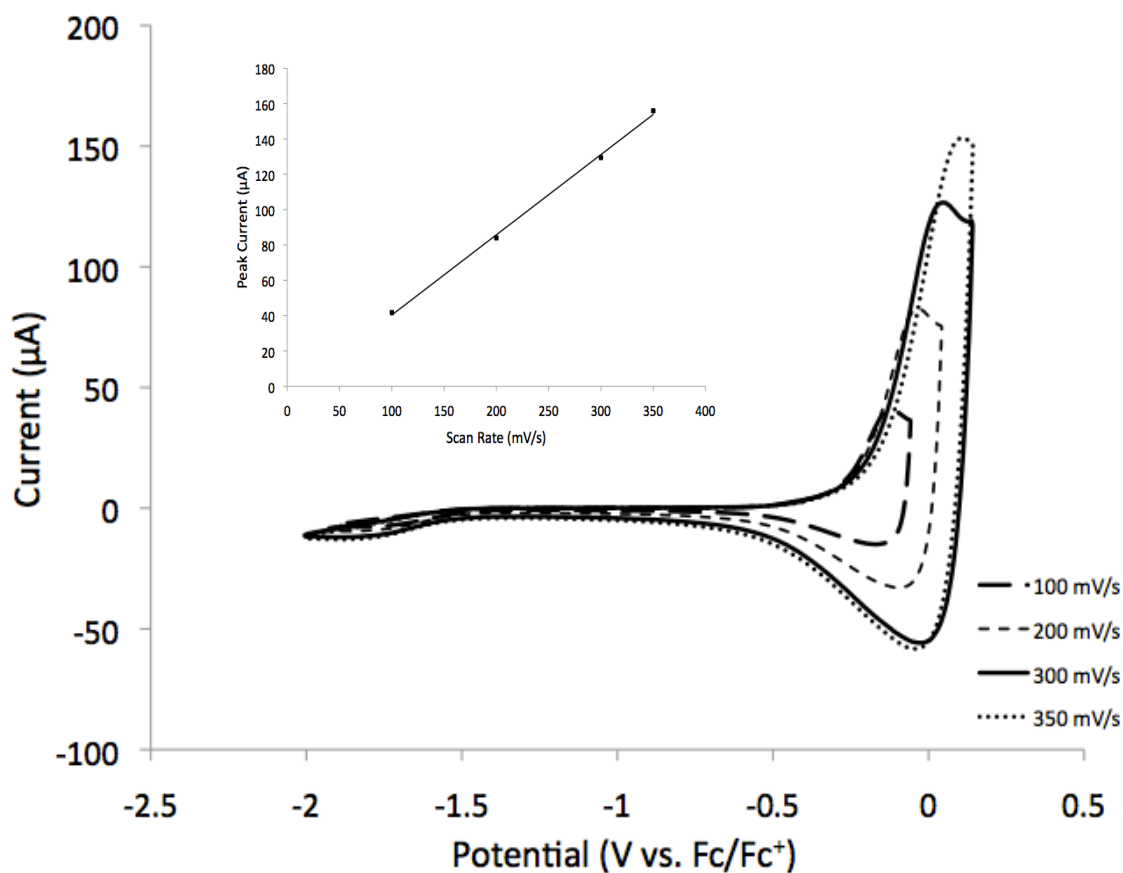


Figure 36. PBEPm cyclic voltammetry in 0.1 M EMIBTI/CH₃CN. Inset: The linear relationship between peak current and scan rate reveals that the polymer film is adhered to the electrode and is electroactive.

Electrolyte: BMPBTI

The electropolymerization process was repeated using 0.1 M BMPBTI/CH₃CN as the supporting electrolyte while keeping the 0.005 M BTPm monomer solution.

Similarly, the onset of monomer oxidation ($E_{\text{on,m}}$) can be seen at +0.78 V, and the peak ($E_{\text{p,m}}$) is observed at approximately +1.12 V (Figure 37).

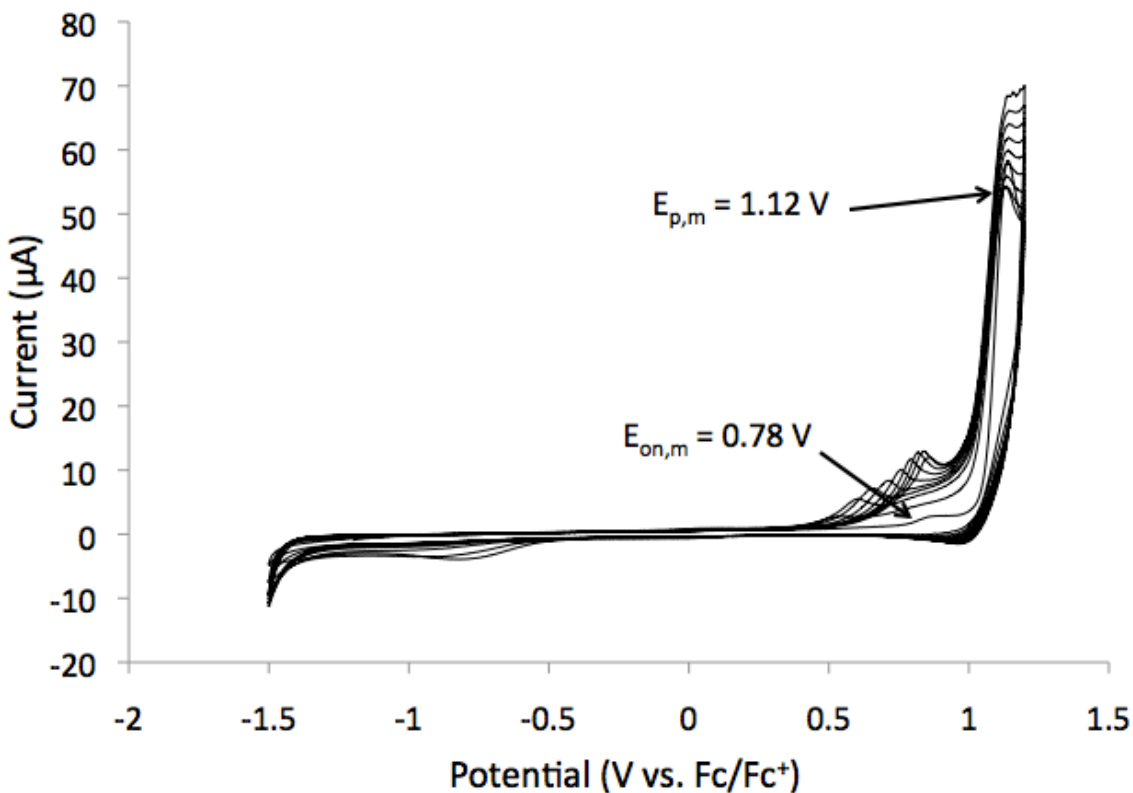


Figure 37. Repeated potential scanning electropolymerization of BTPm (0.005 M in 0.1 M BMPBTI/CH₃CN) Vs. Fc/Fc⁺ at 100 mV/s.

Once more the PBTPm film deposited on the platinum electrode was rinsed with monomer free electrolyte and placed in monomer free electrolyte solution, 0.1M BMPBTI/CH₃CN, the polymer electrochemistry was investigated at 50, 100, 200, 300, and 450 mV/s (Figure 38). While the beginning of polymer oxidation is clearly visible, the peak of the oxidation process is outside the electrolyte stability window and cannot be discerned. The reduction peak is observed at approximately -0.3 V. From this it can be seen that the p-doping process is too high to be utilized.

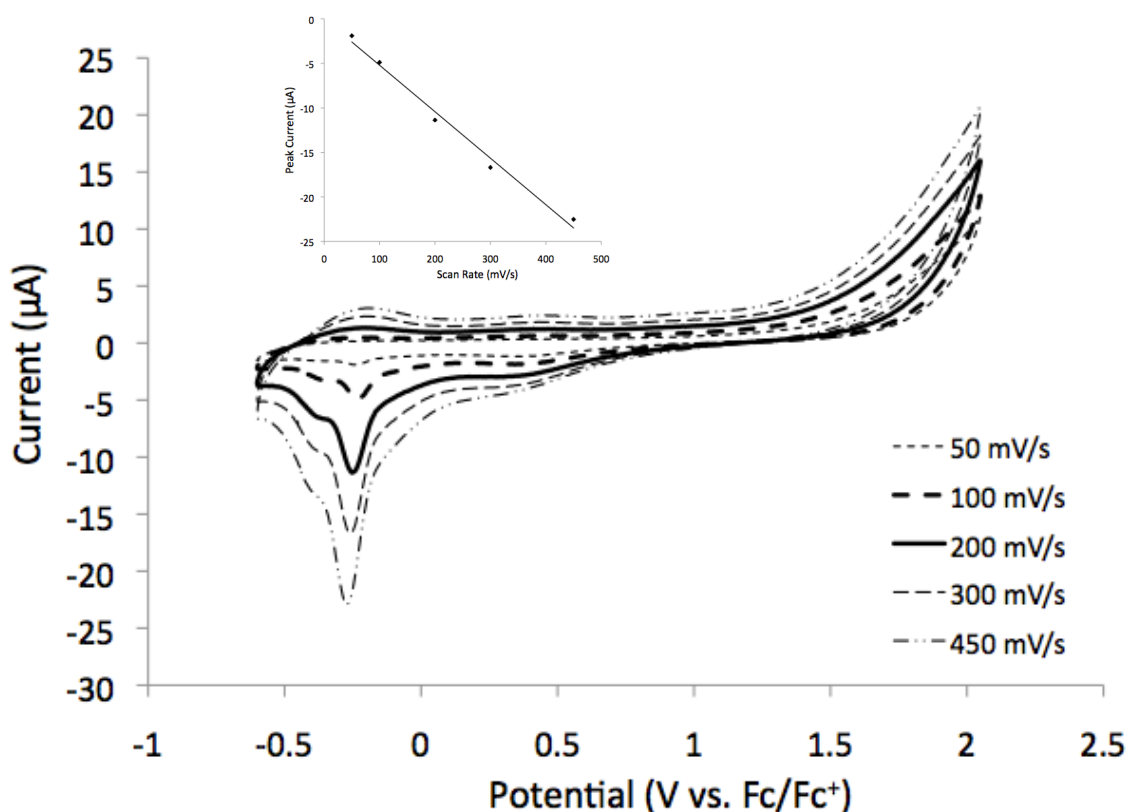


Figure 38. PBTPm cyclic voltammetry in 0.1 M BMPBTI/CH₃CN. Inset: The linear relationship between peak current and scan rate reveals that the polymer film is adhered to the electrode and is electroactive.

Polymer growth from BEPm was accomplished using 0.01 M BEPm in a 0.1 M BMPBTI/CH₃CN electrolyte solution. Onset of monomer oxidation ($E_{\text{on,m}}$) can be seen at +0.7 V, with a peak ($E_{\text{p,m}}$) at approximately +0.82 V (Figure 39). Polymer reduction is observed with a much greater current response than previously seen, from approximately -0.75 V to -0.3 V, with the change in monomer and electrolyte. The redox process seen centered at -0.6 V during polymerization, and not seen during polymer electrochemistry (Figure 40), likely indicates that the process belongs to a soluble species, possibly a soluble oligomer, that was removed during the film rinsing process.

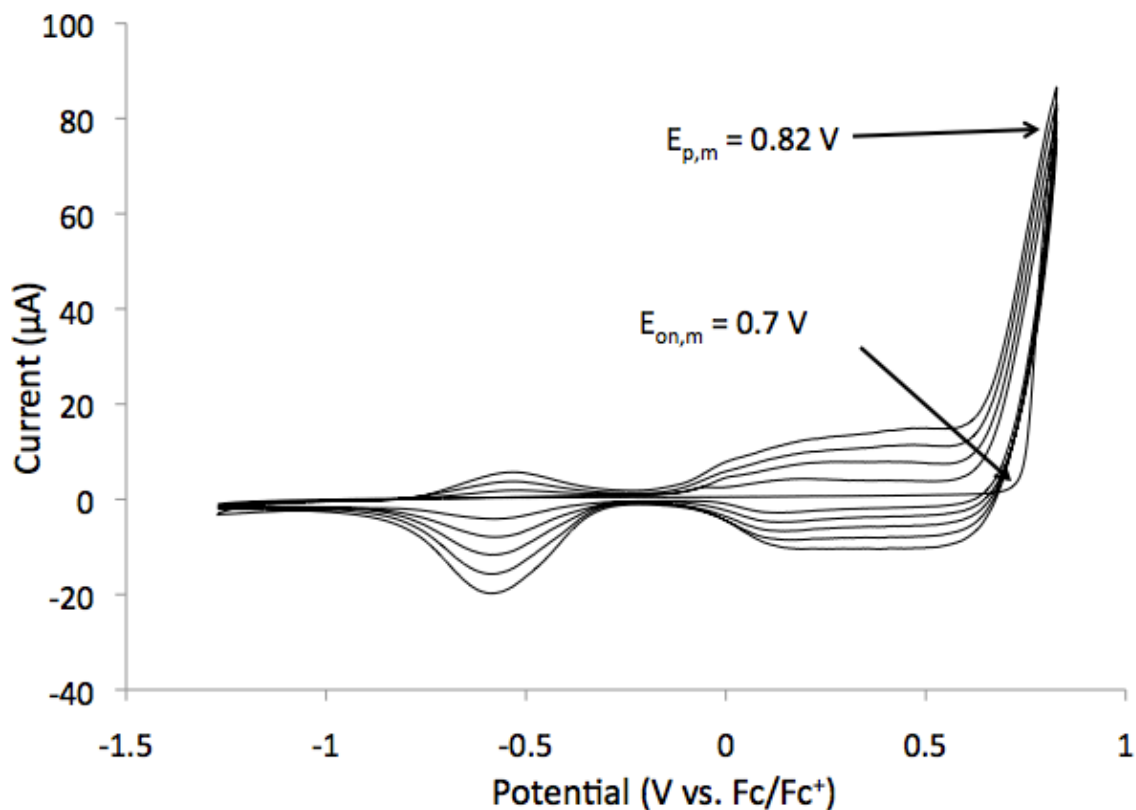


Figure 39. Repeated potential scanning electropolymerization of BEPm (0.01 M in 0.1 M BMPBTI/CH₃CN) Vs. Fc/Fc⁺ at 100 mV/s.

Cyclic voltammetry was conducted at rates of 50, 100, 200, 300, and 450 mV/s (Figure 40). The linear dependence of current response on scan rate (Figure 40 inset) indicates that the polymer film is electroactive and adhered to the electrode. As depicted in Figure 40 the observed p and n-doping peaks show consistent linearity with increasing scan rate. In comparison to cyclic voltammogram for BTPm (Figure 39), the window has shifted to lower potentials when looking at the n-doping peaks at approximately -1.95 V. Also, the p-doping process has become visible at +0.9 V.

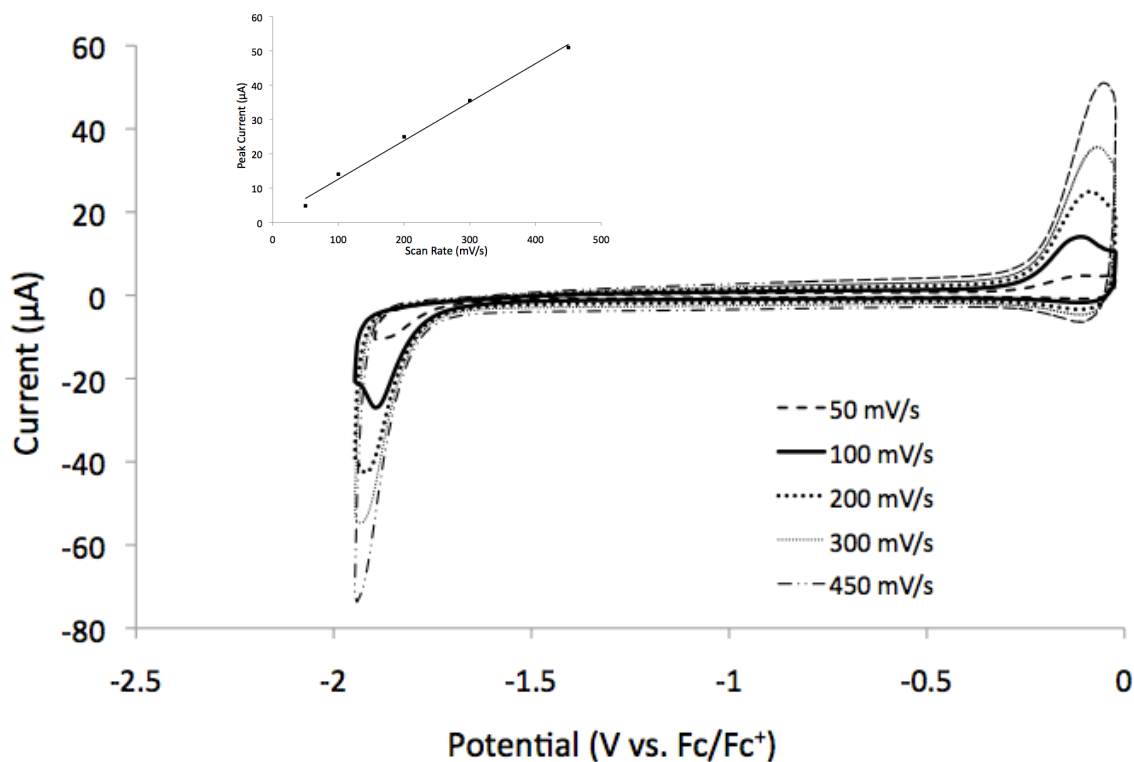


Figure 40. PBEPm cyclic voltammetry in 0.1 M BMPBTI/CH₃CN. Inset: The linear relationship between peak current and scan rate reveals that the polymer film is adhered to the electrode and is electroactive.

A comparison of the cyclic voltammograms of PBEPm and PBTPm (Figure 41) reveals that PBEPm gives a greater current response than PBTPm at lower potentials in BMPBTI/CH₃CN. However, a larger current response is observed for PBEPm due to the preparation from a 0.01 M monomer solution, while PBTPm was prepared from a 0.005 M monomer solution. Also, both p and n-doping processes are shown to be more prominent for PBEPm. The shift in potential for the EDOT analog, PBEPm, is, again, due to the electron donating ethylenedioxy substituents lowering the oxidation potential significantly.

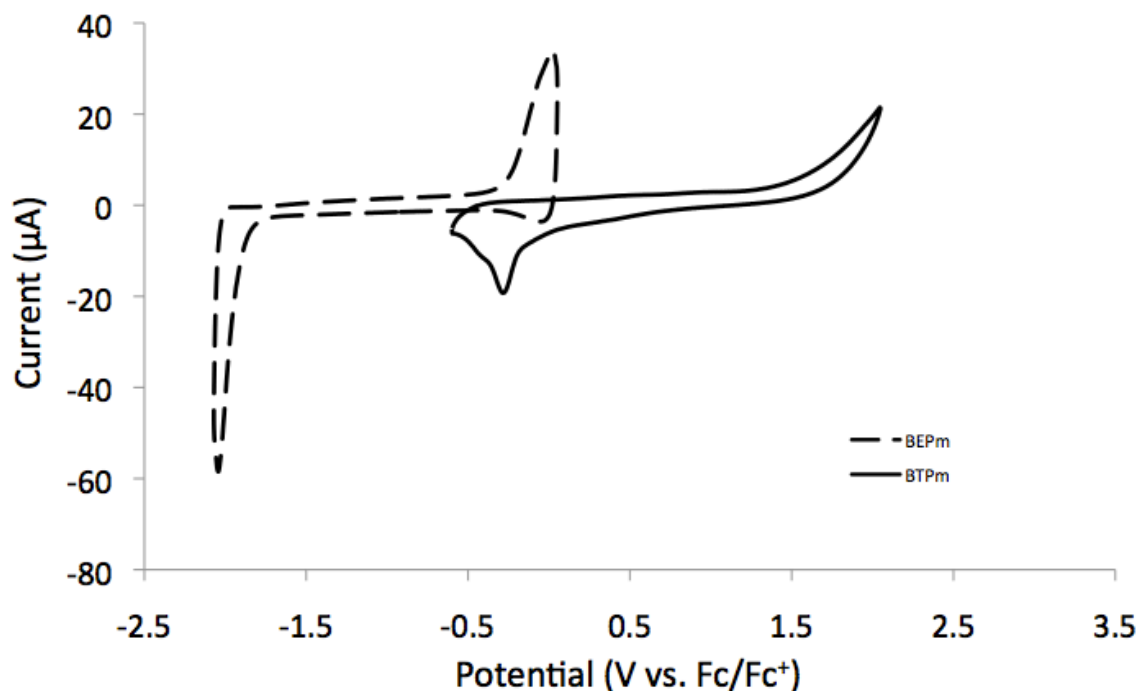


Figure 41. Cyclic voltammetry of PBEPm (dashes line, prepared from 0.005 M BEPm) vs. PBTPm (solid line, prepared from 0.005 M BTPm) in 0.1 M BMPBTI/CH₃CN at 450 mV/s.

A summary of the preceeding data is provided in Table 1. The EDOT monomers, BEPm and BEIPz, have nearly identical monomer oxidation peak potentials ($E_{p,m}$), showing that oxidation potential is determined by the donor group. The thiophene monomer, BTPm, exhibits a much higher oxidation potential due to the lack of electron donating ethylenedioxy groups. The much lower $E_{on,m}$ observed for BEIPz may indicate that the monomer underwent spontaneous dimerization prior to electropolymerization. The very low observed E_g for BEIPz (2.5 eV) also supports this hypothesis.

Table 1. Tabulated data for each monomer and its respective polymer in 0.1 M BMPBTI/CH₃CN. Values for the band gap determination are discussed in the spectroelectrochemistry section below.

	E _{a,p} (V)	E _{on,m} (V)	E _g (eV) (Echem)	E _g (eV) (Optical)
BEPm	0.82	0.70		3.18
PBEPm	-1.10		1.45	1.85
BTPm	1.12	0.78		3.33
PBTPm			1.25	2.25
BEIPz	0.80	0.20		2.50
PBEIPz	0.35		1.50	

Spectroelectrochemistry

Energy gap, E_g, determination was accomplished from 1.25 x 10⁻³ M monomer in a 0.1 M BMPBTI/CH₃CN. The optical energy gaps for BTPm and BEPm are approximately 3.33 eV and 3.18 eV respectively (Figure 42). The observed differences are due to the ethylenedioxy derivative donating electron density and raising the HOMO, thus lowering the E_g.

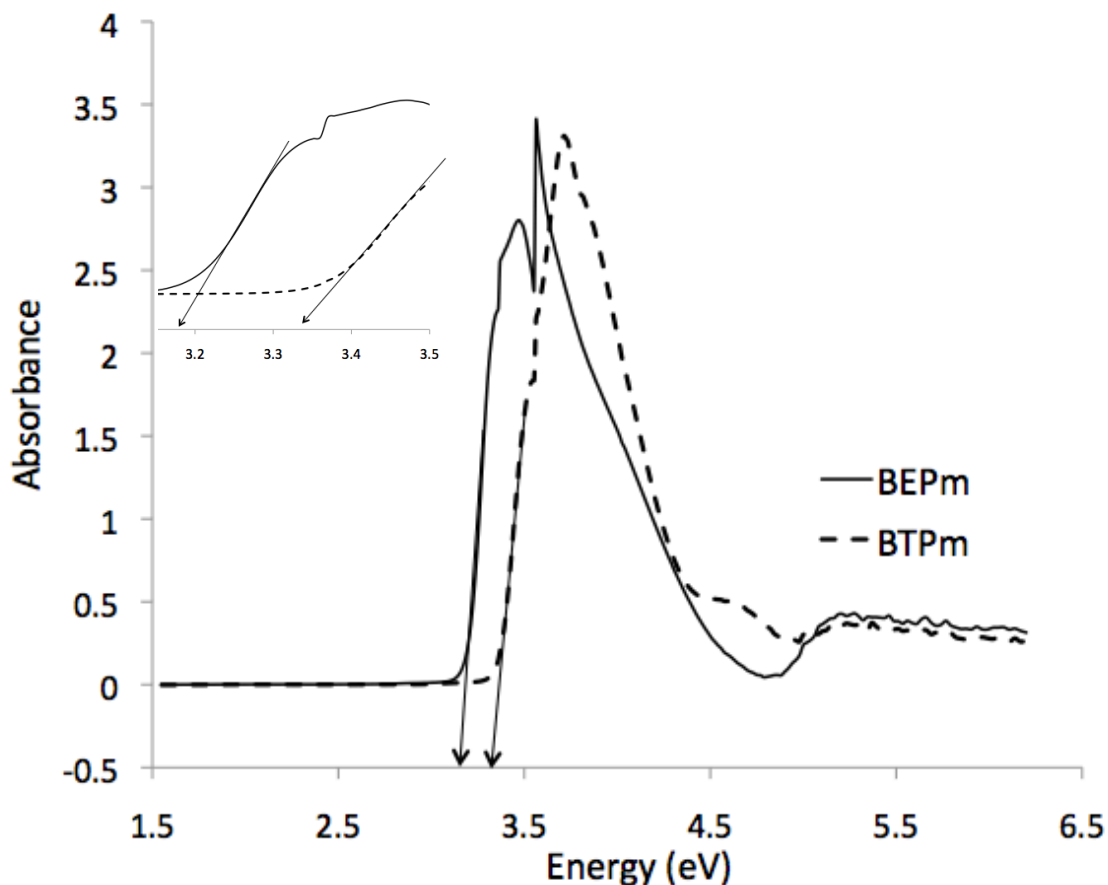


Figure 42. Monomer energy gap, E_g , depicted for BTPm and BEPm using 1.25×10^{-3} M monomer concentrations. Inset: magnified portion of energy gap determination.

Spectroelectrochemical analyses of PBTPm and PBEPm were conducted after electrochemically depositing the polymer films onto indium-tin oxide (ITO) coated working electrodes; ITO provides a transparent conductive surface to use as the working electrode in place of opaque platinum or gold button electrodes (Figure 43 & 44), thus facilitating acquisition of absorption spectra. During deposition, a platinum wire was used as the counter electrode while a silver wire was utilized as a pseudo-reference electrode. Once the polymer was adhered to the ITO surface, the polymer was rinsed and placed in a monomer free electrolyte solution with the platinum counter electrode

replaced by a transparent ITO electrode to allow the beam to pass through the polymer and ITO electrodes without disruption.

At the lowest potential, -0.9 V, the burgundy red PBEPm film is in its reduced state. The blue-purple observed for the oxidized form was similar to that of poly[2,5-bis(3,4-ethylene-dioxy-2-thien-2-yl)pyridine] (PBEPy)] also seen by David Irvin and colleagues.⁵³ The band gap is determined from the onset of the π to π^* transition. The excitation of electrons from valence to conduction band causes the only significant absorption. For PBEPm, the transition onset occurs at approximately 1.85 eV with a peak at 2.5 eV (Figure 43). With an increase in applied potential, the polymer becomes oxidatively doped. The intensity of the interband transition decreases, and three absorbances develop at a lower energy possibly due to the formation of a bipolaronic species.⁶² In past studies, it has been found that the incorporation of EDOT will contribute to a more evident π to π^* transition.⁶³

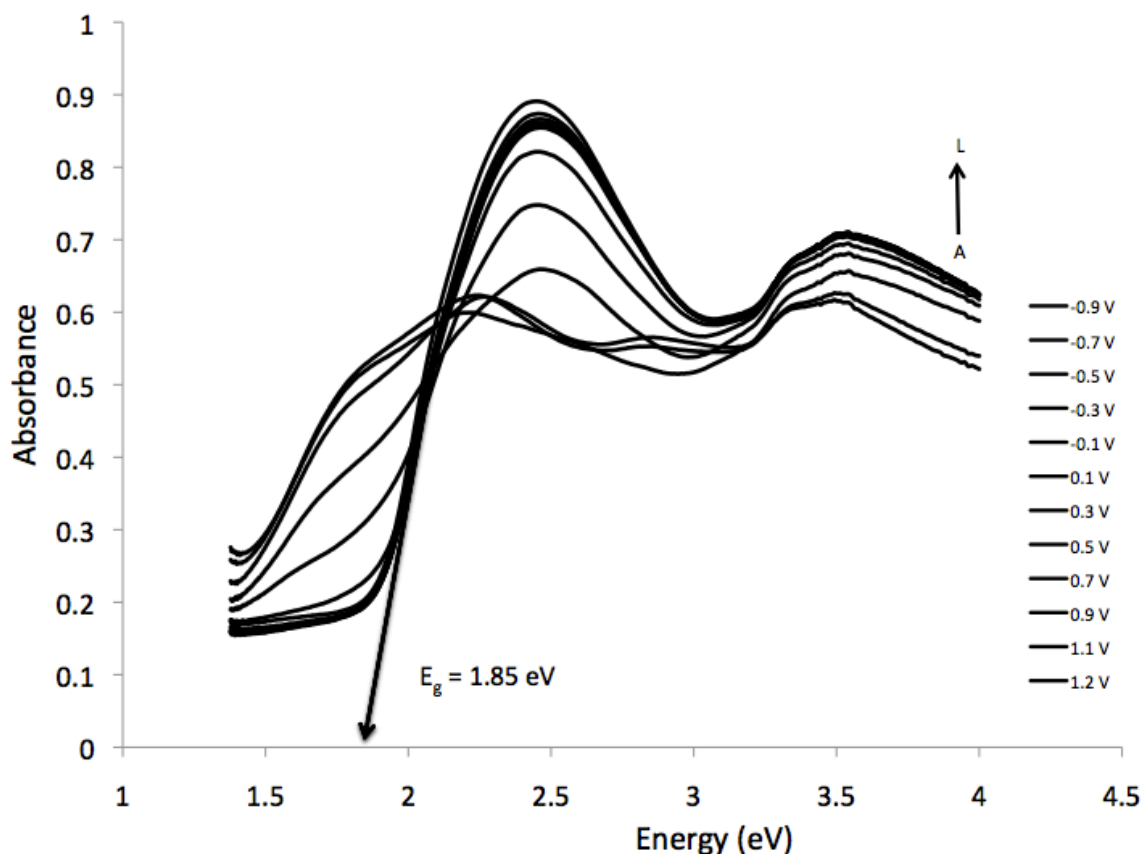


Figure 43. Spectroelectrochemistry of PBEPm in 0.1 M BMPBTI/CH₃CN electrochemically deposited on an ITO working electrode from -0.9 V (A) to 1.2 V (N).

The onset of the π to π^* transition, band gap, determined for BTPm was found to be 2.25 eV with a peak at 3.2 eV and a shoulder at approximately 2.5 eV (Figure 44). Increasing the applied potential from -1.05 V to 1.65 V causes the polymer to become oxidatively doped, p-doped. As with PBEPm the intensity of the interband transition decreases however, it is not as drastic and no clearly depicted absorbances develop at a lower energy. This likely indicates that the polymer is not very electroactive at this point, possibly due to degradation; while electrochemical studies are conducted in an inert atmosphere glove box, spectroelectrochemical studies are conducted in air because the spectrophotometer cannot be placed in the glove box.

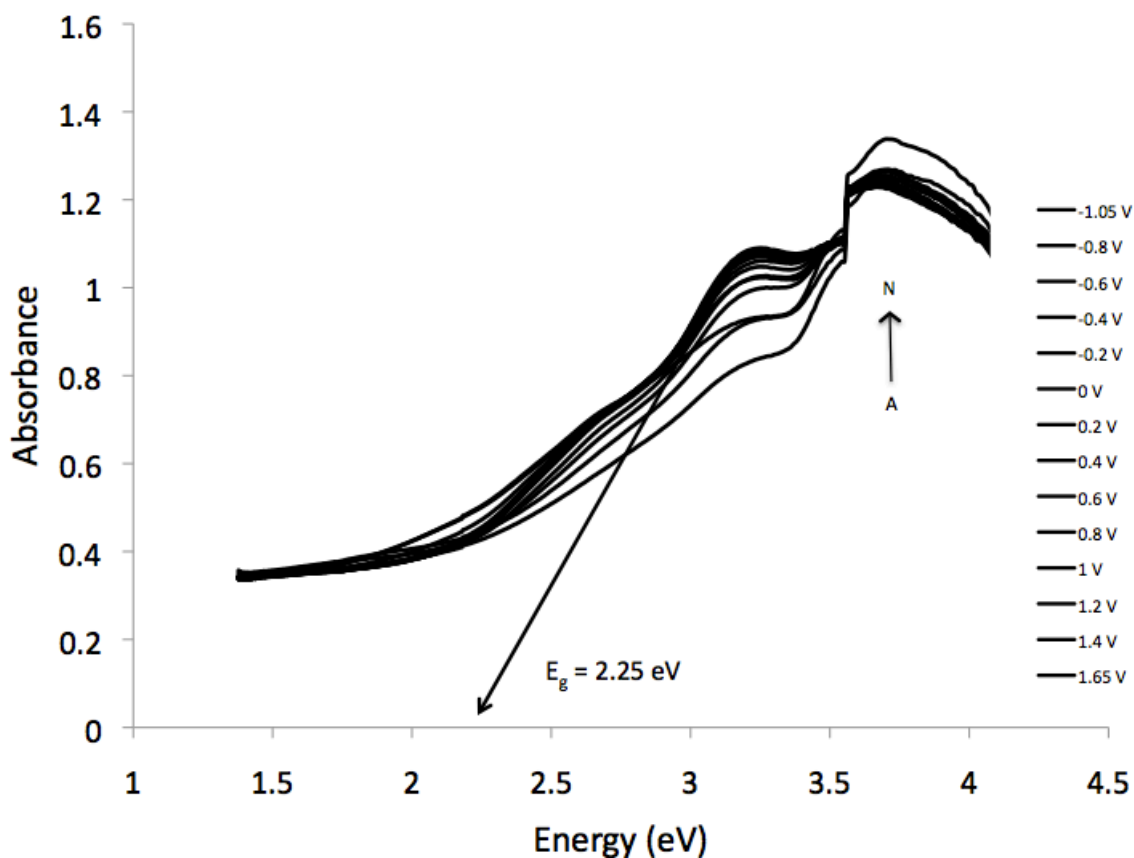


Figure 44. Spectroelectrochemistry of PBTPm in 0.1 M BMPBTI/CH₃CN electrochemically deposited on an ITO working electrode from -1.05 V (A) to 1.65 V (N).

The spectroelectrochemistry of PBEPm (Figure 43) differs slightly from that of PBTPm (Figure 44). With the EDOT moiety contributing to a more evident π to π^* transition, a significant interband transition decrease is observed. Also, with the electron donating EDOT moiety, the HOMO and LUMO become closer, forming a smaller band gap. The same is true for each polymers n-doped state.

Molecular Modeling and X-Ray Diffraction

Both BEPm and BTPm contain two single bonds attaching the pyrimidine group to the two EDOT or thiophene groups, respectively. The single bonds present between the two have the ability to twist and turn freely thus flipping the attached EDOT or thiophene rings in any given direction. This ring flipping raised question as to the possibility that steric properties may be affecting the electrochemistry. Also, the EDOT electron donating groups lower the oxidation potential for BEPm significantly. However, previous studies have shown that barrier properties caused by ring flipping remain unaffected even with a change in oxidation potential.⁶⁴

Using the Cerius 2 Program it can be seen that ring flipping appears likely with both BEPm and BTPm. This places the thiophene rings, in BTPm for example, both facing up or in an opposite orientation (Figure 45). The same is true for BEPm. The barrier of rotation found for BTPm with sulfurs on the same side was 762.77 J while the energy with sulfurs on opposing sides was 765.83 J. These energies are so similar that there is likely no preference for either orientation.

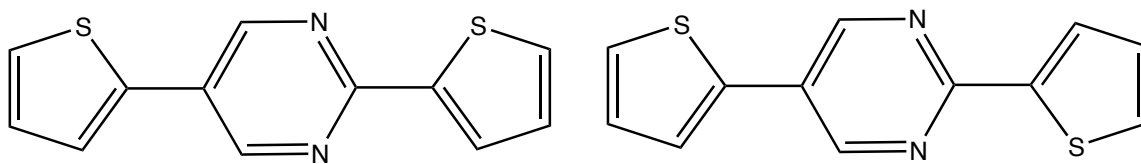


Figure 45. BTPm conformers.

Because these molecules have freedom of rotation, the orientation of the thiophene or EDOT moieties can be observed through the torsion angle. The torsion

angle, or dihedral angle, depicts an angle between two planes. The torsion angle of two planes is visible when looking along their line of intersection (Figure 46).

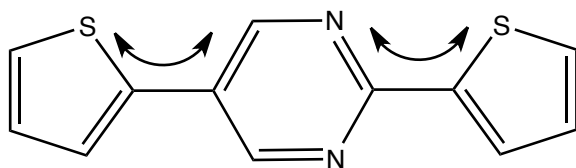


Figure 46. Determination of torsion angles through plane intersection.

After minimization and dynamics for the monomer solution, it can be seen that the torsion angle on the opposing side of the nitrogens in BEPm is 33.4° while the torsion angle for BTPm was found to be 21.6° (Figure 47). Larger torsional angles reduce pi overlap, limiting conjugation.⁶⁵ The crystal structure, found by Makda Araya, of BTPm showed complete planarity with a torsion angle less than 5° .⁶¹ In solution the monomers have freedom to rotate and move, creating the ability to endure a larger torsion angle. However, in a crystal they are locked in place with no freedom of motion. This is due principally to crystal packing and π - π stacking that reinforces the planarity. The barrier of rotation calculated for BEPm and BTPm in solution was 64.4 J and 33.5 J respectively.



Figure 47. Molecular models of BTPm and BEPm showing torsion angles occurring on the opposite side of the pyrimidine nitrogens.

As a crystal, stacked together, the monomers show a planar geometry with torsion angles less than 5° . X-Ray crystallography experiments conducted on a BTPm single crystal, by fellow graduate student Makda Araya, revealed a spacing of 3.4 Å between adjacent monomers. By molecular modeling the distance was found to be 3.4 Å as well (Figure 48); distances this small are indicative of π - π overlap between adjacent molecules.⁶⁶

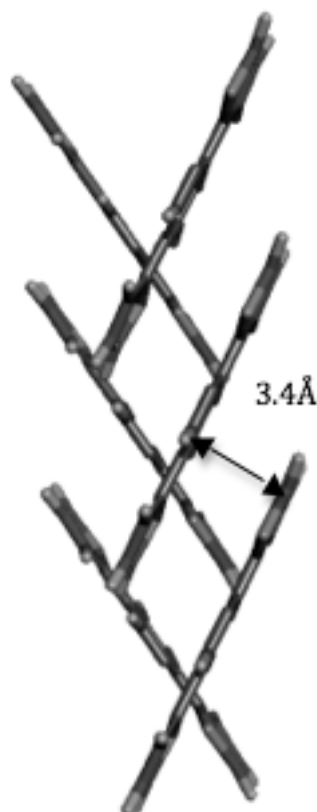


Figure 48. Molecular model of BTPm with distance of 3.4 Å between each monomer.

The crystal structure of BEPm could not be determined however, molecular modeling predicts a 3.9 Å distance between monomers (Fig 49). The increased spacing, which is still close enough to allow for pi-pi overlap, is likely due to the disorder induced by the ethylenedioxy substituents. The barrier of rotation was found to be 740.77 J for BEPm with sulfurs on the same side and 750.54 J with sulfurs on opposing sides. As with BTPm, these energies are so similar that there is likely no preference for either orientation; in BEPm, this appears to increase disorder, preventing the monomer from crystallizing well.

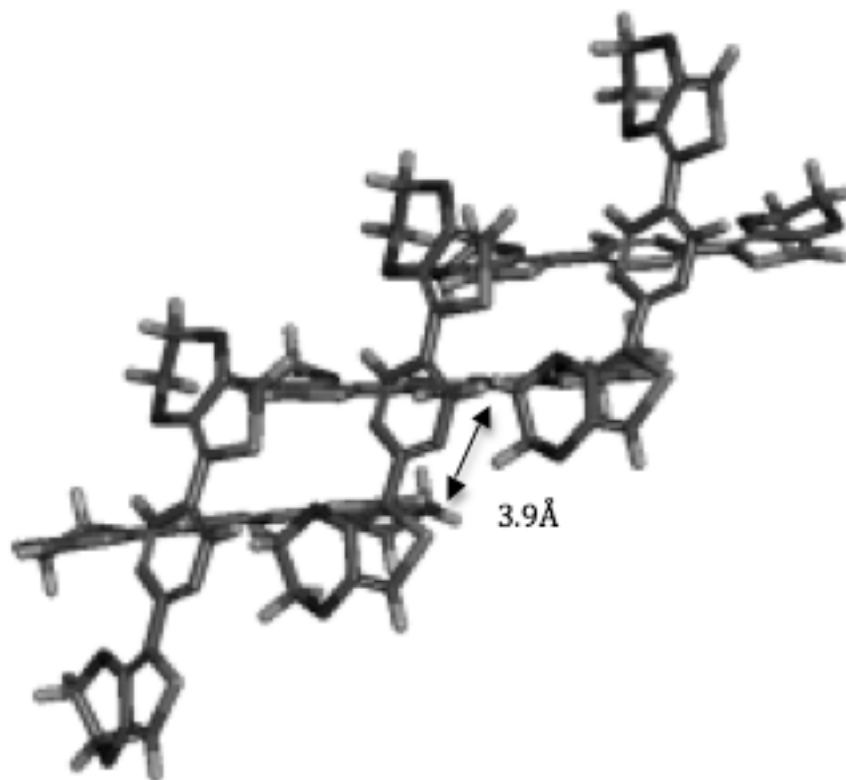


Figure 49. Molecular model of BTPm with distance of 3.9 Å between each monomer.

Conclusions

The electron affinities and ionization potentials of the high nitrogen heterocycles determine the success of the polymers' electrochemistry, creating a better n-doping polymer, through stabilizing the negative charge more effectively. The low monomer concentration was necessary due to poor solubility of BTPm. To obtain a lower oxidation potential for both the monomer and polymer, BEPm was synthesized to increase the donor groups' electron density. Addition of electron-donating ethylenedioxy substituents resulted in BEPm monomer oxidation potentials considerably lower than those of BTPm. The voltammograms reveal a significant p-doping current response, but the n-doping portion was relatively insignificant, particularly in comparison to the voltammograms of

PBTPm; it is possible that the electron donating ethylenedioxy substituents lowered the reduction potential enough that only the edge of the reduction process is accessible within the electrochemical stability window of the electrolyte solution. As observed with BTPm using EMIBTI as the supporting electrolyte, scanning to n-doping potentials during electropolymerization has not improved polymer n-doping electrochemical response. The lack of an irreversible process may be due to the pyrimidine ring containing a better acceptor, more electron withdrawing, than the isopyrazole, creating more stabilized ether linkages. The n-doping process is not seen for PBEPm when using EMIBTI as the supporting electrolyte possibly due to the small electrolyte window. The electropolymerization process for each monomer was repeated using 0.1 M BMPBTI/CH₃CN as the supporting electrolyte. From this it can be seen that the p-doping process is too high to be utilized in PBTPm. However, for BEPm the redox process during polymerization, and not seen during polymer electrochemistry likely indicates that the process belongs to a soluble species, possibly a soluble oligomer, that was removed during the film rinsing process. Voltammograms of PBEPm and PBTPm reveals that PBEPm gives a greater current response and more prominent p- and n-doping processes than PBTPm at lower potentials in BMPBTI/CH₃CN.

Using the EDOT moiety for isopyrazoles and pyridines, the band gap has steadily lowered with electropolymerization of the monomer and n-doping of the polymer. The band gap determination was found from the π to π^* transition, where in BEPm the intensity of the interband transition decreased, and three absorbances developed at a lower energy possibly due to the formation of a bipolaronic species. Optical energy gaps for BTPm and BEPm are approximately 3.33 eV and 3.18 eV respectively. The observed

differences are possibly due to the ethylenedioxy derivative donating electron density and raising the HOMO, thus lowering the E_g . The band gap determined for BTPm for the onset of the π to π^* transition was found at approximately 2.25 eV. With the EDOT moiety contributing to a more evident π to π^* transition, a significant interband transition decrease is observed and the HOMO and LUMO become closer, forming a smaller band gap. The same is true for each polymers n-doped state.

Ring flipping appeared likely with both BEPm and BTPm. This would place the thiophene or EDOT rings both facing up or in an opposite orientation. There is no preference for one or the other. Larger torsional angles reduce pi overlap, limiting conjugation. X-Ray crystallography experiments conducted on a BTPm single crystal, by fellow graduate student Makda Araya, revealed a spacing of 3.4 Å between adjacent monomers similar to the calculated molecular modeling distance of 3.4 Å. The increased spacing, which is still close enough to allow for pi-pi overlap, is likely due to the disorder induced by the ethylenedioxy substituents. For both BEPm and BTPm, the energies are so similar that there is likely no preference for either orientation.

CHAPTER IV

FERROCENE-CONTAINING POLYMERS

Background

Ferrocene-containing polymers have gained much attention since their debut in the mid 1970s due to their exceptional stability during the redox process.⁶⁷ The inherent properties of ferrocene-containing polymers, such as redox stability, reversible oxidation, and controlled chemistry, have been extensively studied. It has been found that ferrocene polymers display semiconductive properties when produced from poly(vinylferrocene), poly(ethynylferrocene), and poly(3-vinylbisfulvalenediiron).^{13,68} These organometallic polymers, with metal containing backbones or constituents, are widely studied for their intrinsic properties and their ability to be precursors in nanocomposite ceramic materials.⁶⁹ Technological advancements for applications, such as automobile components, and protective coatings can be accomplished using ceramic materials derived from ferrocene-based, metal-containing polymers.⁶⁹ Furthermore, conceivable electrochemical applications, such as electrochemical sensors, electrode coatings, and batteries have been of interest due to the reversible redox processes of ferrocene.^{70,71,72} Electrochemical behavior of ferrocene-containing polymers for use in enzymatic biosensors and bio-fuels is of particular interest, as well as the development of ferrocene-

containing polymers in aqueous media.^{73,74} Styrene can be co-polymerized with ferrocene-containing vinyl monomers such as the one shown in Figure 50. However, the resulting copolymers may be composed of randomly distributed ferrocenophane and styrene units, consequently producing a backbone structure that is poorly defined. Research with these monomers has centered on attaining high molecular weight copolymers comprised of well-defined backbones.⁶⁸

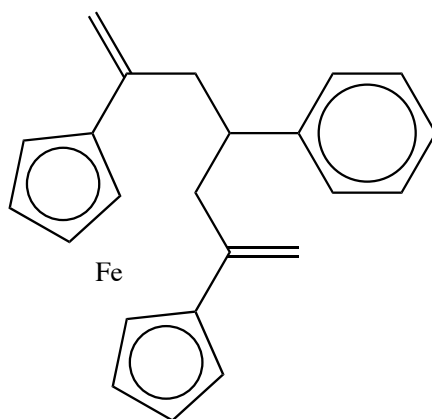
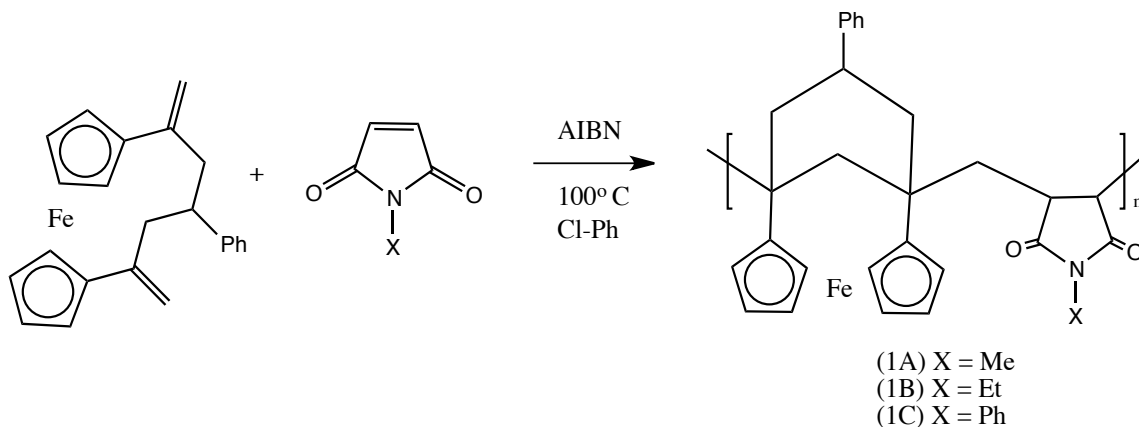
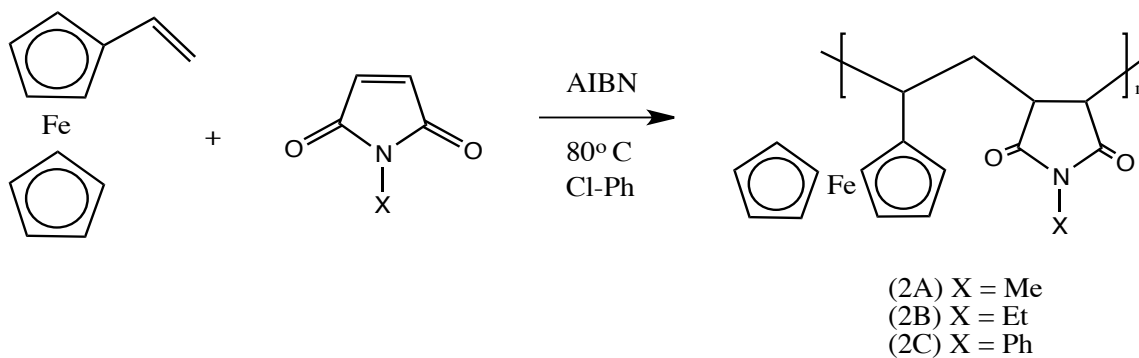


Figure 50. A typical ferrocene-containing vinyl monomer.

Various copolymers derived from 3-phenyl[5]ferrocenophane (Figure 51), denoted as copolymers 1A-C, and from vinylferrocene (Figure 52), denoted as copolymers 2A-C, with various N-substituted maleimides were prepared by another member of the Irvin Research Group. The compounds undergo free-radical polymerization with azobisisobutyronitrile (AIBN) as the free radical initiator. Copolymerization of these monomers has been thought to produce high molecular weight polymers with recurrent distribution of monomers.⁷⁵ Electrochemical characterization of these polymers was necessary to determine their utility for the applications mentioned above.



Scheme 5. Copolymerization of 3-Phenyl[5]ferrocenophane-1,5-dimethylene with Various N-Substituted Maleimides.



Scheme 6. Copolymerization of Vinylferrocene with Various N-Substituted Maleimides.

Experimental

Materials

Aqueous 0.1 M solutions were prepared from deionized water and sodium chloride (NaCl) purchased from Acros. Experiments were conducted on a lab bench exposed to air. Ferrocene copolymers were prepared by Dr. Charles Neef as described

below. Polymers were prepared as shown in Figures 51 & 52 above via free-radical polymerization with AIBN as the free radical initiator.

Instrumentation

Chronoamperometry and cyclic voltammetry experiments were accomplished using a Pine WaveNow potentiostat. The working (WE), auxiliary (CE), and pseudo-reference (RE) electrodes were a platinum button (0.2 cm diameter, Bioanalytical Systems Inc.), a platinum wire, and a silver wire respectively. All chronoamperometry experiments used the following parameters: induction period: 0 V for 15 seconds, forward step period: 0.5 V for 120 seconds, and relaxation period: 0.5 V for 120 seconds. Monomer concentrations were 0.01 M while monomer-free aqueous sodium chloride was 0.1 M. Once polymer deposition was accomplished, the films were placed in a 0.1 M NaCl monomer-free electrolyte solution. Cyclic voltammetry experiments were accomplished with 2 scans at scan rates of 20, 40, 60, 80, and 100 mV/s for all ferrocene-containing polymers.

Results and Discussion

Electrodeposition

The copolymers were electrochemically deposited via chronoamperometry onto a platinum working electrode from a 0.1 M aqueous NaCl, solution. A platinum counter

electrode and silver wire pseudo-reference electrode were used as well. At multiple scan rates the CV's for copolymers 1A-C and 2A-C revealed a linear relationship between current and scan rate, which is expected for surface-immobilized electroactive materials.

At slower scan rates a minor current increase for copolymers 1A-C was discovered preceding the reduction peak slower scan rates of 20, 40, and 60 mV/s than those depicted at 100 mV/s in Figures 53 & 54. This occurrence could be a result of anions rapidly diffusing to the surface followed by a slower diffusion through the polymer film. In the polymers oxidized state, it is assumed to be swollen with water due to Van der Waal interactions.

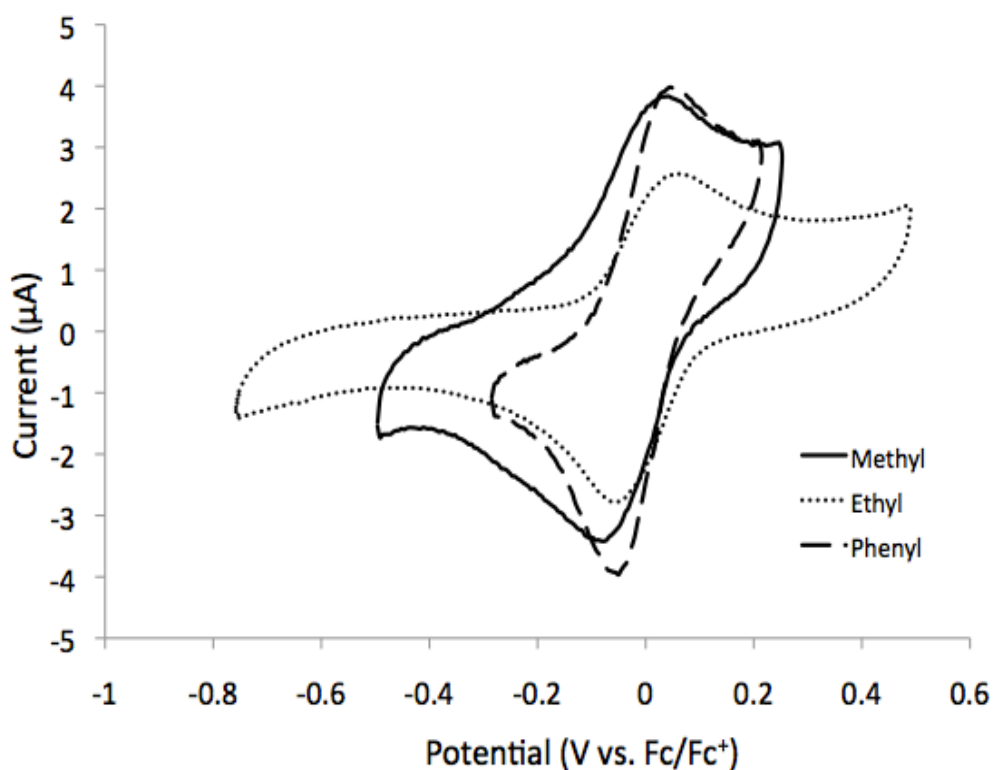


Figure 51. Cyclic Voltammogram of copolymer 1A-C at 100 mV/s. WE: Pt (0.2 cm diameter); RE: Ag wire; CE: Pt wire.

For comparison of the electrochemical behavior of copolymers derived from vinylferrocene, cyclic voltammograms for the three polymers were obtained at 100 mV/s and have been overlayed (Figure 54). Copolymers 2A and 2B show similar trends for reduction and oxidation with corresponding current response. However the 2C (phenyl) copolymer has greater current response for both reduction and oxidation processes. Possible reasoning for the copolymers, 1C and 2C, to obtain more intense current responses, Figure 53 and 54, than the comparative copolymers may be that it contains the phenyl ring rather than the straight alkyl chain.

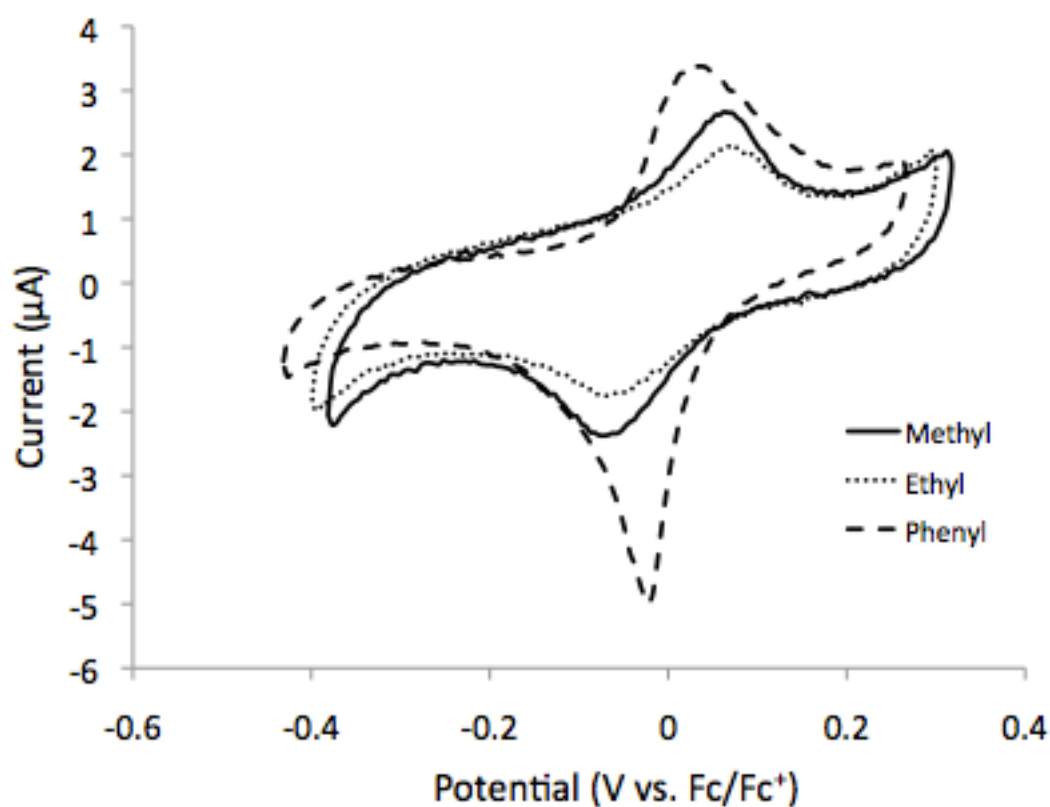


Figure 52. Cyclic voltammogram of copolymer 2A-C at 100 mV/s. WE: Pt (0.2 cm diameter); RE: Ag wire; CE: Pt wire.

During polymer neutralization, a denser film is formed from removal of water causing the film to flatten resulting in a slower diffusion of ions. For copolymers 2A-C and 1A-C, this phenomenon was not observed and was consistent with the diffusion coefficients obtained using chronoamperometry (Table 2). The expected redox potentials are lower for copolymers 1A-C and 2A-C than what was observed. The increased potentials could be caused by conformational changes when moving from solution to the electrode to become immobilized which in turn causes chain compression increasing ferrocenyl and maleimide interactions. Cyclic voltammograms were obtained at 100 mV/s for 20 scans to assess the stability of the CME's. A small change from the first scan to the second was observed however, the consecutive scans showed insignificant loss in I_{pa} and I_{pc} .

Diffusion coefficients rely on the electrolyte's rate of diffusion through the polymer film and show evidence of polymer swelling on the electrode.³¹ Diffusion rates for copolymers 1A-C were in the range of $10^{-9} \text{ cm}^2 \text{ s}^{-1}$ and signifying that the electrolyte easily diffused through the polymer film inducing swelling (Table 2). Similarly, diffusion rates for the copolymers 2A-C were in the range of $10^{-9} \text{ cm}^2 \text{ s}^{-1}$ signifying similar diffusion through the polymer film.

Table 2. Oxidation and reduction potentials for electrodeposited copolymers, 1A-C and 2A-C, in 0.1 M NaCl/H₂O with corresponding diffusion coefficients, D. WE: Pt (0.2 cm diameter); RE: Ag wire; CE: Pt wire.

Copolymer	E _{ox} (V)	E _{red} (V)	D (cm ² /s)
1A	0.04	-0.08	6.0 x 10 ⁻⁹
1B	0.06	-0.06	4.9 x 10 ⁻⁹
1C	0.05	-0.05	1.3 x 10 ⁻⁹
2A	0.06	-0.07	5.5 x 10 ⁻⁹
2B	0.07	-0.07	1.2 x 10 ⁻⁹
2C	0.02	-0.02	4.9 x 10 ⁻⁹

Conclusions

The resulting ferrocene-containing copolymers displayed good solubility in aqueous media, as done by Dr. Charles Neef, providing the ability to develop solution cast amorphous films. Diffusion rates of all the copolymers were in the 10⁻⁹ range, depicting good diffusion throughout the polymer. In aqueous sodium chloride solutions, oxidative electrochemical deposition produced films with satisfactory redox activity making these copolymers good targets for use as chemically modified electrodes that can eventually be utilized as sensors.

CHAPTER V

CONCLUDING REMARKS

Conclusions

Our research group has focused its efforts on the synthesis and characterization of high nitrogen heterocyclic acceptor units flanked by thiophene- and EDOT- based donor units to explore the effectiveness of various acceptor groups. Both p-doping and n-doping processes and spectroelectrochemistry were studied for all of the pyrimidine and isopyrazole monomers and polymers. For the ferrocene-containing copolymers, oxidative electrochemical deposition produced films with satisfactory redox activity making these copolymers good targets for use as chemically modified electrodes that can eventually be utilized as sensors.

Irreversible reduction during isopyrazole studies made it impossible to avoid electrochemically induced cleavage of the alkyl aryl ethers using gold or platinum working electrodes. After electropolymerization using all four electrolytes/solvent systems, BMPBTI/CH₃CN, TMABF₄/CH₃CN, TBAP/PC, and TBAP/CH₃CN were compared and BMPBTI/CH₃CN showed to be the best system due to the lower oxidation potential alongside the good current response. Linear dependence of current response on scan rate also indicated that the polymer film was electroactive and had adhered to the

electrode. Deprotection of BEIPz TMS failed due to an unavailability of water to complete the deprotection process. Addition of electron-donating ethylenedioxy substituents resulted in BEPm monomer oxidation potential considerably lower than that of BTPm. Voltammograms of PBEPm and PBTPm reveals that PBEPm gives a greater current response and more prominent p- and n-doping processes than PBTPm at lower potentials in BMPBTI/CH₃CN.

Failed attempts were made to determine the spectroelectrochemical behavior of PBEIPz due to the polymers inability to adhere to the ITO-coated glass electrode. Using the EDOT moiety for pyridines, the band gap obtained steadily lowered, as expected, with electropolymerization of the monomer and n-doping of the polymer.

BEPm and BTPm appeared to have no preference for thiophene ring orientation based on barrier of rotation calculations. X-Ray crystallography experiments conducted on a BTPm single crystal, by fellow graduate student Makda Araya, revealed a spacing of 3.4 Å between adjacent monomers similar to the calculated molecular modeling distance of 3.4 Å.

Ferrocene-containing copolymers displayed good solubility in aqueous media, providing the ability to develop solution cast amorphous films. In aqueous sodium chloride solutions, oxidative electrochemical deposition produced films with satisfactory redox activity making these copolymers good targets for use as chemically modified electrodes that may eventually be utilized as sensors. Diffusion rates of all copolymers depicted good diffusion throughout the polymer.

Future Work

The extent of this research focused on electronic and spectroelectronic properties of only a few known and novel monomers and polymers as well as electrolyte/solvent systems. Continuing with experimentation using several other electrolytes may provide for further understanding of the monomer and polymer processes.

Determining band gap, E_g , for PBEIPz would be beneficial after finding a proper working electrode that the polymer would adhere to. Utilizing other acceptors such as pyrazine, fluoropyrazine, or piperidine to determine n-doping capabilities and compare electron affinities. Also, experimenting with these polymers' long term switching stability to see if they contain capability to be used as sensors.

REFERENCES

- ¹ Natta, G.; Mazzanti, G.; Corradini, P. "Stereospecific Polymerization of Acetylene," *Atti accad. nazl. Lincei Rend. Classe Sci. Fis. Mat. e Nat.* **1958**, *25*, 3-12.
- ² Shirakawa, H.; Louis, E.J.; MacDiarmid, A.G.; Chiang, C.K.; Heeger, A.J. "Synthesis of Electrically Conducting Organic Polymers: Halogen Derivatives of Polyacetylene," (CH)_x. *J.C.S. Chem. Comm.* **1977**, *16*, 578-580.
- ³ Vaschetto, M. E.; Monkman A. P.; Springborg, M. "First-principles studies of some conducting polymers: PPP, PPy, PPV, PPyV, and PANI," *J. Molec. Struc.* **1999**, *486*, 181-191.
- ⁴ Kanatzidis, M. G.; Hubbard, M.; Tonge, L. M.; Marks, T. J. "In situ intercalative polymerization as a route to layered conducting polymer-inorganic matrix microlaminates. Polypyrrole and polythiophene in FeOCL," *Synth. Met.* **1989**, *28*, 89-95.
- ⁵ Zainudeen, U. L.; Careem, M. A.; Skaarup, S. "PEDOT and PPy conducting polymer bilayer and trilayer actuators," *Sensors and Actuators B.* **2008**, *134*, 467-470.
- ⁶ Naik, R.; Ganesan, R.; Adarsh, K. V.; Sangunni, K. S.; Takats, V.; Kokenyesi, S. "Light and heat induced interdiffusion in Sb/As₂S₃ nano-multilayered film," *J. Non-Crystalline Solids.* **2009**, *355*, 1939-1942.
- ⁷ Moliton, A.; Hiorns, R. C. "Review of electronic and optical properties of semiconducting π -conjugated polymers: applications in optoelectronics," *Polym Int.* **2004**, *53*, 1397-1412.
- ⁸ Tarkuc, S. "Tuning the optoelectronic properties of conjugated polymers via donar-acceptor-donor architechture," Ph. D. Thesis, Middle East Technical University, **2010**.
- ⁹ Tarkuc, S.; Udum, Y.A.; Toppare, L. "Tuning of the Neutral State Color of the π -conjugated Donor-Acceptor-Donor Type Polymer from Blue to Green via Changing the Donor Strength on the Polymer," *Polymer.* **2009**, *50*, 3458-3464.
- ¹⁰ Hissler, M.; Lescop, C.; Reau, R. "Functional phosphorus-based π - conjugated systems: Structural diversity without multistep synthesis," *Pure Appl. Chem.* **2007**, *79*, 201-212.

- ¹¹ Apperloo, J. "Interactions between π - conjugated molecules in their charged and photoexcited states," Thesis, Technische Universiteit Eindhoven. **2001**.
- ¹² Jian, L.; Sano, T.; Hirayama, Y.; Shibata, K. "White polymer light emitting diodes with multi-layer device structure," *Synth. Met.* **2009**, *159*, 36-40.
- ¹³ Chen, H.; Hou, J.; Zhang, S.; Liang, Y.; Yang, G.; Yang, Y.; Yu, L.; Li, G. "Polymer solar cells with enhanced open-circuit voltage and efficiency," *Letters: Nat. Phot.* **2009**, *3*, 649-653.
- ¹⁴ Sugata, M.; Kaloni T. P. "Electronic properties of boron and nitrogen doped graphene: A first principles study," S. N. Bose National Centre for Basic Sciences. **2012**.
- ¹⁵ Ahonen H. J.; Lukkari, J.; Kankare, J. "n- and p- Doped poly(3,4-ethylenedioxythiophene): Two electronically conducting states of the polymer," *Macromolec.* **2000**, *33*, 6787-6793.
- ¹⁶ Witker, D. L.; Clancy, S. O.; Irvin, D. J.; Stenger-Smith, J. D.; Irvin, J. A. "Electrochemical Deposition of a new n-doping polymer based on bis(thienyl)isopyrazole," *J. Electrochem. Soc.* **2007**, *154*, G95-G98.
- ¹⁷ Bishop, B. M.; McCafferty, D. G.; Erickson, B. W. "4'-Aminomethyl-2,2'-bipyridyl-4-carboxylic Acid (Abc) and Related Derivatives: Novel Bipyridine Amino Acids for the Solid-Phase Incorporation of a Metal Coordination Site Within a Peptide Backbone," *Tetrahedron.* **2000**, *56*, 4629-4638.
- ¹⁸ Jakle, Frieder. "Conjugated organoborane oligomers, macrocycles and polymers for organic electronics and sensors."
- ¹⁹ Dai, L.; Soundarrajan, P.; Kim, T. "Sensors and sensor arrays based on conjugated polymers and carbon nanotubes," *Pure Appl. Chem.* **2002**, *74*, 1753-1772.
- ²⁰ Gospodinova, N.; Terlemezyan, L. "Conducting polymers prepared by oxidative polymerization: Polyaniline," *Prog. Polym. Sci.* **1998**, *23*, 1443-1484.
- ²¹ Anzari, R.; Keivani, M. B. "Polyaniline conducting electroactive polymers: Thermal and environmental stability studies," *Electrochem. J. of Chem.* **2006**, *3*, 202-217.
- ²² Thieblemont, J. C.; Gabelle, J. L.; Planche, M. F. "Polypyrrole overoxidation during its chemical synthesis," *Synth. Met.* **1994**, *66*, 243-247.
- ²³ Stepnicka, P. *Ferrocenes: Ligands, materials, and biomolecules*; John Wiley & Sons Ltd. West Sussex, **2008**.
- ²⁴ Stenger-Smith, J.; Irvin J. A. "Ionic liquids for energy storage applications," **2009**, *4.4*, 103.

- ²⁵ Dennany, L.; Wallace, G. C.; Forster, R. J. "Luminescent metal complexes within polyelectrolyte layers: Tuning electron and energy transfer," *Am. Chem. Soc.* **2009**, 25(24), 14053-14060.
- ²⁶ Sawyer, D. T.; Sobowiak, A.; Roberts, J. L. *Electrochemistry for chemists*. New York, **1995**.
- ²⁷ Borges, R. S.; Queiroz, A. N.; Mendes, A. P. S.; Araujo, S. C.; Franca, L. C. S.; Franco, E. C. S.; Leal, W. G.; Da Silva, A. B. F. "Density functional theory (DFT) study of edaravone derivatives as antioxidants," *Int. J. Molec. Sci.* **2012**, 13, 7594-7606.
- ²⁸ Zarras, P. "Novel electroactive polymers as environmentally compliant coatings for corrosion control," Naval Air Warfare Center Weapons Division. **2006**.
- ²⁹ Bard, A. J.; Faulkner, L. R. *Electrochemical Methods*. John Wiley and Sons. **2001**.
- ³⁰ Kissinger, P. T.; Heineman, W.R. In *Laboratory Techniques in Electroanalytical Chemistry*, Marcel Dekker, INC, New York. **1984**.
- ³¹ Suarez, I. J.; Otero, T. F.; Marquez, M. "Diffusion coefficients in swelling polypyrrole; ESCR and Cottrell models," *J. Phys. Chem.* **2005**, 109, 1723-1729.
- ³² Simon, P.; Gogotsi, Y. "Materials for electrochemical capacitors," *Nat. Mat.* **2008**, 7, 845-854.
- ³³ Irvin, J.A.; Irvin, D.J.; Stenger-Smith, J.D. "Electroactive Polymers for Batteries and Supercapacitors," *Handbook of Conducting Polymers*, 3rd ed.; Skotheim, T.A.; Reynolds, J.R., eds.; CRC Press: Boca Raton, FL. **2007**, 9-1-9-29.
- ³⁴ Irvin, J.A.; Winkel, K. "Thin-Film Applications of Electroactive Polymers," In *Functional Polymer Films*, 1st ed.; Knoll, W.; Advincula, R.C., eds.; Wiley VCH: Weinheim, Germany: **2011**, 983-1015.
- ³⁵ Bohler, A.; Dirr, S.; Johannes, H.; Ammermann, D.; Kowalsky, W. "Influence of the process vacuum on the device performance of organic light-emitting diodes," **1997**, 91, 95-97.
- ³⁶ Dalton, L. R.; Thomson, J.; Nalwa, H. S. "The role of extensively delocalizing π -electrons electrical conductivity, non-linear optical properties and physical properties of polymers," *Polymer*. **1987**, 28, 543-552.
- ³⁷ Nolot, E. S.; Andre, A.; Doyeux, H.; Vaurfey, D. "Characterization of organic light emitting diodes by spectroscopic ellipsometry," <http://www.science24.com/paper/15507> (accessed 6/2012).

- ³⁸ Bian, L.; Zhu, E.; Tang, J.; Tang W.; Zhang, F. "Recent progress in the design of narrow bandgap conjugated polymers for high-efficiency organic solar cells," *Prog. in Poly. Sci.* **2012**.
- ³⁹ Wilken, S.; Hoffman, T.; Von Hauff, E.; Borchert, H.; Parisi, J. "ITO-free inverted polymer/fullerene solar cells: Interface effects and comparison of different semi-transparent front contacts," *Solar Energy Materials and Solar Cells.* **2012**, 96, 141-147.
- ⁴⁰ Wang, P.; Yao, K.; Chen, L.; Chen, Y.; Li, F.; Wang, H.; Yu, S. "Self-assembled mesogens modified fullerene for efficiently stable bulk heterojunction solar cells," *Solar Energy and Solar Cells.* **2012**, 97, 34-42.
- ⁴¹ Downard, A. J.; Surridge, N. A.; Gould, S.; Meyer, T. J. "Photocurrents in thin polymeric films. Chromophore/quencher assemblies based on polypyrrole," *J. Phys. Chem.* **1990**, 94, 6754-6764.
- ⁴² Beaujuge, P. M.; Reynolds, J. R. "Color control in π - conjugated organic polymers for use in electrochromic devices," *Chem. Rev.* **2010**, 110, 268-320.
- ⁴³ Savenije, T. J. Organic Solar Cells. Delft University of Technology.
- ⁴⁴ Nagarajan, S.; Kumar, J.; Bruno, F. F.; Samuelson, L. A.; Nagarajan, R. "Bioanalytically synthesized poly(3,4-ethylenedioxythiophene)," *Macromolecules.* **2008**, 41, 3049-3052.
- ⁴⁵ Sotzing, G. A.; Reynolds, J. R.; Steel, P. J. "Poly(3,4-ethylenedioxythiophene) (PEDOT) prepared via electrochemical polymerization of EDOT, 2,2'-Bis(3,4-ethylenedioxythiophene) (BiEDOT), and their TMS derivatives," *Communications.* **1997**.
- ⁴⁶ Winkel, K. "Low band gap donar-acceptor strategies for stable n-doping polymers," Masters Thesis, Texas State University-San Marcos, San Marcos, TX. **2011**.
- ⁴⁷ Macfarlane, D. R.; Meakin, P.; Sun, J.; Amini, N.; Forsyth, M. "Pyrrolidinium Imides: A new family of molten salts and conductive plastic crystal phases," *J. Phys. Chem.* **1999**, 103, 4164-4170.
- ⁴⁸ Coetzee, J. F.; Cunningham, G. P. "Evaluation of single ion conductivities in acetonitrile, nitromethane, and nitrobenzene using tetraisoamylammonium tetraisoamylboride as reference electrolyte," **1965**, 87, 2529-2534.
- ⁴⁹ J. R. Aranzaes, M. Daniel, D. Astruc, *Can. J. Chem.*, **84**, 288-299, (2006).

- ⁵⁰ Azzena, U.; Denurra, T.; Melloni, G. "Electron-transfer-induced reductive demethoxylation of anisole: evidence for cleavage of a radical anion," **1992**, *57*, 1444-1448.
- ⁵¹ Franco, D.; Panyella, D.; Rocamora, M.; Gomez, M.; Clinet, J. C.; Muller G.; Dunach. "Electrochemical cleavage of allyl aryl ethers and allylation of carbonyl compounds: umpolung of allyl-palladium species," *Tetrahedron Letters*. **1999**, *40*, 5685-5688.
- ⁵² Hillman, A. R., Daisley, S. J., Bruckenstein, S. "Ion and solvent transfers and trapping phenomena during n-doping of PEDOT films," *Electrochimica Acta*. **2008**, *53*, 3763-3771.
- ⁵³ Irvin, D.; DuBois, C. J.; Reynolds, J. R. "Dual p- and n-type doping in acid sensitive alternating bi(ethylenedioxythiophene) and pyridine polymer," *Chem. Comm.* **1999**, 2121-2122.
- ⁵⁴ Yamaguchi, I.; Mitsuno, H. "Synthesis of n-type π - conjugated polymers with pendant crown ether and their stability of n-doping state against air," *Macromolecules*. **2010**, *43*, 9348-9354.
- ⁵⁵ Ruiz, V.; Colina, A.; Heras, A.; Lopez-Palacios, J. "Study of electrochemical stability of conducting polymers by bidimensional spectroelectrochemistry: p- and n-doping of poly(4,4'-bis(butylthio)-2,2'-bithiophene) films," *Polymer Degradation and Stability*. **2006**, *91*, 3117-3123.
- ⁵⁶ Higgins, Roger W.T. "Enhancement of polymer light-emitting diode performance through doping and improved charge injection," Masters thesis, Durham University. **2001**.
- ⁵⁷ Dillow, G. W.; Kebarle, P. "Electron affinities of aza-substituted polycyclic aromatic hydrocarbons," *Can. J. Chem.* **1989**, *67*, 1628-1631.
- ⁵⁸ Tanaka, S.; Kaeriyama, K.; Hirajde, T., "Properties of poly[2,5-bis(2-thienyl)thiazole] and poly[bis(2-thienyl)pyridine]s," *Die Makromolekulare Chemie, Rapid Communications*. **1988**, *9*, 11, 743-748.
- ⁵⁹ Schwenn, P. E.; Gui, K.; Zhang, Y.; Burn, P. L.; Meredith, P.; Powell, B. J. "Kinetics of charge transfer process in organic solar cells: Implications for the design of acceptor molecules," *Organic Electronics*. **2012**.
- ⁶⁰ Mosquera, A.; Riveiros, R.; Sestelo, J. P.; Sarandeses, L. A. "Cross-coupling reactions of indium organometallics with 2,5-dihalopyrimidines: synthesis of hytinadine A," *Organic letters*. **2008**, *10*, 3745-3748.

- ⁶¹ Araya, A. "Synthesis of donor-acceptor-donor molecules for preparation of stable n-doping polymers," Master, Thesis, Texas State University-San Marcos, San Marcos, TX, **2012**.
- ⁶² Neudeck, A.; Petr, A.; Dunsch, L. "Separation of the Ultraviolet-Visible Spectra of the Redox States of Conducting Polymers by Simultaneous Use of Electron-Spin Resonance and Ultraviolet-Visible Spectroscopy," **1999**, *103*, 912-919.
- ⁶³ Thomas, C. A.; Zong, K.; Abboud, K. A.; Steel, P.; Reynolds, J. R. "Donar-mediated band gap reduction in homologous series of conjugated polymers," *J. Am. Chem. Soc.* **2004**, *126*, 16440-16450.
- ⁶⁴ Schmittl, M.; Keller, M.; Burghart, A.; Rappoport, Z.; Langels, A. "Electronic effect in polyarylviny propellers. Sold state structures and dynamic behaviour in solution of several crowded enol derivatives," *J. Chem. Soc.* **1998**, 869-875.
- ⁶⁵ Steckler, T. T.; Abboud, K. A.; Craps, M.; Rinxler, A.; Reynolds, J. R. "Low band gap EDOT-benzobis(thiadiazole) hybrid polymer characterized on near-IR transmissive single walled carbon nanotube electrodes," *Chem. Comm.* **2007**, 4904-4906.
- ⁶⁶ Liu, J.Q., Wang, Y.Y., Zhang, Y.N., Liu, P., Shi, Q.Z., Batten, S.R., *Eur. J. Inorg. Chem.* **2009**, 147-15.
- ⁶⁷ Hudson, R. "Ferrocene polymers: current architechtures, syntheses and utility," *J. Organomatallic Chem.* **2001**, 637-639.
- ⁶⁸ Abd-El-Aziz, A. S. Organoiron polymers. *Coordination Chemistry Reviews.* **2003**, *246*, 3-52.
- ⁶⁹ Dumitru, A.; Morozan, A.; Mirea, C.; Mihaiescu, D.; Panaiotu, C.; Ciupina, V.; Stamatin, I. "Inorganic copolymers based on silanes and ferrocene monomers, precursors for advanced nanostructured ceramics," *Composite Science and Technology.* **2005**, *65*, 713-717.
- ⁷⁰ Cao, Q.; Zhang, J. F.; Ren, W. X.; Choi, K.; Kim, J. S. "Ferrocene-based novel electrochemical In³⁺ sensor," *Tetrahedron Letters.* **2011**, *52*, 4464-4467.
- ⁷¹ Taylor, C. E.; Creager, S. E. "Electrochemiluminescence-based detection of ferrocene derivatives at monolayer-coated electrodes," *J. Electroanalytical Chem.* **2000**, *485*, 114-120.
- ⁷² Fujiwara, K.; Akutsu, H.; Yamada, J.; Satoh, M.; Nakatsuji, S. "Structures and charge-discharge properties of spin-carrying ferrocene derivatives," *Tetrahedron Letters.* **2011**, *52*, 6655-6658.

- ⁷³ Padeste, C.; Seiger, B.; Grubelnik, A.; Tiefenauer, L. "Molecular assembly of redox-conductive ferrocene–streptavidin conjugates — towards bio-electrochemical devices," *Biosensors and Bioelectronics*. **2004**, *20*, 545-552.
- ⁷⁴ Osman, M. H.; Shah, A. A.; Walsh, F. C. "Recent progress and continuing challenges in bio-fuel cells. Part I: Enzymatic cells," *Biosensors and Bioelectronics*. **2011**, *26*, 3087-3102.
- ⁷⁵ Neef, C. "Reactive and Functional Polymers," Submitted.

VITA

Jamie R. Carberry was born in Huntsville, Texas, on September 15, 1988, to Martha Knox Carberry, to her brother Norman Phillip Carberry Jr., and sisters Heather Senta Carberry, and Amanda Ann Carberry. After completing her work at New Braunfels High School, New Braunfels, Texas, in May 2007, she entered Texas State University-San Marcos in August 2007. In August 2010, she entered the Graduate College of Texas State as an early entry masters student. She received her Bachelor of Science in Chemistry from Texas State in May 2011.

Permanent Address: 186 Rosemary Loop

New Braunfels, Texas 78130

This thesis was typed by Jamie R. Carberry.